FEASIBILITY OF EUGENOL ENCAPSULATED POLY(LACTIC ACID)(PLA) FILMS VIA ELECTROSPINNING AS A NOVEL DELIVERY SYSTEM FOR VOLATILE COMPOUNDS IN FOOD PACKAGING SYSTEMS

A Thesis Submitted to
the Graduate School of Engineering and Sciences of
İzmir Institute of Technology
in Partial Fulfillment of the Requirements for the Degree of

DOCTOR OF PHILOSOPHY

in Food Engineering

by
Dılhun Keriman ARSERİM UÇAR

July 2017
İZMİR

We approve the thesis of **Dılhun Keriman ARSERİM UÇAR**

Examining Committee Members:

Prof. Dr. Figen KOREL
Department of Food Engineering, İzmir Institute of Technology

Prof. Dr. Ahmet YEMENİCİOĞLU
Department of Food Engineering, İzmir Institute of Technology

Prof. Dr. Sacide ALSOY ALTINKAYA
Department of Chemical Engineering, İzmir Institute of Technology

Prof. Dr. Kamile Nazan TURHAN
Department of Food Engineering, İzmir University of Economics

Prof. Dr. Taner BAYSAL
Department of Food Engineering, Ege University

25 July 2017

Prof. Dr. Figen KOREL
Supervisor, Department of
Food Engineering
İzmir Institute of Technology

Prof. Dr. Kit L. YAM
Co-Supervisor, Department of
Food Science
Rutgers University

Prof. Dr. Ahmet YEMENİCİOĞLU
Head of the Department of
Food Engineering

Prof. Dr. Aysun SOFUOĞLU
Dean of the Graduate School of
Engineering and Sciences

ACKNOWLEDGEMENTS

Primarily my sincere gratitude needs to be expressed to a number of people throughout this journey who made this thesis possible. First, my deepest appreciations go to my supervisor Prof. Dr. Figen KOREL for her great mentorship throughout not only for my academic career but also in life. Second, I would like to thank Prof. Dr. Kit L. Yam, my co-supervisor who has provided me with a great chance of being a member of his research group and making kind cooperation with Dr. LinShu Liu and Prof. Dr. Paul Takhistov during my stay at Rutgers University. I would like to give him my special thanks for his guidance, practical approach for conducting research, and professionalism throughout for my PhD research. I am indebted to Dr. Yam and his lab members, Xi, Han, Carol, Şerife, Chang, Ally, Elham and everyone in the research group for providing me with an inspiring and motivating environment.

Special thanks go to Dr. LinShu Liu, under whose supervision I worked throughout my research at United States Department of Agricultural (USDA) as he invested tremendous effort in my research and made me feel so welcome in his research group.

I would like to thank several researchers whose contributions allowed me to complete my thesis. First, Prof. Dr. Paul Takhistov, Dr. Phong Huynh at Rutgers University, and Dr.Tony Jin, Dr. Ana Margarida Moriera de Sousa, Joseph Uknalis and Audrey Thomas-Gahring at United States Department of Agricultural (USDA) and also Weiqiao Yang whom I had a wonderful time while working at the same lab.

In addition, special thanks go to my thesis committee, Prof. Dr. Ahmet YEMENİCİOĞLU, Prof. Dr. Sacide ALSOY ALTINKAYA, Prof. Dr. Kamile Nazan TURAN and Prof. Dr. Taner BAYSAL for their support, guidance and helpful suggestions.

I am grateful to Assist. Prof. Dr. Umut ADEM for his help in the interpretation of the X-ray results. I would like to thank Assist. Prof. Dr. Ümit Hakan YILDIZ who provided me the electrospinning equipment in IZTECH and special thanks to Assoc. Prof. Dr. Ayşe Handan BAYSAL for her guidance during my antifungal experiments.

I am grateful to Esra TUZCUOĞLU YÜCEL for her guidance and patience during my GC analysis at the IZTECH Environmental Development Application and Research

Center. I also appreciate the members of IZTECH Biotechnology and Bioengineering Research and Application Center, especially Yekta Oğuz GÜNAY, for her help and patience. I would like to thank the specialist of IZTECH Center for Materials Research of Izmir Institute of Technology, especially Mine BAHÇECİ and Işın ÖZÇELİK, for their valuable guidance during my research. I am very thankful to my friends Esra KAÇAR, Canan CANAL, Gökçen KAHRAMAN, Çelenk MOLVA, Duygu BÜYÜKTAŞ, Derya BOYACI, Gözde Seval SÖZBİLEN and Oğuz UNCU and I am indebted to all members of the Food Enginnering-IZTECH.

I would like to thank Scientific and Technological Research Council of Turkey (TUBITAK)–2214/A International Doctoral Research Fellowship Program, and Scientific Research Project of Izmir Institute of Technology (Project no: İYTE06 2016-2017).

Lastly, I am grateful to my husband Mehmet UÇAR, my lovely daughter Zerya UÇAR for their support to get through the difficult times, encouragment and a being a part of my life during this journey. My deepest appreciations go to my whole family; my mother Türkan ARSERİM, my father Eyyüp Sabri ARSERİM and my brothers, specials thanks my brother Ender Hikmet ARSERİM.

ABSTRACT

FEASIBILITY OF EUGENOL ENCAPSULATED POLY(LACTIC ACID)(PLA) FILMS VIA ELECTROSPINNING AS A NOVEL DELIVERY SYSTEM FOR VOLATILE COMPOUNDS IN FOOD PACKAGING SYSTEMS

Food safety and quality are important issues in food industry. The aim of this research was to evaluate the feasibility of delivering eugenol via poly(lactic) acid (PLA) emulsion fibers-grafted PLA films with bacterial cellulose into the package headspace. For this purpose, first, bacterial cellulose crystals as a natural carrier for eugenol were produced. The influence of hydrolysis temperature, time, and acid to cellulose ratio, acid concentration and type with the addition of the neutralization step on the structure, and the properties of bacterial cellulose crystals were studied. Nanocrystals, which had high thermal stability and high crystallinity bacterial cellulose, were produced. Bacterial cellulose stabilized oil-in-water Pickering emulsions were produced as carriers for eugenol. The emulsion formulations consisting of cellulose fibers and crystals, eugenol, and surfactants were characterized for food packaging applications. PLA films were produced with obtained eugenol emulsions and poly(lactic) acid which were obtained via the electrospinning method. The produced films revealed a significant antibacterial effect on *L. innocua,* and *E. coli* inoculated tomato stem scars as real food model. The fabricated films also had significant antifungal activity on *B.cinerea* inoculated table grapes. Developed novel biodegradable-PLA cellulose composite films had a great potential for delivering bioactive volatile compounds for intelligent food packaging applications. The findings of this research supports the technical feasibility of delivering eugenol for antimicrobial active packaging applications via electrospun fibers.

ÖZET

ELECTROEĞİRME İLE EUGENOL ENKAPSÜLE EDİLMİŞ PLA FİLMLERİN UÇUCU BİLEŞİKLER İÇİN YENİ TAŞINIM SİSTEMİ OLARAK GIDA AMBALAJ SİSTEMLERİNDE UYGULANABİLİRLİĞİ

Gıda güvenliği ve kalitesi gıda endüstrisinin en önemli konularındandır. Bu çalışmanın amacı eugenol enkapsüle edilmiş poli(laktik) asit emülsiyon lifleri ile aşılanmış PLA filmlerinin gaz fazındaki bioaktif bileşiklerin paketlenmiş gıda tepeboşluğuna taşınımının uygulanabilirliğini test etmektir. Bu amaç için üretilen bakteriyel selüloz kristallerinin (BSK) yapı ve özelliklerine hidroliz sıcaklığı ve zamanı, asit selüloz oranı, asit konsantrasyonu ve türüne, nötralizasyon basamağının eklenmesinin etkileri test edilmiştir. Yüksek kristal yapılı ve sıcaklığa dayanıklı BSK'ler üretilmiştir. Bakteriyel selüloz ile stabilize edilmiş su içinde yağ emülsiyonları eugenol'ün taşınımı için üretilmiştir. Selüloz fiberleri ve kristalleri, eugenol ve yüzey etkin bileşiklerden oluşan emülsiyon formülasyonları gıda ambalaj uygulamaları için karakterize edilmiştir. PLA filmleri eugenol emülsiyonları ve poli(laktik) asit ile birlikte elekroeğrime yöntemi ile üretilmiştir. Üretilen filmler, gıda modeli olarak, *L. innocua,* ve *E. coli* aşılanmış domates sap yaralarına karşı önemli antimikrobiyal etki göstermiştir. Filmler ayrıca *B.cinerea* inoküle edilmiş üzümler üzerine de önemli antifungal etki gösterdiği saptanmıştır. Geliştirilen yeni biyobozunur PLA selüloz kompozit filmler, gaz fazındaki bioaktif bileşiklerin akıllı gıda ambalajlama uygulamaları ile birlikte taşınımının büyük bir potansiyele sahip olduğunu göstermektedir. Bu çalışmanın sonuçları eugenol'ün gaz fazının paketlenmiş gıdalara elekroeğirme yöntemi ile üretilen fiberler ile taşınımının teknik olarak uygulanabilirliğini desteklemektedir.

TABLE OF CONTENTS

LIST OF FIGURES

Figure **Page**

LIST OF TABLES

Table **Page**

CHAPTER 1

INTRODUCTION

Food safety and quality are important issues in fresh produce. In recent years, consumer demand for natural and organically produced foods has created an interest for researchers to produce renewable, biodegradable antimicrobial packaging for food preservation. Antimicrobial packaging is an application of active packaging that can control the release of antimicrobial agents to food surface and provide adequate shelf life (Appendini & Hotchkiss, 2002). According to the reports of Food and Agriculture Organization of the United Nations one-third of the produced foods are wasted each year (FAO, 2011).

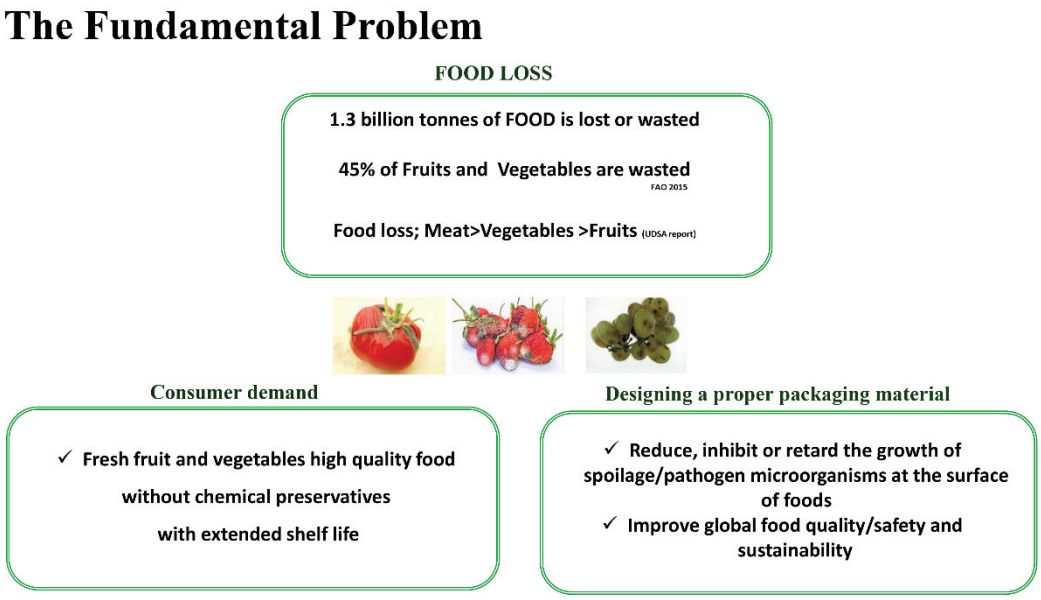

Figure 1.1. Food waste as a fundamental problem

Industrial utilization of biobased products and metabolic by-products are expected to significantly contribute to the sustainability of the national economy. Poly(lactic) (PLA) acid is a biobased polymer derived from lactic acid (2-hydroxyl propionic acid), which can be produced from carbohydrate fermentation or chemical synthesis from corn. According to the amount of the isomers in the structure poly(D-lactide), poly(L-lactide) and L(+)or D(-) lactide can be processed (Auras, Harte, & Selke, 2004).

Bacterial cellulose (BC) is a metabolite by product of *Gluconacetobacter xylinus* (Chawla, Bajaj, Survase, & Singhal, 2009) and has a nanoscale dimension and three-dimensional nano-fibrillar network. In addition, it is a non-toxic, sustainable, and green nanomaterial (Dufresne, 2013). Cellulose whiskers obtained by chemical acid hydrolysis, have various potential applications in different areas such as; reinforcing agents in nanocomposites (due to its impressive mechanical properties) (Habibi, Lucia, & Rojas, 2010), and interfacial stabilization of emulsions especially formations of Pickering emulsions (Kalashnikova, Bizot, Bertoncini, Cathala, & Capron, 2013) and biomedical applications (Picheth et al., 2017).

In terms of the economic feasibility, BC can be produced from agricultural cellulosic wastes such as coconut husk (Rosa et al., 2010) and sugarcane bagasse (Kumar, Negi, Choudhary, & Bhardwaj, 2014) as a source. Corn steep liquor, a by-product of wet corn milling, was used in the growth culture media during this study. In terms of the industrial application level, genetically modified type of *G. Xylinus* bacteria can be used as an industrial strain, and new bioreactors and fermentors could be designed for the production of BC (Chawla et al., 2009). From the practical point of view, bacterial cellulose is an available and sustainable green material, it can be produced in different surface modifications, in shape and size, and that is required according to the system needs. BC is commercially available, and Nata de coco brand in the Philippines produced jelly-like dessert from BC by the fermentation of coconut water (Chawla et al., 2009).

PLA is an economically feasible material, which is a good candidate bio-based polymer for food packaging, besides being an abundant and a cheap biomaterial (Auras et al., 2004). Essential oils are volatile aromatic oily liquids, which are naturally non-toxic and have a wide range of bioactive properties including antimicrobial and antioxidant properties even at vapor-phase (Burt, 2004).

The economic feasibility of the vapor phase of bioactive agents that are either antimicrobial or antifungal is still under investigation, and more study is needed to prove the economic feasibility of eugenol in the food packaging systems in commercial applications.

The problem statement and research gap of this Ph.D. research is based on the main problem of food waste in fresh produce. The gap is the current limitations of using volatile lipophilic bioactive compounds with biobased polymers for bioactive food packaging sytems. Essential oils (EOs) are highly volatile, and due to the volatility of essential oils, using EOs in packaging systems is a current major problem. Another

problem is limitations of the film processing methods such as films/fibers with EOs in the film.

The motivation of this study is that BC may create a large surface area to the volume ratio. This surface area would provide an active side to enhance the release, and using BC may improve the barrier, reduce the mobility and make an allignment for encapsulation. Pickering emulsion formulations (eugenol, bacterial cellulose, lauric arginate) with eugenol active compound in packaging systems is a novel delivery system for the lipophilic volatile active compound. The use of biodegradable, biobased nanoparticles (cellulose) and polymers, for food packaging, a major contributor to environmental sustainability.

The rationale of this study is to develop of a novel active biobased composite packaging film/labels with antimicrobial volatile compound (eugenol) in order to increasing the shelf life of fresh produce by an active protection against microbial contaminations.

This Ph.D. study is comprised of four main parts;

In the first part of the study; the investigation on the production of cellulose from *Acetobacter Xylinum*, preparation of cellulose nanocrystals via two acid hydrolyzes and the characterization of obtained fibers and crystals by scanning electron microscopy, thermogravimetric analysis, X-ray diffraction, and Fourier-Transform infrared spectroscopy will be explained.

In the second part of this study, the research regarding the emulsion formulations and characterization with bacterial cellulose crystals (BCNCs) and bacterial cellulose fibers (BCNFs) in the presence of eugenol essential oil with different types of surfactants will be presented.

In the third part of this study; the investigation of the feasibility of electrospun PLA composite fibers with eugenol encapsulated BCNCs emulsion formulations with PLA polymer solution via the electrospinning technique and characterization of produced films and fibers morphology will be presented. Moreover, observations regarding the antimicrobial efficiency of encapsulated eugenol vapor on artificially inoculated tomato stem scars as a food model will be provided.

In the fourth part of this study; the observations about the water vapor and temperature as an external stimulus to trigger the release profile study of eugenol from fabricated PLA films at the headspace, and to test the antifungal efficacy of PLA films

on the artificially *B.cinerea* contaminated table grapes without direct contact with the grapes will be provided.

In the present study, electrospun PLA fibers-grafted to PLA films were prepared by electrospinning, and these cellulose encapsulated eugenol electrospun fiber mats were used as a carrier for eugenol for delivering the eugenol vapor to the headspace of the food package.

The objective of this Ph.D. research is to test the feasibility of delivering encapsulated eugenol gaseous bioactive compounds with nanoscale/microscale formulations of BCNCs (Bacterial cellulose nanocrystals), as a carrier with PLA(poly-lactic-acid) nanofibers and to prove a novel concept of the delivery stem for volatile compounds. Table grapes and tomato stem scars were used as a food model for food packaging applications.

To achieve the objective, five hypotheses were proposed.

Hypothesis one; Bacterial cellulose crystals without losing their thermal stability and crystallinity could be produced from cellulose fibers under controlled acid hydrolysis conditions. To test this hypothesis hydrolysis conditions; low acid concentrations, short hydrolysis time and low cellulose acid ratios combining the post-treatment neutralization were used.

Hypothesis two; BCNFs or BCNCs could be formed oil-in-water Pickering emulsions with a combination of different surfactants. This surfactant can provide electrostatic, hydrophobic, and steric interactions with BCNFs and BCNCs to stabilize the cellulose to form the Pickering emulsions for the encapsulation of volatile eugenol essential oil. To test this hypothesis cetyltrimethylammonium bromide (CTAB), sodium dodecyl benzene sulfate (SDS), Tween 20, and lauric arginate (LA) were used for emulsion formulations.

Hypothesis three; Cellulose emulsions could be spun with PLA polymer to fabricate the antimicrobial electrospun fibers for food packaging applications. Active fibers/films could deliver the volatile eugenol vapors from the electrospun fibers to the headspace of the package. To test this hypothesis PLA, eugenol, LA and Pickering emulsions of BCNCs were used at spinning solution formulations to fabricate the beaded free active PLA-composite homogeneous films.

Hypothesis four; Water vapor and temperature could act as an external stimulus to trigger the release of eugenol vapor from the electrospun PLA/emulsions fibers-grafted to PLA films and vaporize into the headspace of the package in a controlled manner for

food packaging applications. To test this hypothesis electrospun PLA/emulsions fibers-grafted to PLA films with/without bacterial cellulose was used. To stimulate the fresh produce packaging conditions 4±1°C and 22±1 °C temperature and low (60±2 %RH) and high (87±2 % RH) relative humidity were used.

Hypothesis five; An appropriate amount of eugenol could be released from electrospun PLA/emulsions fibers-grafted to PLA films into the headspace of the package for inhibition/retarding of the growth of food spoilage m/o. To test this hypothesis, the efficacy of electrospun PLA/emulsions fibers-grafted to PLA films was tested on artificially *B.cinerea* contaminated table grapes and artificially *E. coli* K12 and *L. innocua* contaminated grape tomatoes stem scars without direct contact with table grapes and grape tomatoes.

CHAPTER 2

ACTIVE PACKAGING TECHNOLOGIES

2.1. Active Packaging

Conventional food packaging has a passive barrier in order to protect the food from the surrounding environment (Brody, Bugusu, Han, Sand, & McHugh, 2008). However, ‘’Active packaging is packaging in which subsidiary constituents have been deliberately included in or on either the packaging material or the package headspace to enhance the performance of the package system’’(Robertson, 2014). Active food packaging has many concepts such as antimicrobial and antioxidant, moisture, flavor absorber, carbon dioxide absorbers/emitters and oxygen scavengers (Brody, Bugusu, Han, Sand, & McHugh, 2008; Otoni, Espitia, Avena-Bustillos, & McHugh, 2016). Antimicrobial food packaging is the form of active packaging, which contains antimicrobial compounds to extend shelf life and increase the quality and safety of the packed food. Antimicrobial agents can release/migrate from the surface of food product in the package/food system or headspace, and the air gap between the package and absorb/diffuse onto the surface of food in the package/headspace/food systems (Ayala-Zavala, Del-Toro-Sánchez, Alvarez-Parrilla & Aguilar, 2008b; Quintavalla & Vicini, 2002). Intelligent or smart packaging is composed of smart devices to detect and monitor the changes in the product and the condition of the packaged product. There are smart devices including time temperature and ripeness indicators, radio-frequency identification systems, and sensors that are the decision-makers of the packaging system (Biji, Ravishankar, Mohan, & Srinivasa Gopal, 2015; Vanderroost, Ragaert, Devlieghere, & De Meulenaer, 2014).

2.2. Foodborne Illness Associated with Fresh Produce

According to the Center for Disease Control and Prevention (CDC) in the USA, each year approximately 48 million people suffered from foodborne illness and based on

the 2006 US population 31 pathogens caused illness estimated (CDC, 2016). *Salmonella* (tomatoes, sprouts, mangoes), *Escherichia coli* O157 (spinach and lettuce), and *Listeria* are the common food pathogens that caused the foodborne disease outbreaks. Bacterial outbreaks are associated with grains and beans 5 %, vegetables 20.7 %, and fruits and nuts 6.3 % (Painter et al., 2013). The main microbial infection can occur during pre and post-harvesting processing, storage, transporting, handling and food preparation. Fresh tomatoes may be contaminated with *Listeria*, (Beuchat & Brackett, 1991), *Salmonella Enteritidis* and *Escherichia coli* O157:H7 infections (Deza, Araujo, & Garrido, 2003). Volatile essential oils can be the alternative to chemical compounds for decreasing or preventing the foodborne illness associated with fresh produce. Dorman and Deans (2000) determined the antibacterial effect of the clove, oregano, thyme, black pepper, geranium and nutmeg volatile essential oil against 25 different bacteria including spoilage bacteria, and animal and plant pathogens. Numerous antimicrobial compounds and applications were proposed to prevent and decrease the microbial contamination of fresh tomatoes. Soylu, Soylu, and Kurt (2006) reported the thyme and oregano oil vapor antimicrobial effect against tomato blight disease Phytophthora infestans.

In another study, the vapor phase of cinnamaldehyde, allyl isothiocyanate and carvacrol to decrease the microbial contamination of *Salmonella* and *Escherichia coli* O157:H7 on the whole and sliced tomatoes were used (Obaidat & Frank, 2009). Volatile antimicrobials showed not only antibacterial activity but also antifungal activity one of which is hexanal. Hexanal vapor decreased the *Botrytis cinerea* infection on the tomatoes (Utto, Mawson, & Bronlund, 2008). In their study, Jin and Gurtler (2012) investigated the inactivation effect of edible chitosan and organic acids coatings on four *Salmonella* strain contaminated tomatoes stem scar. Other techniques such as package ozonation were used to decreasing the microbial populations of *Listeria innocua*, *Escherichia coli* O157:H7 and *Salmonella Typhimurium* on the surface and stem scar of the fresh tomatoes (Fan, Sokarai, Engemann, Gurtler, & Liu, 2012).

Botrytis cinerea, gray mold, is the important omnipresent pathogen that can cause food loss in many fruits and vegetables such as strawberry, tomatoes and table grapes, which results in economical losses in pre and post-harvesting process (Parafati, Vitale, Restuccia, & Cirvilleri, 2015; Vu, Hollingsworth, Leroux, Salmieri, & Lacroix, 2011). Sulfur dioxide (SO_2), a commercially available chemical compound, is generally used for reducing the gray mold. However, due to the hazardous human health effect of SO_2, researchers aim to develop a new biofumigants with the aim of controlling the gray mold

disease on table grapes. Cinnamon leaf oil vapor (Melgarejo-flores et al., 2013), eugenol, thymol and carvacrol vapor mixture (Guillén et al., 2007), thymol and linalool (Guillén et al., 2007), eugenol and thymol vapor (Valero et al., 2006), and eugenol, menthol and thymol (Valverde et al., 2005) were used as biofumigants for controlling the post-harvest decay of table grapes and improve the food safety.

2.3. Food Loss and Waste Associated with Fresh Produce

The main problem for the food industry is the keeping the quality and safety of fresh produce. According to the Food Agriculture Organisation (FAO) of the United Nations 1.3 billion tons of food is lost and wasted every year in the whole world (FAO, 2011). In the economical point of food loss and waste is relative US$ 990 billion in industrialized and developing countries. Fruits, vegetables, and root crops are the wasted foods in high amount among the others roughly 40-50% per year (FAO, 2017)

2.4. Cellulose

Cellulose $(C_6H_{10}O_5)_n$ is the abundant plant-derived biodegradable polymer on the earth. Not only the plants, but also some bacteria species, algae, fungi, and animals can produce cellulose (George, 2015).

Acetobacter xylinum, the former name is *Glucanacetobacter xylinus* bacterium, has been used as a model microorganism for producing the extracellular bacterial source cellulose (Chawla, Bajaj, Survase, & Singhal, 2009). *Acetobacter xylinum* is a Gram-negative, obligate aerobic bacterium which was first reported in 1886 by A.J Brown (Chawla et al., 2009; Rangaswamy, Vanitha, & Hungund, 2015). Gram-negative species including *Agrobacterium, Azotobacter, Aerobacter, Pseudomonas, Salmonella,* and *Sarcina* are the other reported examples of cellulose produced bacteria. The biosynthesis of cellulose from bacteria has two steps. First, β-1,4 glucan chain with the polymerization of glucose units is produced, and in the second step, self-assembly of the produced fibrils for crystallization of cellulose is observed. Nata de coco is the commercially available jelly-like product of bacterial cellulose, and it is used as a snack in the Philippines. (Chawla et al., 2009).

The unique properties of BC including high surface to the volume ratio, high crystallinity and low density make it a promising material for many applications such as a reinforcing agent in the packaging of nanocomposites and stabilisation of oil/water interface for Pickering emulsion formulations and pH sensors (George, Ramana, Bawa, & Siddaramaiah, 2011; George & Sabapathi, 2015; Kalashnikova et al., 2013).

Cellulosic sources are bacterial cellulose, cotton, sisal, ramie, flax, tunicates, hemp, microcrystalline cellulose and tunicates (Habibi, 2014). Cellulose fibers are composed of crystalline and amorphous regions. Cellulose crystals can be obtained by chemical and enzymatic hydrolysis via degrading the amorphous disorder regions and leave the crystalline regions (Lisias Pereira Novo, Bras, Garcia, Belgacem, & Curvelo, 2016). Strong acids such as hydrochloric, sulfuric and phosphoric acids can easily hydrolyze the amorphous regions of cellulose and leave the crystalline regions (Sadeghifar, Filpponen, Clarke, Brougham, & Argyropoulos, 2011).

Cellulose source, nature of acid, acid concentration, acid to pulp ratio, reaction time and temperature can affect the structure and properties of produced crystals to make it more compatible with systems needs. The final product can have differences in dimensions, surface charge, crystallinity, thermal stability and yield of the produced cellulose crystals (Habibi et al., 2010). For example, sulfuric acid and phosphoric acid introduce the negatively charged groups at the surface of crystals. The hydrolyzed crystals of phosphoric and sulfuric acids with the negatively charged groups are produced electrostatically stabilized suspensions (Eyley & Thielemans, 2014). Chemical modification methods including non-covalent surface modifications, sulfonation, TEMPO-mediated oxidation, esterification, etherification, silylation, urethanization, amidation, click chemistry and polymer grafting have been used for changing the hydrophilic-hydrophobic properties of cellulose to make it more compatible with different applications (Habibi, 2014).

Cellulose has a potential application in many areas in industrial and biomedical applications. It can be used as a drug carrier; it can also be used in medical implants, wound healing, cornea replacement, cardiovascular surgery and tissue engineering (Jorfi & Foster, 2015). Bacterial cellulose has been used as a gel stabilizing, thickening and emulsifying agents, and it has also been used to produce low calorie and low cholesterol products in the food industry (Shi, Zhang, Phillips, & Yang, 2014).

.

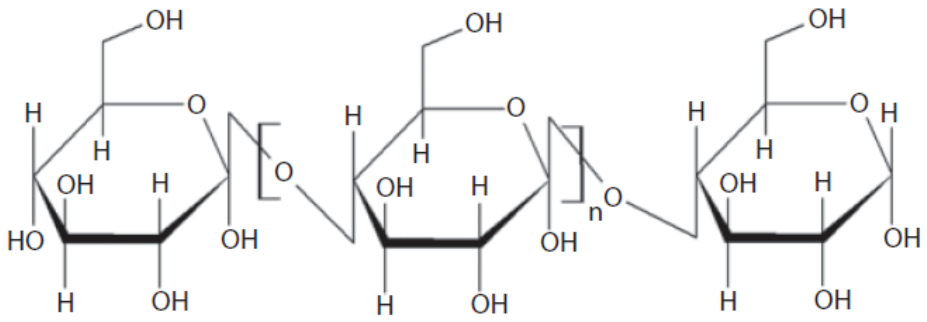

Figure 2.1. Structure of Cellulose

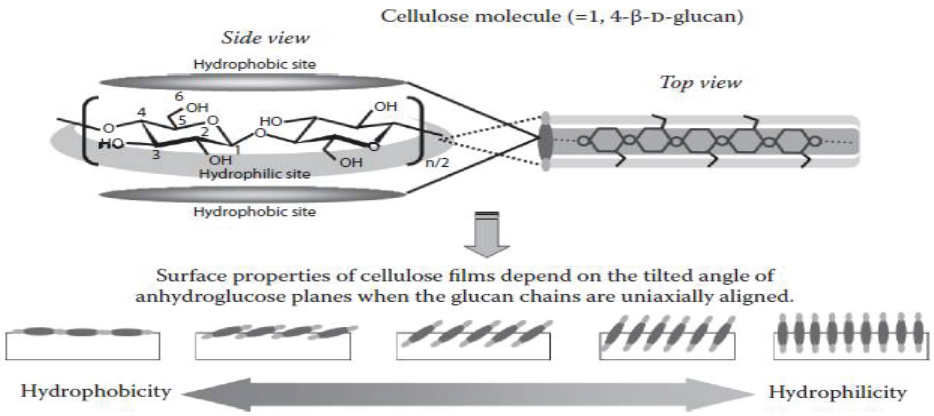

Figure 2.2. Structure of bacterial cellulose
(Source: Gama, Gatenholm, Klemm, & Al, 2012)

2.5. Pickering Emulsions Systems

Emulsion systems are composed of two immiscible liquids such as oil and water. Emulsions can be either oil-in-water (O/W) or water-in-oil (W/O) according to the distribution of the aqueous and oil phase (McClements, 2005). The stabilization of emulsions with colloidal particles was first described by Ramsden (Ramsden, 1903) and Pickering (Pickering, 1907). Pickering emulsions are the type of emulsions that are stabilized by a solid particle in the presence and absence of surfactants. Pickering emulsions can be formed as oil-in-water (O/W) (Kalashnikova, Bizot, Cathala, & Capron, 2011), water-in-oil (W/O) (Lee, Blaker, Heng, Murakami, & Bismarck, 2014b) and water-in-water (W/W) emulsions (Peddireddy, Nicolai, Benyahia, & Capron, 2016). Particle stabilized emulsion type depends on the particle wetting properties and the adsorption of the particle at the oil-water interface. Solid particles that have contact angle

(θ)> 90 forms water-in-oil emulsions and contact angle (θ)< 90 forms the oil-in-water Pickering emulsions (Lee et al., 2014b; Scarlett, Morgan, & Hildebrand, 1926).

Organic and inorganic particles have been reported for Pickering emulsions including, clays, carbon nanotubes (Chevalier & Bolzinger, 2013), starch nanoparticles (Haaj, Magnin, & Boufi, 2014), soy protein nanoparticles (Liu & Tang, 2013), silica particles (Liu, Jiang, Cui, & Binks, 2017) chitosan particles (Ho et al., 2016) and cellulose and cellulose derivatives (Lee et al., 2014b). Cellulose types used in the formulations of Pickering emulsions for encapsulation were given in Table 2.1.

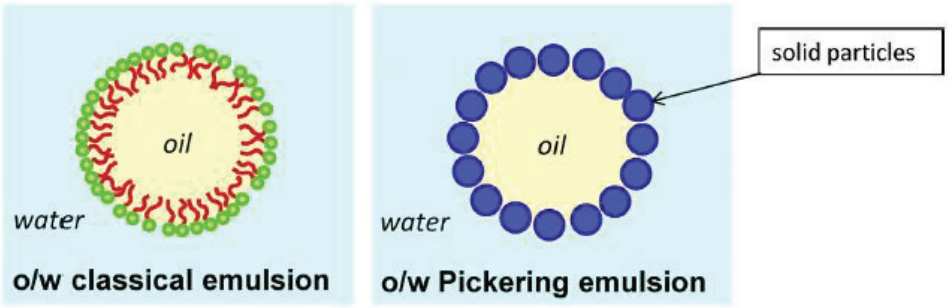

Figure 2.3. Pickering emulsions
(Source: Chevalier & Bolzinger, 2013)

Table 2.1. Cellulose types used in the formulations of Pickering emulsions for encapsulation

Cellulose Type	Emulsion Type	References
Rice straw/Halocellulose nanocrystals	O/W Pickering emulsion	(Jiang & Hsieh, 2015)
Wood cellulose nanocrystals	Pickering Emulsions(O/W)	(Gong, Wang, & Chen, 2017a)
Cotton cellulose nanocrystals/Nanofibers	Pickering Emulsions(O/W)	(Gestranius, Stenius, Kontturi, Sjöblom, & Tammelin, 2017a)
Cotton cellulose nanocrystals	Water-in-water Emulsions(W/W)	(Peddireddy et al., 2016)
Cotton liners cellulose	Pickering Emulsions(O/W)	(Cherhal, Cousin, & Capron, 2016)
Birch Pulp Cellulose Crystals	Oil-in-water Emulsions	(Ojala, Sirviö, & Liimatainen, 2016)
Bacterial cellulose fibers	Oil-in-water Emulsions	(Paximada, Tsouko, Kopsahelis, Koutinas, & Mandala, 2016)
Green algae crystals		
Avicel cellulose nanocrystals/ microfabricated cellulose	Oil-in-water Emulsions	(Mikulcova, Bordes, Kasparkova, & Vera, 2016)
Asparagus cellulose nanocrystals	Pickering Emulsions(O/W)	(Wang et al., 2016)
Cotton cellulose	Pickering Emulsions(O/W)	(Hu, Ballinger, Pelton, & Cranston, 2015)
sisal fibers nanowhiskers	Pickering Emulsions	(Liu et al., 2015)
Bacterial cellulose fibers	Pickering Emulsions(O/W)	(Fu et al., 2015a)
Softwood fibers	Multiple emulsions(W/O/W)	(Carrillo, Nypelö, & Rojas, 2015)
Cotton/Wood cellulose	Double Emulsions(O/W/O)	(Cunha, Mougel, Cathala, Berglund, & Capron, 2014)
Corncob cellulose	Pickering Emulsions	(Wen, Yuan, Liang, & Vriesekoop, 2014)
Bacterial cellulose fibers from nata de coco	Pickering Emulsions(W/O)	(Lee et al., 2014b)
Bacterial cellulose nanofibers	High internal phase emulsions(w/O)	(Lee, Blaker, Murakami, Heng, & Bismarck, 2014a)
Bacterial cellulose/Cotton	Pickering Emulsions(O/W)	(Kalashnikova et al., 2013)
Cotton cellulose	High internal phase emulsions(O/W)	(Capron, 2013)
Bacterial cellulose crystals/Cotton cellulose	Pickering Emulsions(O/W)	(Kalashnikova, 2012)
Ramie fibers	Pickering Emulsions(O/W)	(Zoppe, Venditti, & Rojas, 2012)
Bacterial cellulose crystals	Pickering Emulsions(O/W)	(Kalashnikova et al., 2011)
Softwood microfibrilated cellulose	Oil-in-water Emulsions	(Xhanari, Syverud, & Stenius, 2011a)
Spruce microfibrilated cellulose	Oil-in-water Emulsions	(Andresen & Stenius, 2007)

2.6. Eugenol Essential Oil and Encapsulation of Eugenol

The challenge with using essential oil in practical applications is that essential oils are highly volatile compounds, and they are sensitive to environmental factors (moisture, heat, oxygen, and light) (Turek & Stintzing, 2013). If they are not stored at ideal conditions, they could lose their volatility and bioavailability. The encapsulation of hydrophobic bioactive agents via emulsion based delivering systems may increase the physical stability and enhance the bioactivity of the bioactive compounds (Bilia, Ravishankar, Mohan & Gopal, 2014). In the last decade, considerable efforts have been made on the encapsulation of essential oils. Oil-in-water emulsions of clove oil were formed with sodium dodecyl sulphate (SDS) (Purwanti, Neves, Uemura, Nakajima, & Kobayashi, 2015), clove oil nanoemulsions were formulated in the presence of canola oil and gum ultra (Majeed et al., 2016), eugenol nanoemulsions were prepared with whey protein isolate (Bejrapha, Choi, Surassmo, Chun, & Min, 2011), thyme, and lemongrass, and sage nanoemulsions were formulated with sodium alginate and Tween 80 (Acevedo-Fani, Salvia-Trujillo, Rojas-Graü, & Martín-Belloso, 2015), cinnamaldehyde oil-in-water emulsions were obtained with cinnamaldehyde and Tween 80 (Otoni et al., 2017) are the examples of emulsion sytems.

Eugenol (2-methoxy-4-allylphenol) is the major component of clove oil (Farag, Daw, Hewedi, & El-Baroty, 1989; Jirovetz et al., 2006). Eugenol has antimicrobial activity against a wide range of microorganisms that are of concern for food safety including *Salmonella typhi* (Devi, Nisha, Sakthivel, & Pandian, 2010), *Staphylococcus aureus*, *Escherichia coli*, *Pseudomonas aeruginosa* (Walsh et al., 2003), and antioxidant activity (Jirovetz et al., 2006), and has antifungal activity against *Botrytis cinerea* (El-Shiekh, Nour El-Din, Mohamed, & Karam EL-Din, 2012; Wang, Zhang, Chen, Fan, & Shi, 2010). Due to the highly volatile and low chemical stability nature of eugenol, it is sensitive to environmental factors. The encapsulation of eugenol may enhance its stability and bioavailability. Eugenol is encapsulated with β-cyclodextrin (Gong et al., 2016; Hill, Gomes, & Taylor, 2013; Seo, Min, & Choi, 2010) and 2-hydroxypropyl- β-cyclodextrin and 2-hydroxypropyl-β-cyclodextrin via molecular inclusion complex and with polycaprolactone by emulsion diffusion system in order to protect eugenol from light oxidation during storage (Choi, Soottitantawat, Nuchuchua, Min, & Ruktanonchai, 2009). And other encapsulations systems that are used for eugenol encapsulations,

include in solid lipid carriers (Cortés-Rojas, Souza, & Oliveira, 2014), in lecithin nanoliposomes (Valencia-Sullca et al., 2016), gelatin-sodium alginate complex coacervation method (Shinde & Nagarsenker, 2011), chitosan nanoparticles (Woranuch & Yoksan, 2013a) and the encapsulation of eugenol in the surfactant micelles (sulfonyl 485W) (Gaysinsky, Davidson, Bruce, & Weiss, 2005).

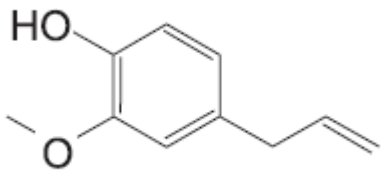

Figure 2.4. Chemical structure of eugenol
(Source: Burt, 2004)

2.7. Surfactants

Surfactants, surface active agents, are amphiphilic molecules that contain hydrophobic and hydrophilic head group. Surfactants lower the interfacial free energy of either immiscible two fluids or solid liquid interface. According to the surfactants chemical structure, surfactants are classified into three groups, anionic, cationic and nonionic (Kumar, Bhattacharjee, Kulkarni, & Kumar, 2015). Lauric arginate (LA), cetyltrimethylammonium bromide (CTAB) and didecyl dimethyl ammonium bromide (DMAB) are the cationic surfactants, sodium dodecyl sulfate (SDS) is anionic, and Tween 80, Tween 20 and span 80 are the examples of nonionic surfactants.

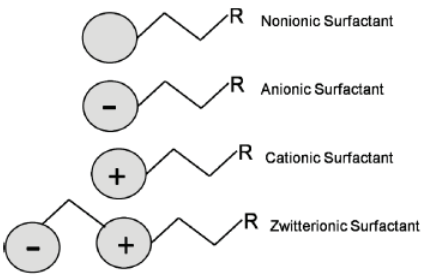

Figure 2.5. Class of surfactants
(Source: Kumar et al., 2015)

The hydrophile-lipophile balance (HLB) value of surfactant was used to decide the surfactant type in either oil-in-water (O/W) or water-in-oil (W/O) emulsion formulations. In W/O emulsions, the surfactant HLB value between 3-7 and in O/W emulsion formulations HLB value 9-15 is generally used (Chevalier & Bolzinger, 2013).

Lauric arginate (LA, N-lauroyl-L-arginine ethyl ester monohydrochloride) is a food grade cationic surfactant. LA is derived from L-arginine, lauric acid, and ethanol. It has a wide range of antimicrobial activity against bacteria, yeast, and mold (Nair, Nannapaneni, Kiess, Mahmoud, & Sharma, 2014). LA was approved by Food and Drug Administration of United states in (FDA, 2005) as generally recognized as safe (GRAS).

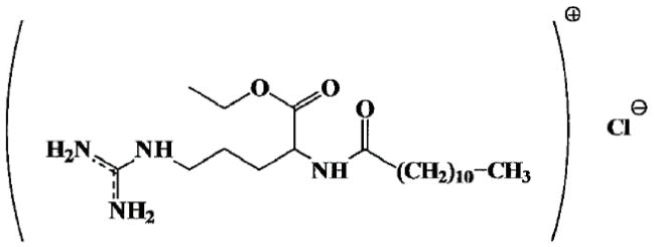

Figure 2.6. Molecular structure of lauric arginate
(Source: Asker, Weiss, & McClements, 2011)

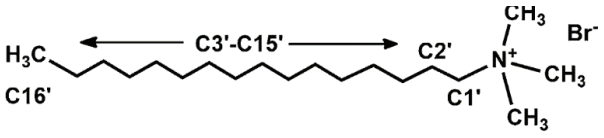

Figure 2.7. Molecular structure of cetyltrimethylammonium bromide
(Source: Baruah et al., 2014)

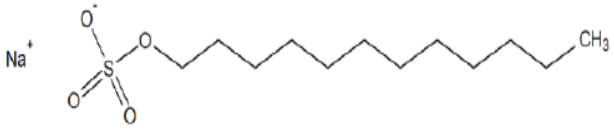

Figure 2.8. Molecular structure of sodium dodecyl sulfate
(Source: Livingstone, Nagata, Bonn, & Backus, 2015)

2.8. Electrospinning Process

Electrospinning is a single one-step process for fabricating the nano and macroscale fibers from natural and synthetic polymers. Electrospinning is not a new technique Rayley was first observed it in 1987, and later, Zeleny studied the main mechanism in 1914 on the electrospraying process. A simple electrospinning set up includes a syringe pump that control solution flow rate, the high voltage supply for producing the voltage, collector (ground metal plate, rotating drums), syringe and solution with a solvent (Burger, Hsiao, & Chu, 2006). Electrospinning applies a high voltage to the solution, evaporates the solvent and results in leaving the fibers (Sousa et al., 2015). In the electrospinning process, many parameters such as polymer concentration, viscosity, electrical conductivity and surface tension of the spinning solution, applied voltage, flow rate, the distance between the needle and collector can affect fabricated fiber morphology (Burger, Hsiao, & Chu, 2006; Neo, Ray, Easteal, Nikolaidis, & Quek, 2012; Okutan, Terzi, & Altay, 2014). Scanning electron microscopy, transmission electron microscopy, and atomic force microscopy can be used for the morphological characterization of the produced fibers. Moreover, Fourier transforms infrared, differential scanning calorimetry and X-ray diffraction methods can be used for the chemical characterization of the produced fibers (Okutan, Terzi, & Altay, 2014). The disadvantage of electrospinning is low production rate, and it is still newly born in the industrial scale applications. Electrospinning has a potential to be used in many areas in near future such as textile industry, filtration, wound dressing, tissue dressing (Mirjalili & Zohoori, 2016), biomedical applications (Agarwal, Wendorff, & Greiner, 2008) and food packaging (Bhushani & Anandharamakrishnan, 2014) as reported in detail in reviews.

The main structural advantage of the electrospinning process is that fibers have sub-micron and nano-size, high surface to the volume ratio and fibrous structure (Kriegel, Kit, Mcclements, & Weiss, 2009). The functional advantages of electrospun fibers are that they have high loading of the encapsulation of the active agent, they are appropriate for thermolabile active agents, they sustain and control the release, maintain the stability of bioactive compounds (Bhushani & Anandharamakrishnan, 2014; Kriegel, Arrechi, Kit, McClements, & Weiss, 2008).

Production of multifunctional electrospun fibers for food packaging applications is feasible. Emulsion spinning is one of the mostly used techniques for enhancing the bioavailability of encapsulated bioactive compounds (Agarwal & Greiner, 2011). Several research studies have been conducted in recent years with polymer emulsion spinning such as (R)-(+)-limonene in poly(vinyl alcohol) (Camerlo, Vebert-Nardin, Rossi, & Popa, 2013), surfactant based emulsion with eugenol in poly(vinyl alcohol) (Kriegel, Kit, McClements, & Weiss, 2009) and lysozyme encapsulated poly(DL-lactide) fibers (Yang, Li, Qi, Zhou, & Weng, 2008). Most recently, the electrospinning method has been used for volatile bioactive compounds encapsulation via nanofibers and with a combination of a different carrier to deliver bioactive compounds to increase the stability, bioavailability and release of active compounds in controlled manner. Recent studies with electrospinning method are presented in Table 2.2.

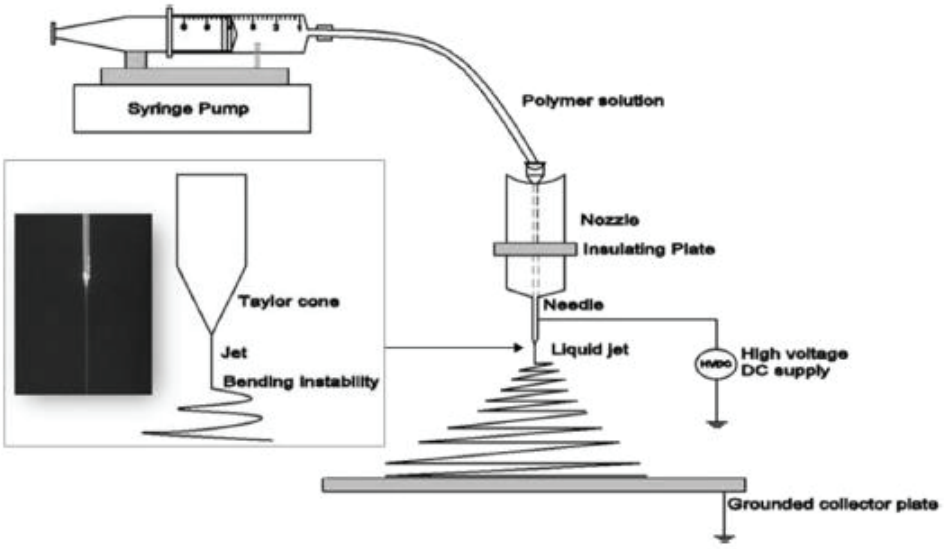

Figure. 2.9. Basic laboratory scale electrospinning setup
(Source: Bhushani & Anandharamakrishnan, 2014)

Table 2.2. Volatile essential oil in electrospinning process

Polymer	Essential oil	References
Polyethylene oxide	Eugenol/SiO2-eugenol liposome	(Cui, Yuan, Li, & Lin, 2017)
Polyvinyl alcohol	β-cyclodextrin/cinnamon EO/lysozyme	(Feng et al., 2017)
Cellulose acetate	Rosemary and oregano essential oil	(Liakos, Holban, Carzino, Lauciello, & Grumezescu, 2017)
Zein prolamine	Orange essential oil	(Yao et al., 2017)
Poly(lactic acid)	Cinnamon/ β-cyclodextrin complex	(Wen et al., 2016)
Poly(lactic acid)	Allyl isothiocyanate	(Kara et al., 2016)
Pullulan	Periladehayde/β-cyclodextrin complex	(Mascheroni et al., 2013)
Chitosan/poly(ethylene oxide)	Cinnamaldehayde	(Rieger & Schiffman, 2014)
Polyvinyl alcohol	Allyl isothiocyanate/β-cyclodextrin complex	(Aytac, Ipek, Durgun, Tekinay, & Uyar, 2017)
Polyvinyl alcohol	Eugenol/Cyclodextrin inclusion complex	(Kayaci, Ertas, & Uyar, 2013)
Polyvinyl alcohol	Limonene	(Camerlo et al., 2013)
Polyvinyl alcohol	Eugenol/emulsion based systems	(Kriegelet al., 2009)
Soy protein/poly(lactic acid)	Allyl isothiocyanate	(Vega-Lugo & Lim, 2009)

2.9. Poly(lactic acid) and Electrospinning of Poly(lactic acid)

Poly(lactic acid) (PLA) is an aliphatic biobased polymer derived from L(+) and D(-) isomers of lactic acid (2-hydroxyl propionic acid) and can be produced from carbohydrate fermentation or chemical synthesis from corn. Physical properties of PLA are associated with the amount of the isomers in the structure poly(D-lactide), poly(L-lactide) and L-or D- lactide. According to the amount of the isomer, it can have either crystalline, amorphous or semi-crystalline polylactide (Auras et al., 2004; Avinc & Khoddami, 2009). PLA has film forming ability, and such as blow, and injection molding, extrusion, casting, and electrospinning are the film forming processing for PLA.

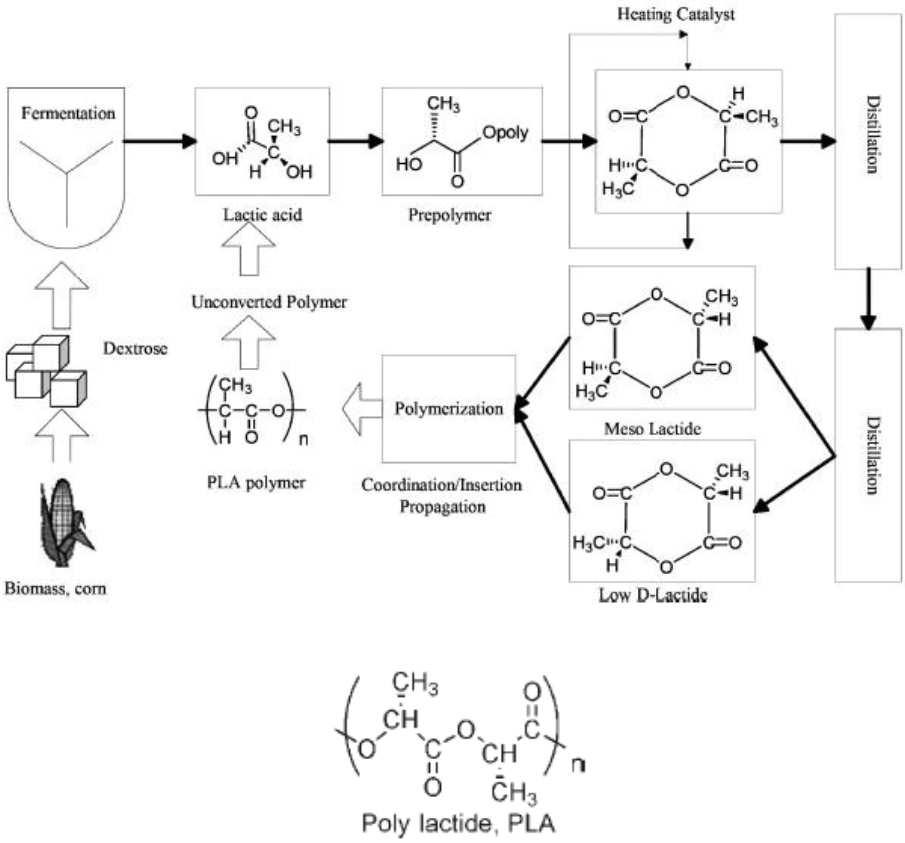

Figure 2.10. Production process and constitutional units of PLA
(Source: Auras et al., 2004)

Poly(lactic acid) is safe in food packaging applications, and PLA has been approved as generally recognized as safe (GRAS) by the United States Food and Drug Administration (FDA) (FDA, 2002). NatureWorks LLC is the manufacturer of PLA and

company use Ingeo™ for producing the food packaging materials such as yogurt, coffee and strawberries.

Polymer type and concentration, solvent type, applied voltage, feed rate, the distance between the collector and needle are the main factors influencing the fiber formation. Chloroform, acetonitrile, dichloroacetic acid, 1,1,2-trichloroethane, methylene chloride and dichloromethane are widely used solvents for PLA, and also acetone and tetrahydrofuran can partly dissolve the PLA. The solvent is the most important parameter on the fiber formation during the electrospinning processing (Casasola, Thomas, Trybala, & Georgiadou, 2014).

Recently, PLA fibers have been used in many delivering systems to produce antimicrobial fibers including triclosan cyclodextrin inclusion (Kayaci, Umu, Tekinay, & Uyar, 2013), antioxidant fibers silver-NP vitamin E (α-tocopherol) (Munteanu, Aytac, Pricope, Uyar, & Vasile, 2014), allyl isothiocyanate (Kara et al., 2016), and silica nanoparticles-eugenol liposome loaded nanofibers (Cui et al., 2017).

2.10. Control Release Packaging for Headspace Applications

"Controlled release packaging (CRP) is defined as a new generation of packaging materials that can release active compounds such as antimicrobials and antioxidants at desirable rates to extend the shelf life of a wide variety of foods " (Yam & Lee, 2012). In controlled release systems, the aim is to create a slow release of active compound in a controlled manner. The release of active compounds from the packaging materials depends on the several factors as can be seen in a conceptual framework that developed by Yam and Lee, 2012 (Figure 2.11).

The active compound release can be controlled in packaging either by direct contact systems or indirect contact systems (Figure 2.12). Indirect contact systems allow the release of aroma, flavoring and volatile compounds to the headspace between the solid food and the package. The indirect contact systems contain three steps: the diffusion of volatile compound from the packaging material to inside the packaging, the desorption of a volatile compound to the interface of food and package, lastly, the adsorption ability of the volatile compound into the food surface (LaCoste, Schaich, Zumbrunnen, & Yam, 2005).

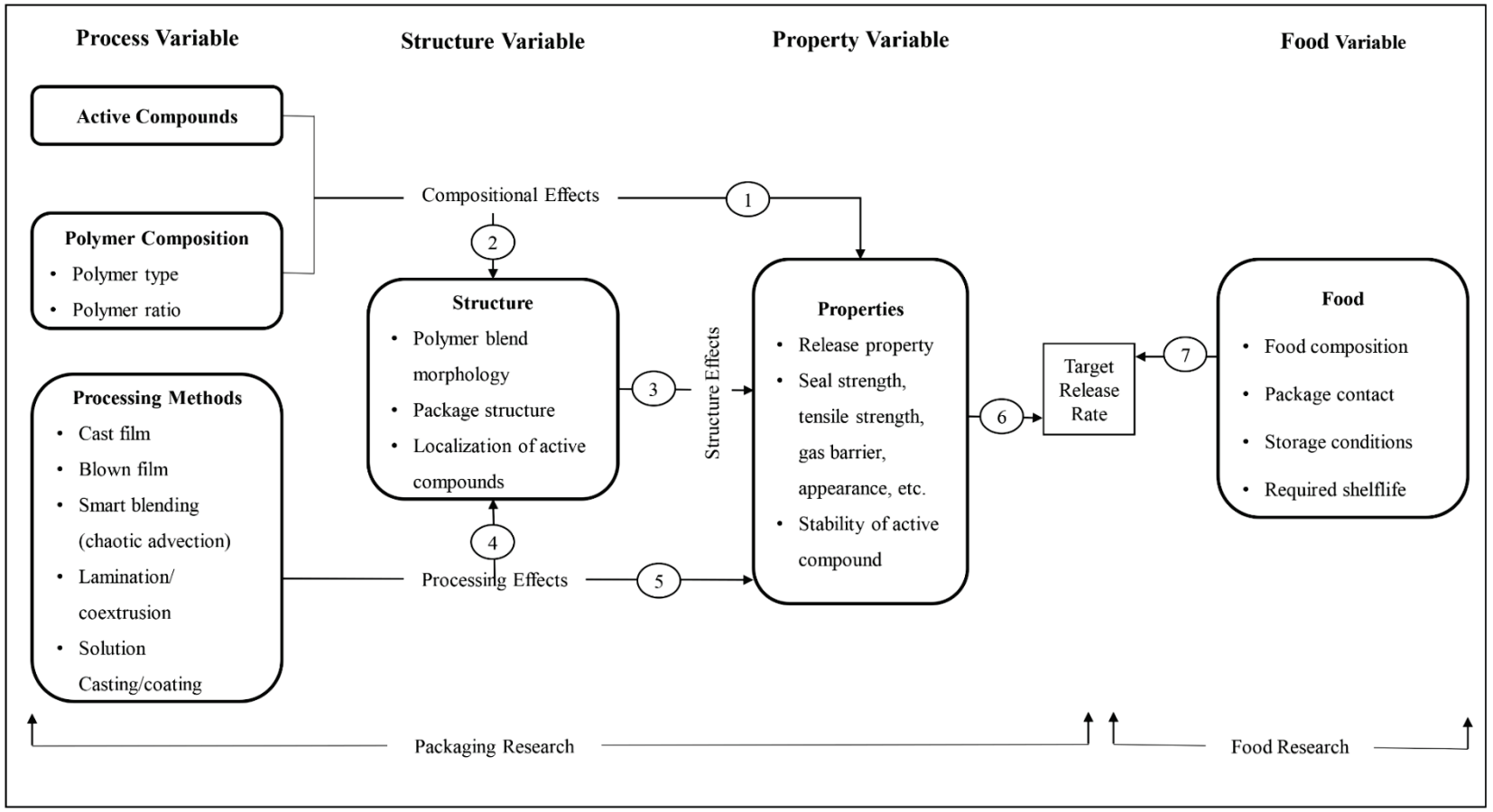

Figure 2.11. Conceptual framework of controlled release packaging
(Source: Adapted from Yam & Lee, 2012)

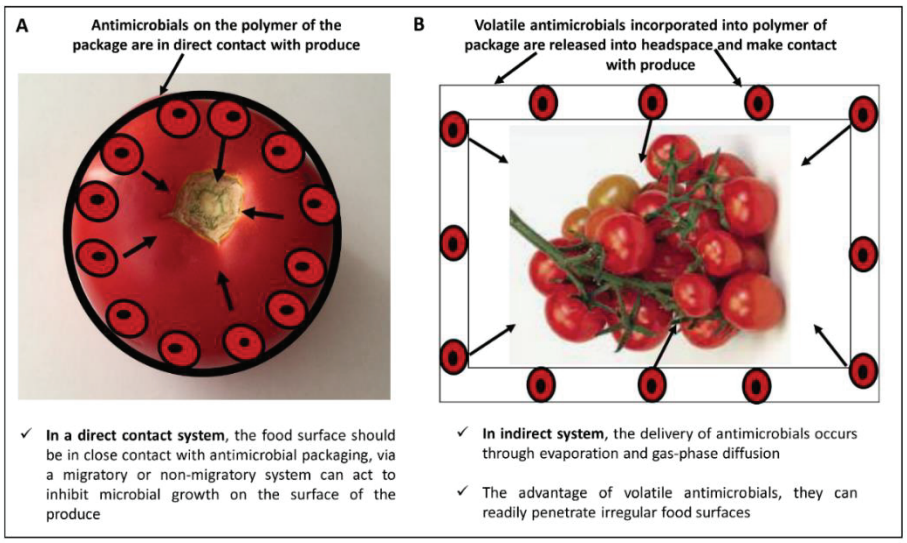

Figure 2.12. Antimicrobial packaging systems for fresh produce a) direct contact b) indirect contact (Source: Adapted from, Yam & Lee, 2012)

The advantage of the electrospun fibers compared to the solution cast film is that electrospun fibers have a porous structure, a high surface area, and high loading efficiency (Fang, Wang, & Lin, 2011; Xie & Hsieh, 2003). Another advantage is to be able to increase stability, bioavailability and the release of active compounds in a controlled manner via nanofibers to deliver bioactive compounds. Many researchers also investigate the release of encapsulated active agents from the electrospun fibers. Soy protein and poly(lactic acid) spun with an ally isothiocyanate (AITC) volatile compound used to test the controlled release of active compound from the fibers under different relative humidity (Vega-Lugo & Lim, 2009). In another study, poly(lactic acid) spun with ally isothiocyanate to test the controlled release of ally isothiocyanate from the fibers at different temperatures has been investigated (Kara et al., 2016). The controlled release of perillaldehyde from perillaldehyde-cyclodextrin pullulan fibers was triggered by relative humidity (Mascheroni, Guillard, Gastaldi, Gontard, & Chalier, 2011). Different carriers such as metal-organic frameworks, different natural and synthetic polymers and different cyclodextrins inclusion complexes have been used to control the release of active compounds. Metal-organic frameworks were used for the encapsulation of volatile ally isothiocyanate, and the release of AITC is triggered by different temperature and humidity (Lashkari, Wang, Liu, Li, & Yam, 2017). Control release of volatile hexanal from various cyclodextrins inclusions complexes (Almenar, Auras, Rubino, & Harte,

2007) and thymol release from zein films (Del Nobile, Conte, Incoronato, & Panza, 2008) are the examples of the volatile compounds release systems.

CHAPTER 3

PRODUCTION AND CHARACTERIZATION OF CELLULOSE NANOCRYSTALS

3.1. Introduction

Cellulose is the most abundant organic renewable and biodegradable polymer in nature. It has potential applications specifically in many areas in industrial and biomedical applications (Duran, Lemes, Duran, Freer, & Baeza, 2011) such as, drug delivery, wound healing, tissue engineering (Jorfi & Foster, 2015), nanocomposite films (Peng, Dhar, Liu, & Tam, 2011) and food industry (Shi et al., 2014). The main source of cellulose is plant cells, and a wide variety of living species, including bacteria, algae, and fungi and some animals like tunicates are capable of producing cellulose (Amano, Ito, & Kanda, 2005; Chawla et al., 2009). *Acetobacter* strains such as *Glucanacetobacter xylinus* have been used as model microorganism to produce the cellulose (BC) extracellularly; this bacterium produced biomaterial which is called bacterial cellulose (Cheng, Catchmark, & Demirci, 2009; Gu & Catchmark, 2012). *Acetobacter xylinum* is a Gram-negative, obligate aerobic bacterium which is found in vinegar, fruits, and vegetables (Rangaswamy et al., 2015). Bacterial cellulose has the similar chemical structure as plant cellulose, however, compared to plant cellulose; it is highly pure without hemicellulose, lignin, and pectin (Chawla et al., 2009; Gu & Catchmark, 2012). BC has gained the rapid interest of among researchers due to its unique properties such as having high surface area, high crystallinity, high tensile strength, high water holding capacity, and low density (George & Sabapathi, 2015). Cellulose nanofibers (CNF) and cellulose nanocrystals (CNC) are the main types of cellulose (Klemm et al., 2011). Nanofibers, nanowhiskers, nanoparticles, microcrystallites, are the different terminology used for nanocrystals, but the term cellulose nanocrystals (CNCs) is the widely-used term in the scientific literature (George & Sabapathi, 2015).

Cellulose nanocrystals have been prepared from various natural resources including bacterial cellulose (Martínez-Sanz, Olsson, Lopez-Rubio, & Lagaron, 2011a), microcrystalline cellulose (Novo, Bras, García, Belgacem, & Curvelo, 2015), natural

fibers (macrophyte typha doming enosis) (César, Pereira-da-Silva, Botaro, & de Menezes, 2015), pine wood and corncob fibers (Ditzel, Prestes, Carvalho, Demiate, & Pinheiro, 2016), sugar plam fibers (Fahma, Hori, Iwamoto, Iwata, & Takemura, 2016), garlic straw residue (Kallel et al., 2016), cotton, avicel, and tunicates (Elazzouzi-hafraoui et al., 2008).

The main modification processes for the production of cellulose nanocrystals are chemical and enzymatic hydrolysis (George, Ramana, Bawa, & Siddaramaiah, 2011). TEMPO (Saito, Kimura, Nishiyama, & Isogai, 2007), subcritical water (Novo et al., 2015), and quaternary ammonium salts (Salajková, Brglund & Zhou, 2012) have also been used as alternative methods for isolation of the cellulose nanocrystals. Strong acid hydrolysis can break the cellulose chains leading to cellulose degradation. Acids can easily hydrolyze the amorphous regions of cellulose; however, due to the high acid resistance, it is hard to hydrolyze the crystalline regions (Sadeghifar et al., 2011).

Sulfuric acid (Araki, Wada, Kuga, & Okano, 1998), hydrochloric acid (Rusli, Shanmuganathan, Rowan, Weder, & Eichhorn, 2011) or a combination of sulfuric and hydrochloric acids (Araki, Wada, Kuga, & Okano, 1999) have been extensively used for extraction of the cellulose crystals, and also phosphoric acid (Camarero Espinosa, Kuhnt, Foster, & Weder, 2013) and hydrobromic acid (Sadeghifar et al., 2011) are preferred for extraction. Cellulose source, hydrolysis conditions such as acid type and concentration, acid to pulp ratio, reaction time and temperature and pre-post treatment can affect the crystals dimensions, surface charge, crystallinity, thermal stability and yield of the produced cellulose crystals (Habibi et al., 2010;Reid, Villalobos, & Cranston, 2016).

Cellulose fibers, when subjected to sulfuric acid, provide the negatively charged surface sulfate ester groups ($-OSO_3^-$) on the surface of nanocrystals. These charged groups permitted the homogeneous dispersion of crystals in aqueous suspension and formed the stable colloidal suspensions. In contrast, hydrochloric acid hydrolyzed cellulose fibers yield the low surface charge crystals or no surface charge compared to sulfuric acid treated-fibers and this led to less stable aqueous suspension due to aggregation of crystals (Araki et al., 1998; Araki, Wada, Kuga, & Okano, 2000; De Souza Lima & Borsali, 2004; Beck-candanedo, Roman, & Gray, 2005).

Type of acid, cellulose source, extraction conditions and post treatments affect the thermal stability of crystals. Sulfuric acid treated fibers have negatively charged sulfate ester groups, which diminished the thermal stability of crystals. Increasing acid concentration, extraction time and cellulose acid ratio increased the sulfate ester groups

and decreased the decomposition temperature (Roman & Winter, 2004). Thermal stability can be improved by post-treatment including desulfation and neutralization with alkaline solutions (Wang, Ding, & Cheng, 2007; Martínez-Sanz et al., 2011a). Thermal stability is an important key factor during the thermoplastics processing of polymers. 200 °C and above temperature requirement is needed for thermoplastic composites (Glasser, Taib, Jain, & Kander, 1999). Cellulose thermal decomposition is around 300°C, and it is enough for thermal processing of composites (Rantuch & Chrebet, 2014).

Up to date, some research efforts have been conducted to obtain bacterial cellulose crystals with the high thermal stability and crystallinity (Martínez-Sanz et al., 2011a; Vasconcelos et al., 2017). Whereas researchers have been observed that cellulose produced from the same source with different extraction conditions did not have same properties and behaviors. Present study hypothesizes that cellulose crystals without losing their thermal stability and crystallinity could be produced from cellulose fibers by proposed acid hydrolysis conditions for both acid type hydrolysis. X-ray, TGA, DTA and SEM analysis results, supported the hypothesis.

Here in our major difference from the other systems is; we aim to obtain the high thermal stability, crystallinity and proper morphology by optimizing the hydrolysis conditions using low acid concentrations, short hydrolysis time and low cellulose acid ratios combining the post treatment.

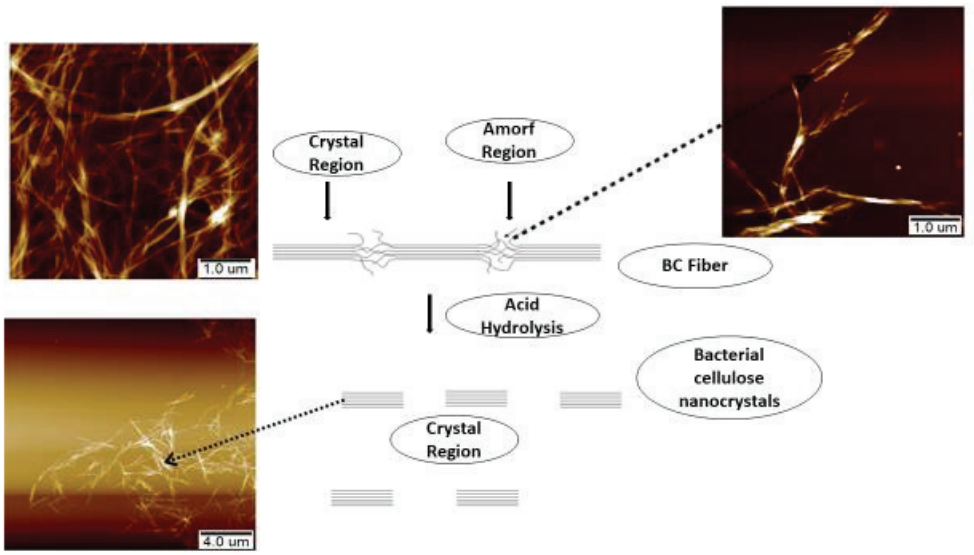

Figure 3.1. Production of bacterial cellulose nanocrystals via acid hydrolysis

3.2. Experimental

3.2.1. Materials and Methods

Gluconacetobacter xylinus (ATCC® 700178™, BPR2001) freeze dried culture was obtained from American Type Culture Collection (Manassas, VA, USA). Corn steep liquor (CLS C4648, 50% solid), calcium carbonate (CaCO3), D-(+)-glucose, yeast extract, citric acid monohydrate and di -Sodium phosphate dibasic dihydrate were bought from Sigma Chem. Co., (St. Louis, MO, USA). Oxoid™ bacteriological peptone, Oxoid™ bacteriological agar, sulfuric acid (H_2SO_4, 95.0 to 98.0 w/w %), hydrochloric acid (HCI, 37%) and sodium hydroxide (NaOH) were purchased from Thermo Fisher Scientific Inc. (Waltham, MA, USA).

3.2.2. Production of Bacterial Cellulose Mats

Gluconacetobacter xylinus (ATCC® 700178™) strain in lyophilized form was purchased from ATCC. YGC (Glucose, 50 (g/l); yeast extract, 5 (g/l); $CaCO_3$, 12.5 (g/l)) medium was used for basal medium. After 72 h, pre-cultured cells were placed in the 90 ml of corn steep liquor (CSL)-glucose medium (Glucose, 20 (g/l); $Na_2HPO_4.2H_2O$, 2.7 (g/l); citric acid monohydrate, 1.15 (g/l); CSL, 80(g/l)) method described by El-Saied, El-Diwany, Basta, Atwa and El-Ghwas (2008). The flasks were incubated at 30 ^oC for 14 days under static conditions. After 14 days, cellulose mats at the air-liquid interface were collected from culture media.

3.2.3. Production of Bacterial Cellulose Nano Fibers

Bacterial Cellulose (BC) pellicles were withdrawn from the culture medium washed with water and BC pellices were cut into small pieces and boiled in 0.2 M NaOH solution with the stirring at 400 rpm for 30 min at 115 ^oC by slightly modified method described by George and Siddaramaiah (2012). Alkali treated BC pellices washed several times with deionized (DI) water. BC pellices were disintegrated in water with a blender (Waring, 8011ES, Stamford CT, USA) for 5 min. Cellulose paste was centrifuged at

13,000 rpm for 15 min, neutralized with hydrochloric acid and sonicated 30 min. The BCNF suspension was freeze-dried at 0.025 bar -50 °C.

3.2.4. Production of Bacterial Cellulose Nanocrystals

Alkali treated cellulose paste was centrifuged at 13,000 rpm for 5 min to remove excess water. For each experiment, 200 (g/L) cellulose/acid ratio was used for both acid hydrolysis. H_2SO_4 and HCl acids were used for hydrolyzing of BCNCs according to the modified method described previously (Araki et al., 1998; George & Siddaramaiah, 2012). The hydrolysis conditions tested in this study were described in Table 3.1. In brief, for both acid treatments 40 (g wet weight basis) cellulose paste was hydrolyzed in 200 ml acid solution. The influence of the acid type, acid concentration and reaction temperature on the production of BCNCs was evaluated with 4N HCl (Reagent grade 37%) acid solution at 95 and 105 °C, and 35 (%, w/w) H_2SO_4 acid solution at 60 and 70^o C at 240 min under continuous magnetic stirring (400 rpm). The reactions were stopped, and suspensions were cooled in an ice bath to room temperature. Both acids were removed from the BCNCs by centrifugation (ThermoFisher Scientific, Sorvall Legend X1R, Osterode, Germany) at 13,000 rpm for 15 min. BCNCs were washed with deionized water and centrifuged at 5 cycles. Following hydrolysis, the neutralization step was applied. All hydrolyzed samples were suspended in deionized water and samples were neutralized with NaOH until the pH 7. After several centrifugation and washing steps, the suspensions were diluted with water. The cellulose dispersion was sonicated for 30 min using an ultrasonicator (Branson Ultrasonic, CPX3800H, 40kHz, Danbury, CT, USA). An aqueous suspension of all hydrolyzed samples was lyophilized by a lyophilizer (VirTis BenchTop 3L, NewYork, USA) at 0.025 bar -50 °C.

Table 3.1. Reaction conditions used to obtain bacterial cellulose nanocrystals (BCNCs)

Sample Name	Cellulose Source	Acid Type	Acid Conc. (N, %)	Reaction Temp.(C)	Reaction Time (h)	Cellulose/acid Ratio (g/L)
H105	BC	HCI	4 N	105	4	200
H95	BC	HCI	4 N	95	4	200
S70	BC	H_2SO_4	35%, w\w	70	4	200
S60	BC	H_2SO_4	35%, w\w	60	4	200

3.2.5. Scanning Electron Microscopy (SEM)

BCNCs and BCNFs aqueous suspensions (0.1 g/L) were sonicated at 80 watts (6 mm probe, Cole polymer ultrasonic processor, USA) for 1 min. Each suspension of 20 µl was allowed to dry on a glass coverslip at room temperature and then mounted on a SEM stub with double-sided adhesive carbon tape. The samples were coated with gold for 30 seconds with EMS 150R ES Sputter Coater (EM Sciences, Hatfield, PA). BCNCs and BCNFs morphology were observed with SEM, FEI Quanta 200 F, (Hillsboro, OR, USA) with an accelerating voltage of 10KV in high vacuum mode. ImageJ software was used to measure the diameter and length of the BCNCs.

3.2.6. Atomic Force Microscopy

Atomic Force Microscopy (AFM) experiments were performed by Bruker MultiMode Nanoscope8 (Bruker, Santa Barbara, USA). Samples used for AFM were prepared by an aqueous suspension of (0.1 g/L) BCNCs and BCNFs. Samples were sonicated for 1 min, and 20 µl of sample suspensions were allowed to dry on glass discs at room temperature. Images were processed in the air with a peak force tapping mode using silicon tip cantilever having nominal spring constant 5 N/m and the resonance frequency of 150 kHz. Images were analyzed by NanoScope Analysis Software (Version 1.7).

3.2.7. Fourier Transform Infrared Spectroscopy of BCNFs and BCNCs

A Fourier transform infrared spectra (FTIR) analysis was recorded with a Perkin-Elmer Spectrometer (LX185255 Spectrum BX II, Llantrisant, UK) equipped with an attenuated total reflection (ATR) accessory, a KBr beam splitter and DTGS detector with triple bounce Diamond/ZnSe crystal plate. The experiment was performed by first taking the background scan of air and spectrum resolution test. All BCNFs and BCNCs powder samples ATR-FTIR spectra were collected over the range from 4000 to 525 cm^{-1} with 4 cm^{-1} resolution averaging 64 scans. Spectrum software (5.3 version) was used for all data analysis.

3.2.8. X-ray diffraction (XRD) Analysis of BCNFs and BCNCs

X-ray diffraction analysis was performed on freeze-dried samples by Philips X'Pert Pro diffractometer (Philips Analytical, PANalytical B.V., Almelo, The Netherlands). The instrument was equipped with a CuKα radiation (λ = 1.5405 Å) at 45 kV, and 40 mA. X'-accelerator detector was used to for X-ray diffraction analysis for 2θ from 5 to 45° with a scan speed of 0.139 (°/s). X'Pert HighScore Plus software (Version 4.1) was used for crystallinity analysis. The crystallinity index CrI (%) was determined by the empirical method developed by Segal, Creely, Martin, & Conrad, (1959) (Eq. (3.1)).

$$\mathrm{CI}(\%) = \frac{(\mathrm{I}_{200} - \mathrm{I}_{\mathrm{am}})}{\mathrm{I}_{200}} \quad (\mathrm{Eq.\ 3.1})$$

I_{200} is the maximum intensity of the diffraction peak from the crystalline region of cellulose, approximately peak at 2θ = 22.7°, and I_{am} is the minimum intensity (between I_{200} and $I_{110)}$ from the amorphous region at approximate peak at 2θ = 18.5°. The crystallite sizes (CS) were obtained from I_{200} crystalline region and were estimated by Scherrer's equation (Eq. (3.2)):

$$\mathrm{CS} = \frac{\kappa.\lambda}{\mathrm{FWHM}.\cos\theta} \quad (\mathrm{Eq.\ 3.2})$$

Where κ is the Scherrer constant (0.94), λ is the wavelength of the X-ray (λ= 0.15416 nm), FWHM is the width of the diffraction peak at half-maximal height (in radians), and θ is the Bragg angle of the crystalline peak.

3.2.9. Thermogravimetric Analysis (TG) of BCNFs and BCNCs

Thermogravimetric (TG) curves were recorded with a Thermogravimetric Analyzer (TG), Perkin Elmer Diamond TG/DTA, (Perkin Elmer Inc. Shelton, CT, USA). The samples (5-7 mg) were heated from 30 to 700°C at 10 °C/min under the 200 ml/min nitrogen gas. Derivative TG curves (DTG) indicated a weight loss rate as a function of temperature.

3.2.10. Zeta Potential Measurement

Zeta potential of the samples was performed on a Malvern Zetasizer Nano (Malvern Instruments Ltd. Worcestershire, UK). BCNCs aqueous suspensions (0.1 g/L) were sonicated for 1 min, and measurements were carried out with folded capillary cells. Reported values are the means and standard deviations of three measurements at 25 °C.

3.2.11. Elemental Analysis

Elemental analysis was used to determine the total sulfur content of the BCNCs samples after the neutralization step. The experiments were carried out by a LECO-CHSN-932 elemental analyzer (LECO Corporation, Michigan, USA). LECO 502-209 sulfamethazine was used for calibration.

3.3. Results and discussion

3.3.1. X-ray Diffraction (XRD) Analysis of BCNFs and BCNCs

X'Pert HighScore Plus software was carried out for the peak fitting of crystallinity analysis. X-ray diffraction (XRD) patterns of hydrolyzed samples were shown in Figure 3.2. All samples represented the main three characteristic diffraction patterns of cellulose I peak intensity at Bragg angle 2θ approximately 14.8, 16.6 and 22.9, corresponding to the (10-1), (101) and (200) lattice plane, respectively (Qiao, Chen, Zhang, & Yao, 2016; Vasconcelos et al., 2017). The crystallite sizes of the native cellulose and acid hydrolyzed cellulose samples were determined from (200) lattice plane in Table 3.2.

The crystalline index of BC increased with both acid hydrolysis conditions. Cellulose structure composed an amorphous and crystalline part, acids and enzymes could easily attack the amorphous parts and released the crystal parts (Park, Baker, Himmel, Parilla, & Johnson, 2010; Trache, Hussin, Haafiz, & Thakur, 2017). The crystallinity index of the HCl and H_2SO_4 hydrolyzed samples were different, H_2SO_4 samples CI were lower than the value of HCI treated samples. Depending on the preparation method (acid type and hydrolysis temperature), BC crystallinity value can be

different. Under controlled acid hydrolysis reactions, increasing hydrolysis temperature increases the crystallinity index and decreases crystallinity sizes of BCNCs compare to native BC (F) for both used acid type. The crystallinity index for the native BC and hydrolyzed BCNCs was in accordance with the previously reported cellulose modification studies. The crystallinity index for 2h and 48h H_2SO_4 (concentration 50.7 % (w/v)) hydrolyzed bacterial cellulose samples CI% 79.64 and 90.31%, respectively (Martínez-Sanz, et al., 2011a). Another research was evaluating the effect of acid concentration and reaction time on crystallinity index; at H_2SO_4 concentrations 50 and 65 % (w/w) for 120 min, BC samples CI was 92 and 22%, respectively. Increasing acid with increasing time may not increase the crystallinity index of BC samples. The combination of high acid concentration and time would digest the crystalline parts of BC; result in the significant decreases in the crystallinity of the material (Vasconcelos et al., 2017).

The critical point is the hydrolysis temperature and time, acid type and acid concentration of the reaction as well as cellulose acid ratio. In our case, the maximum reaction temperature was 105 for HCI at 200 g/L cellulose acid ratio, and maximum cellulose acid ratio was the 200 g/L at 70 ° C for H_2SO_4. During the experimental observations, 115 ºC for HCI acid was used for the extraction process. Boiling solutions turned dark during the reaction. It was observed that 115 ºC was the exaggerated hydrolysis temperature for 4N HCI solution conditions. It can be concluded from the results that for HCI acid extraction process, the max hydrolysis temperature was 105 °C, and 110 g was the maximum cellulose pulp to the acid ratio for H_2SO_4 acid treatment. Acid hydrolysis of cellulose is a complex process, and several parameters should be considered in designing the experiments. More experiments are needed to support this strategy.

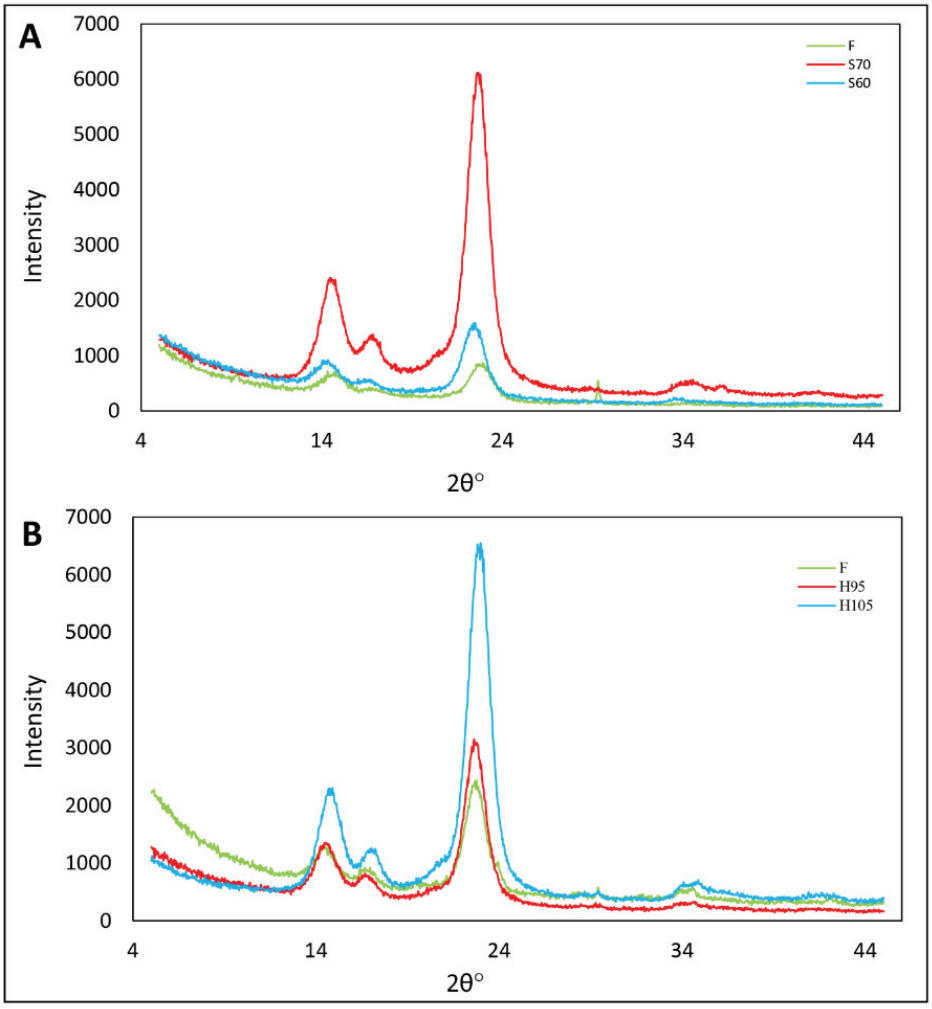

Figure 3.2. X-ray diffraction patterns of native BC (F) and BCNCs after hydrolysis conditions a) F, S60, S70 b) F, H95, H105

3.3.2. Thermogravimetric Analysis (TG) of BCNFs and BCNCs

The thermal stability of freeze-dried BCNFs and BCNCs were investigated by TGA/DTA. By the TGA/DTA results, as can be seen in Figure 3.3 and Figure 3.4, the decomposition temperature of all hydrolyzed BC was not significantly affected by the HCI and H_2SO_4 acids hydrolysis. At proposed acid treatments conditions, acids hydrolysis did not significantly influence the thermal stability of BCNCs in comparison with BCNFs. Native bacterial cellulose fibers had lower degradation temperature than hydrolyzed BCNCs samples. The initial weight loss around 100 °C was related to the evaporation of adsorbed moisture from the bacterial cellulose fibers and crystals. BCNCs and BCNFs maximum thermal degradation temperature occur between 250 and 400°C; this is the specific degradation mechanism of cellulose due to the depolymerization,

dehydration, and decomposition of glycosyl units (Roman & Winter, 2004). By the onset temperature, only minor decomposition differences in thermal stability of all samples can be observed.

In our preliminary examinations, the proposed condition for sulfuric acid treated BCNCs without neutralization step decreased the thermal stability but maintained the same crystallinity degree, structure and morphology (data were not shown). Thermal properties of cellulose depended on the source of cellulose, hydrolysis conditions and post-treatment methods. According to previous studies have been reported in detail; sulfuric acid treatments decreased the thermal stability of cellulose crystals due to the formation of sulfate content ($-OSO_3$) on the BCNCs surface (Camarero Espinosa et al., 2013; Henrique et al., 2015; Martínez-Sanz et al., 2011a; Roman & Winter, 2004). This sulfate groups catalyzed the dehydration reaction by decreasing the decomposition temperature of sulfuric acid treated BCNCs and promoted the accumulation of char residue (Kim, Nishiyama, Wada, & Kuga, 2001; Roman & Winter, 2004). The thermal behavior of neutralized sulfuric acid treated BCNCs was similar to native cellulose fibers, and HCI hydrolyzed BCNCs. The preserved thermal stability may be explained by the replacement of hydrogen ions with alkaline sodium ions for preventing the formation of char residue by the catalytic activity of alkaline ions and improve the thermal stability (Wang et al., 2007).

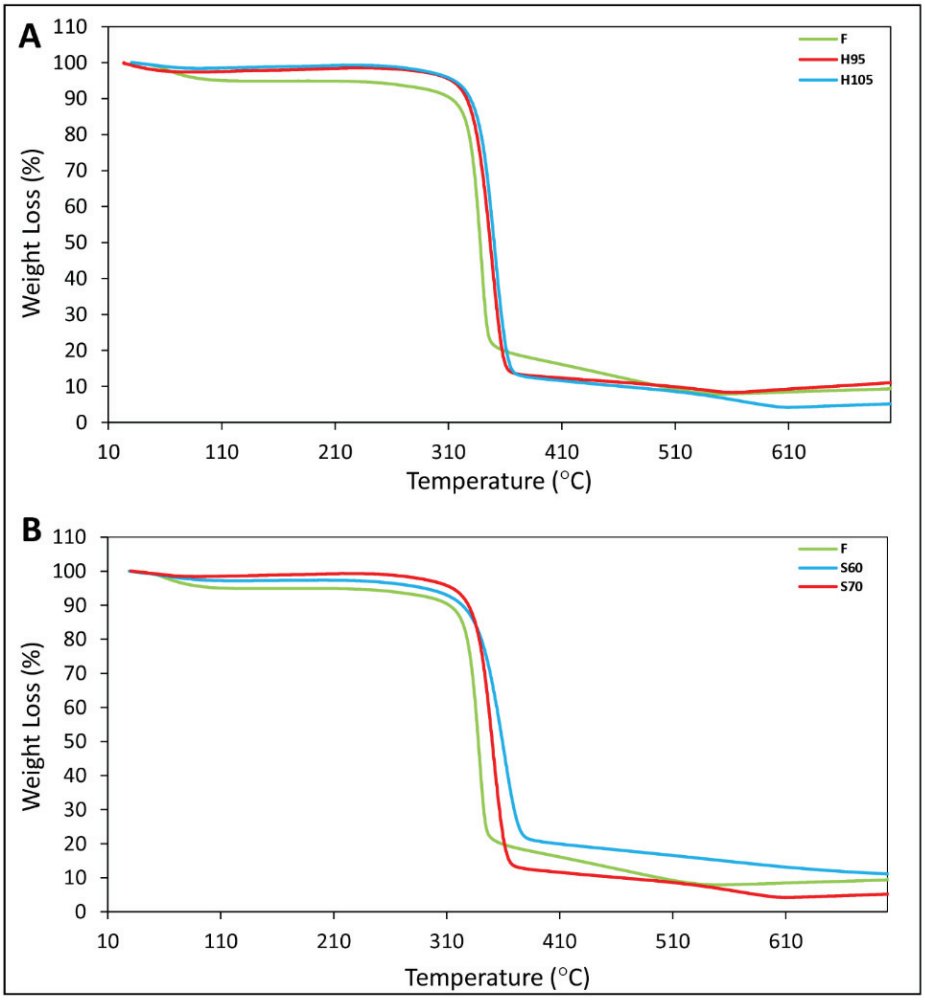

Figure 3.3. TGA curves of native BC and BCNCs obtained after hydrolysis conditions a) F, H95, H105 b) F, S60, S70

Table 3.2. Native BC and BCNCs TGA and XRD results

Sample	Crystallinity Index (%)	Crystallite size (nm)	Temperature Onset (ºC)	Weight losses (%)
F	70.78	18.64	342	90.8
S60	71.23	13.04	369	88.9
S70	86.67	6.52	361	93.2
H95	85.59	10.03	354	88.98
H105	91.36	8.69	358	94.83

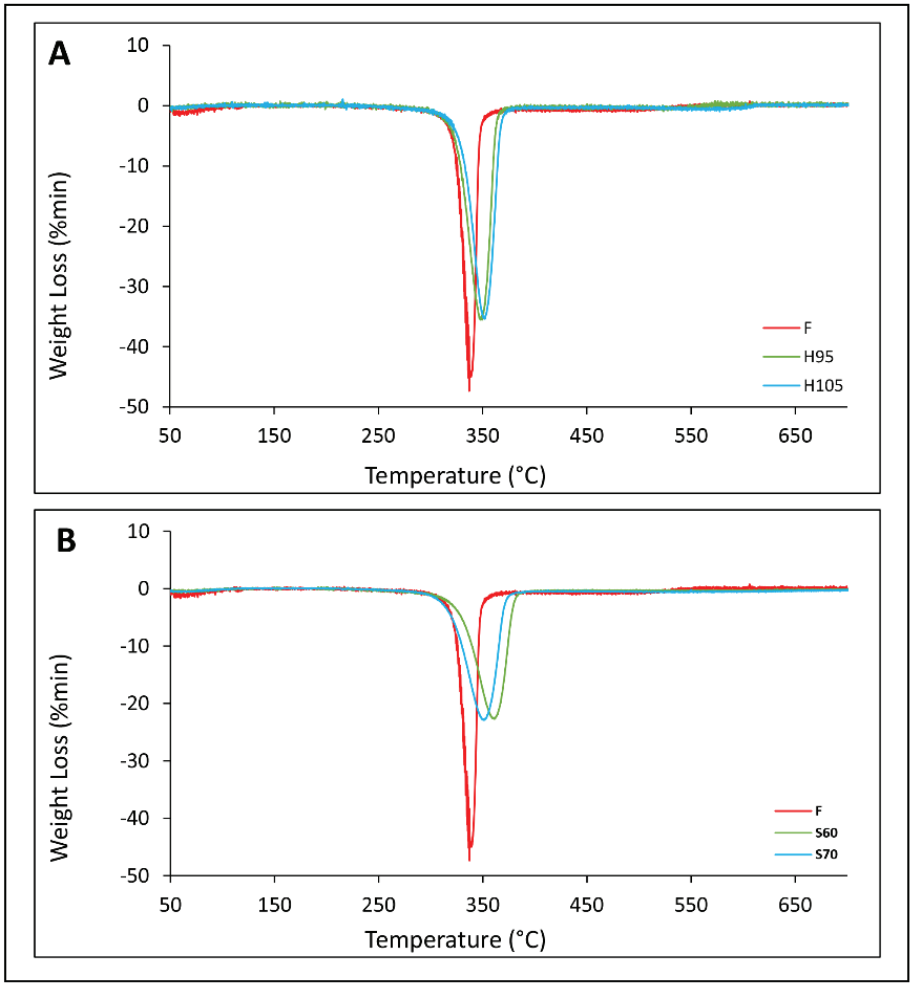

Figure 3.4. DTG curves of native BC and BCNCs obtained from after acid hydrolysis a) F, H95, H105 b) F, S60, S70

3.3.3. Fourier Transform Infrared Spectroscopy of BCNFs and BCNCs

The FT-IR spectra of the structural changes of freeze dried BCNFs, and BCNCs powders were shown in Figure 3.5. FTIR spectra at 3700 to 3000 cm^{-1} (O-H hydroxyl groups), 1277 cm^{-1} (C-H bending) (Castro 2012), 1650 cm^{-1} (absorbed water), 1425-1435 cm^{-1} (HCH and OCH bending), 1111 cm^{-1} (C-C stretching), 665-670 cm^{-1} (C-OH out of plane bending) (Gea et al., 2011), 11620 cm^{-1} (antisymmetric bridge stretching) and 896 cm^{-1} (anomeric carbon group) (Kasprzyk & Wichłacz, 2004), have been reported related to the typical characteristic bands of bacterial cellulose.

The band at 1427, 1277, 896 and 667 cm^{-1} are corresponding to the crystallinity of bacterial cellulose (Castro et al., 2012; Kasprzyk & Wichłacz, 2004). The FT-IR spectroscopy was also used to estimate the 'empirical crystallinity index' of samples in

cellulose samples (Oh, Yoo, Shin, & Seo, 2005). The ratio of absorbance at 1430/900 cm^{-1} gives the proportion of crystallinity index and a fraction of cellulose I in the cellulose samples (Castro et al., 2012; Kumar et al., 2014).

The peaks of cellulose at 3344 cm^{-1} (O-H stretching) for S70, 3343 cm^{-1} for both F and S60, the peak is slightly shifted to lower wave number at 3340 cm^{-1} for both H95 and H105. The spectra at 898 cm^{-1} (C-O-C stretching), which is corresponding to the cellulosic β-(1-4)-glycosidic linkages (Pandey, Mustafa Abeer, & Amin, 2014), broadened at sulphuric acid treated samples S60 and S70.

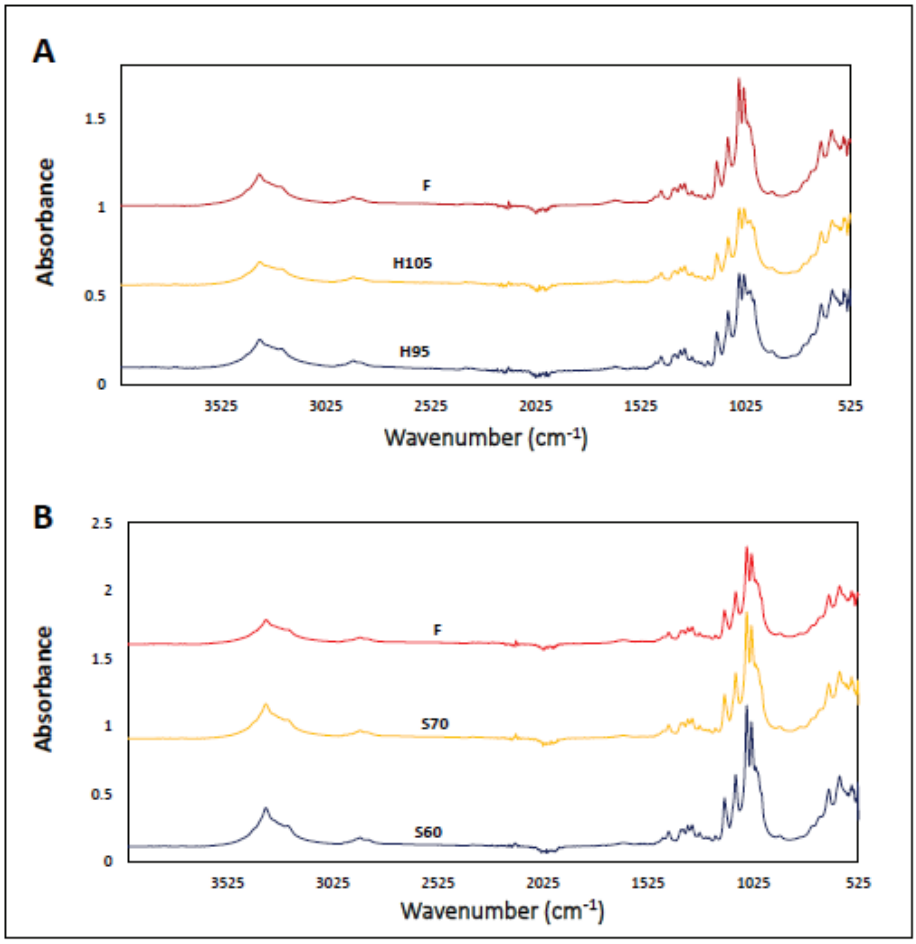

Figure 3.5. FTIR spectra of native BC and BCNCs obtained from after acid hydrolysis a) F, H95, H105 b) F, S60, S70

From the FT-IR spectra of sulfuric acid treated samples it can be observed that there is an absence of spectra at 807 cm^{-1} (C-O-S symmetric vibration bonds corresponding to C-O-SO_3 groups) because of neutralization (Vasconcelos et al., 2017). For all hydrolyzed samples, it can be concluded that after hydrolyzing with both acids, the chemical composition of hydrolyzed BCNCs was similar to BCNFs.

3.3.4. Scanning Electron Microscopy (SEM), Atomic Force Microscopy and Zeta Potential Measurements

Bacterial cellulose fibers were subject to different acid hydrolysis conditions, and fibers broke down into the needle-like shaped BCNCs with a micro and nano scale dimensions (Figure 3.6, Figure 3.7 and Figure 3.8). The dimensions of crystals can be roughly estimated from SEM images. BCNCs cross sections varied from 18.13 ± 4.76 to 22.43 ± 4.59 nm, and the length ranged from 921.85 ± 426.05 to 1232.19 ± 400.38 nm (Table 3.3). BCNCs dimensions were in the average range as found in the literature (Kalashnikova et al., 2013; Martínez-Sanz et al., 2011; Vasconcelos et al., 2017). It can be observed from SEM measurements increasing the 10 ºC for each treatment decrease the length of crystals. Increasing temperature, both acids can diffuse more amorphous region of the cellulose, hydrolyzes the glycosidic bond and result in more crystalline regions with a decrease in length (Elazzouzi-Hafraoui, Putaux, & Heux, 2009). Depending on the hydrolysis conditions, produced crystals have a wide variety of aspect ratios. This aspect ratio (L/d, L is the length and d is the diameters of the crystal) is an important key factor when cellulose crystals are used as a reinforcing agent in polymeric matrixes (Azizi Samir, Alloin, & Dufresne, 2005) and also for the formation of Pickering emulsions to stabilize the oil-water interfaces (Hu et al., 2015; Kalashnikova et al., 2011).

The use of sulfuric acid hydrolysis provides some negatively charged sulfate groups on the surface of BCNCs, and with increasing temperature 60 to 70, the surface charge of crystals is increased. These results are in good agreement with the literature (Araki et al., 1998; Elazzouzi-Hafraoui et al., 2009). Hydrochloric acid-treated BCNCs have low surface charge compare to sulfuric acid-treated BCNCs (Kalashnikova et al., 2013) or undetectable surface charge (Araki et al., 1998).

Table 3.3. BCNCs samples zeta potential and dimensions measurements obtained from SEM

Sample	Length (nm)	Cross-section (nm)	Aspect Ratio (L/D)	Zeta Potential (mV)
H95	1031.67 ± 392.71	18.13 ± 4.76	56.90 ± 21.66	-5.96 ± 3.28
H105	921.85 ± 426.05	21.94 ± 6.95	42.07 ± 19.41	-3.20 ± 3.11
S60	1232.19 ± 400.38	22.43 ± 4.59	54.93 ± 17.85	-13.07 ± 3.16
S70	831.30 ± 355.58	18.42 ± 4.63	45.67 ± 19.30	-24.60 ± 4.27

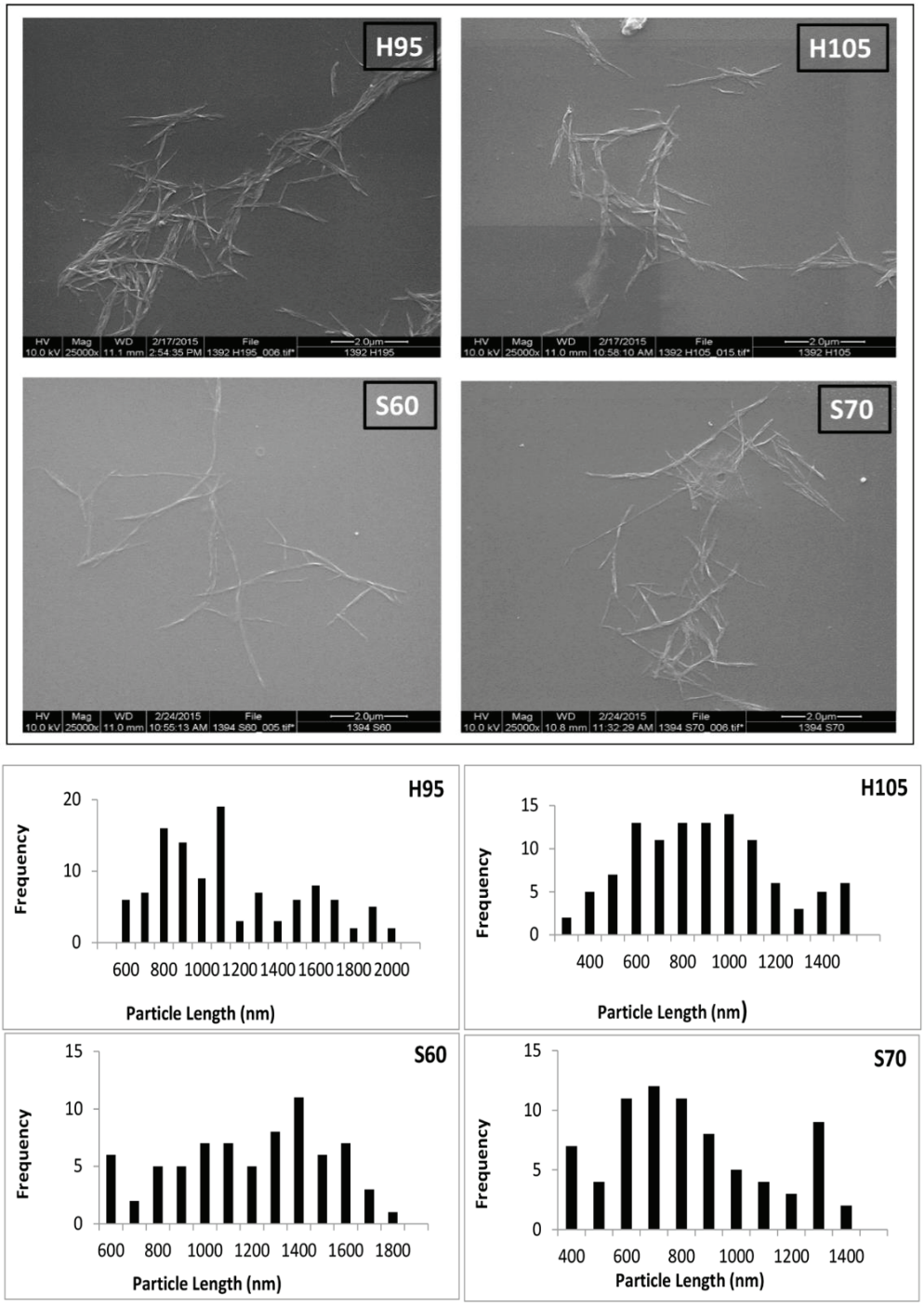

Figure 3.6. SEM images and histogram of the length distribution of H95, H105, S60, and S70

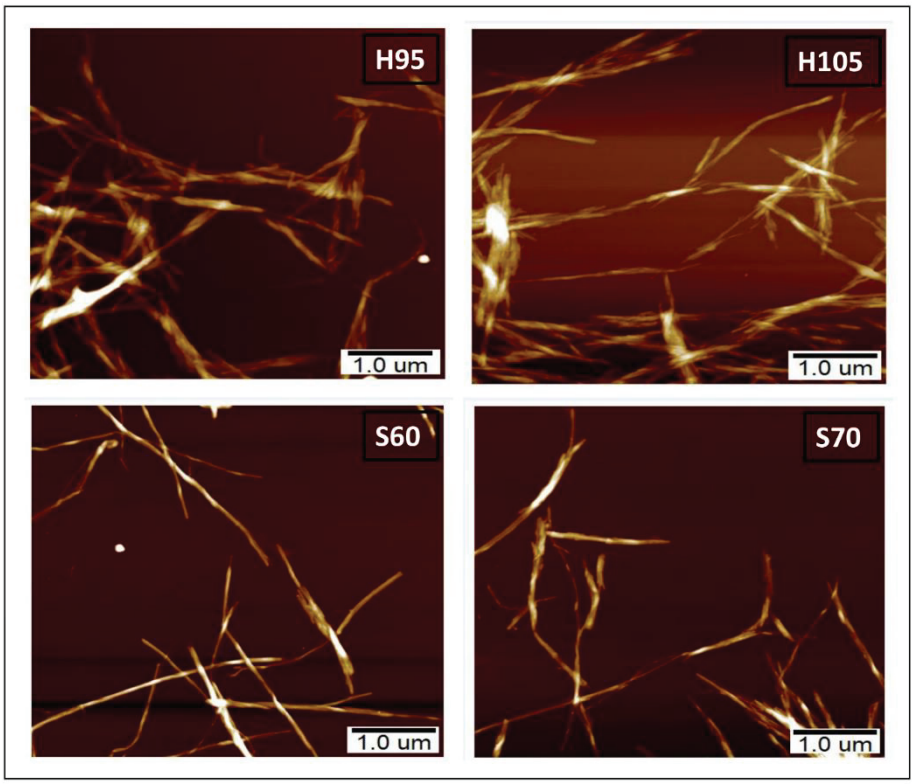

Figure 3.7. AFM images of the of hydrochloric acid (H95, H105) and sulphuric acid (S60 and S70) hydrolyzed crystals

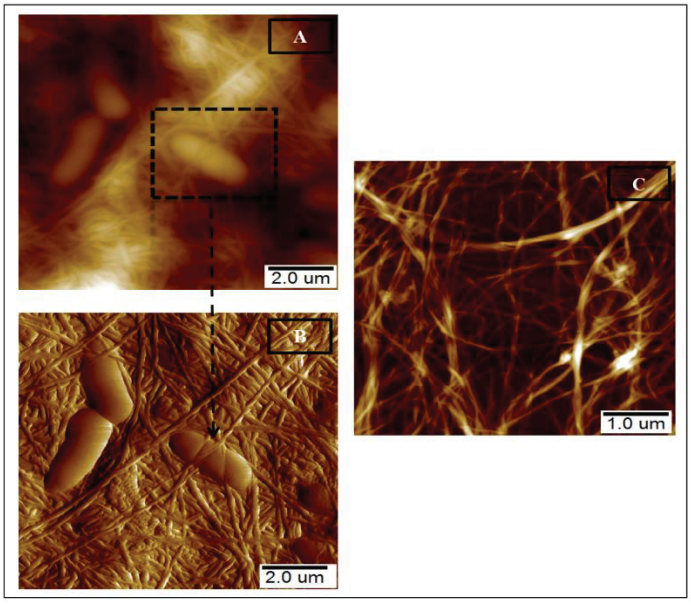

Figure 3.8. AFM image of a) *Gluconacetobacter xylinum* on fibers b) AFM peak force error image of *Gluconacetobacter xylinum* on fibers c) AFM image of cellulose fibers

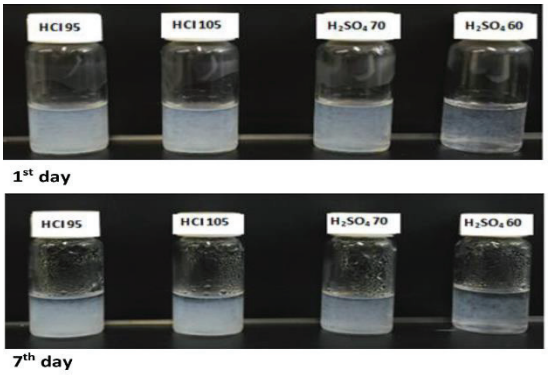

Figure 3.9. Dispersion of BCNCs in water(c=1 g/L), after ultrasonication

The stability of the aqueous suspension of the BCNCs is depended on the size and surface properties of the BCNCs (Ji et al., 2016). Acids treated BCNCs almost have same surface morphology. Both acids treated BCNCs well dispersed in the water and formed homogenous dispersion even after 7 days (Figure 3.9). This good colloidal stability might be due to the negative charge introduced on the surface, which could electrostatically stabilize the BCNCs.

3.3.5. Elemental Analysis

According to the elemental analysis results, sulfur (S%) content is very low in the sulfuric acid treated samples (S60 and S70) (Table 3.4). There was no significant changes in sulfur content compare to native cellulose (F) and hydrochloric acid (H95, H105). These results confirmed the totally removal of the sodium sulfate salt which was formed due to the neutralization step of sulfuric acid hydrolysis. Also, X-ray results did not give any peak for the formation of the salts for both acid hydrolysis.

Table 3.4. Elemental analysis results for native BC and acid treated BCNCs

Sample	C %	H %	N %	S %
F	37.77	6.45	7.830	0.082
S60	43.50	5.15	1.074	0.078
S70	43.19	5.38	0.819	0.030
H95	45.90	6.64	9.830	0.070
H105	45.25	8.17	12.780	0.080

3.4. Conclusion

Micro and nano scale dimensions BCNCs without affecting the thermal stability and crystallinity with negatively charged and aqueous stable crystals were successfully produced from bacterial cellulose fibers under different controlled acid hydrolysis conditions with a neutralization step. X-ray, TGA, DTA analysis and SEM images results, supported the hypothesis. TGA, DTA analysis results indicated that sulfuric acid extraction conditions with post-treatment did not alter the thermal stability of hydrolyzed BCNCs fibers**,** which is one of the disadvantages of sulfuric acid hydrolysis. The result of this research suggested that high thermal stable BCNCs can be produced by optimizing the chemical hydrolysis conditions with low acid concentrations, short hydrolysis time and low cellulose acid ratios including the post-treatment.

CHAPTER 4

PICKERING EMULSIONS

4.1. Introduction

Attention to the utilization of biodegradable and sustainable biopolymers in emulsions systems has currently been growing. Cellulose is the abundant, biocompatible, biodegradable, and commercially available organic polymer in the world. Rod-like colloidal particles such as cellulose nanocrystals can adsorb at the interface to produce oil in water Pickering emulsions in the presence and absence of surfactants (Capron, 2013; Hu, Marway, Kasem, Pelton, & Cranston, 2016).

The mechanism of emulsion stability with hydrocolloids particles generally can relate to particle characteristics (hydrophobicity and /hydrophilicity). The contact angle of hydrophilic solid particles $\theta<90$ and the contact angle of hydrophobic solid particles is $\theta>90$ (Aveyard, Binks, & Clint, 2003). Hydrophobic particles are used in water-in-oil (W/O) emulsions at the oil-water interface, but hydrophilic particles prefer the oil-in-water interface to form oil-in-water (O/W) emulsions (Binks & Lumsdon, 2000, Xhanari et al., 2011).

Stabilization of emulsions with colloidal particles were first described by Ramsden (Ramsden, 1903) and Pickering (Pickering, 1907). A variety of hydrocolloid particles has been studied in Pickering emulsions formations and stabilizers such as starch nanoparticles (Haaj e al., 2014), chitosan particles (Ho et al., 2016), silica particles (Liu et al., 2017) and soy protein nanoparticles (Liu & Tang, 2013). Recently, researchers have shown an increased interest in cellulose fibers, and cellulose crystals stabilized oil in water emulsions. Oza and Frank (1989) mentioned first time stabilization of emulsions via microcrystalline cellulose in the presence of a surfactant. A number of researchers have demonstrated the use of cellulose derivatives and cellulose from different sources such as bacterial cellulose fibers and cellulose crystals (Kalashnikova et al., 2012; Lee, Blaker, Heng, Murakami, & Bismarck, 2014; Ougiya, Watanabe, Morinaga, & Yoshinaga, 1997), micro-fibrillated cellulose (Xhanari, Syverud, & Stenius, 2011), ramie

fibers (Zoppe et al., 2012) and also other cellulosic materials including cotton and wood (Cunha et al., 2014) were used in different kinds of emulsion formulations.

Bacterial cellulose fibers and crystals itself have an emulsion stabilizing effects (Kalashnikova et al., 2011). Paximada et al. (2016) indicated that bacterial cellulose stabilization properties in oil-water emulsions are better than the commercial cellulose; carboxymethyl cellulose and hydroxypropyl methylcellulose. Another study focused on the water–soluble cellulosic derivates methylcellulose and hydroxyethyl cellulose nanocrystals (CNCs) stabilization ability, as the tannic acid encapsulated Pickering emulsions (Hu et al., 2016).

However, due to the nature characteristic (hydrophobicity and hydrophilicity) of hydrocolloid particles, the type of produced emulsions can be different either oil-in-water (O/W) or water–in oil (W/O). Surface modification is required to utilize the cellulose crystals in hydrophobic systems (Abitbol, Marway, & Cranston, 2014) due to the hydrophilicity of cellulose surface (Zoppe et al., 2012). Hydrophilicity of cellulose particle can limit its adsorption ability at the interface. Different modification methods have been used for the hydrophobization of cellulose crystals. Lee et al. (2014b) used bacterial cellulose fibers, which were esterified with acetic, dodecanoic and hexanoic acids. These hydrophobized bacterial cellulose fibers were used as an emulsifier to produce the W/O high internal phase emulsions. Another example is wood cellulose modified with phenyl trimethylammonium chloride to produce oxidized cellulose nanocrystals with hydrophobic domains for electrostatically stabilized oil-in-water Pickering emulsions (Gong et al., 2017). Moreover, mechanically disintegrated cellulose fibers, TEMPO-oxidized nanofibers, and acid-hydrolyzed cellulose nanocrystals were also able to stabilize oil-in-water Pickering emulsions with dodecane which has been investigated by Gestranius et al. (2017).

A number of studies on cellulose fibers and surfactants interactions have been reported in the literature, such as the interaction of cellulose fibers with different alkyl chain length of cationic surfactants (Alila, Boufi, Belgacem, & Beneventi, 2005), an anionic surfactant, sodium dodecylbenzene sulfate (NaDBS) and a non-ionic surfactant, Triton X-100 in the presence and absence of electrolytes (Paria, Manohar, & Khilar, 2005) and nonionic surfactants C_2E_5, $C_{12}E_7$ and $C_{14}E_7$ adsorption on the cellulose surface (Torn, Koopal, De Keizer, & Lyklema, 2005).

In a few studies in literature, cellulose fibers and crystals in the presence of surfactants were used to improve the Pickering emulsions stability. One example is

cationic surfactants cetyltrimethylammonium bromide (CTAB), and didecyl dimethyl ammonium bromide (DMAB) with cellulose crystals and fibers stabilized Pickering emulsions (Hu et al., 2015) and another one is mini-emulsion polymerization with cellulose crystals and poly(methyl methacrylate) by CTAB and SDS surfactants (Kedzior, Marway, & Cranston, 2017).

The objective of this chapter is to produce the BCNFs or BCNCs stabilized Pickering emulsions in the presence of cetyltrimethylammonium bromide (CTAB), sodium dodecylbenzene sulfate (SDS), Tween 20, and lauric arginate (LA) for encapsulation of volatile eugenol essential oil. To achieve the objective, the proposed hypothesis was that BCNFs or BCNCs could be formed oil-in-water Pickering emulsions with a combination of CTAB, LA and SDS surfactants. This surfactant can provide electrostatic, hydrophobic, and steric interactions with BCNFs and BCNCs to stabilize the cellulose to form the Pickering emulsions for encapsulation of volatile eugenol essential oil and main driving forces could be the electrostatic forces.

Based on this hypothesis, the research in this chapter was focused on the first screening experiment with cellulose fibers and crystals interactions with a different type of surfactants and volatile eugenol oil. Zeta potential and particle size measurement of each component along with the combination of emulsions components were examined. After screening, experiments formulated, and all produced emulsions for bacterial cellulose fibers and crystals were characterized by zeta potential, particle size, conductivity, pH measurement and stability tests; morphology of emulsions was also examined by SEM and fluorescence microscope.

The problem statement of this chapter 4 is that eugenol is volatile essential oil and it is hard to protect eugenol from environmental factors such as moisture, heat, oxygen, and light during processing and handling. In order to enhance its stability, volatile eugenol oil encapsulated in emulsion formulation via bacterial cellulose fibers and crystals as carriers. Encapsulation of volatile essential oils by polymer based particles can be a promising way for the enhancing the stability of active compounds from environmental factors and promising alternative delivering system for volatile compounds.

Pickering emulsions stabilized by bacterial cellulose nanocrystals with lauric arginate, cetyltrimethylammonium bromide, didecyl dimethyl ammonium bromid and eugenol oil have been reported. In this part of the research, the utilization of BCNFs and chemically modified BCNCs as bio-based, green materials for oil-in-water emulsion formulations with a combination of different surfactants were reported.

4.2. Experimental

4.2.1. Materials

Sodium dodecyl sulfate (SDS), Tween 20, eugenol oil (Natural ≥98 % W246719), Nile red (N3013) and calcofluor white stain were purchased from Sigma-Aldrich (St. Louis, MO, USA). Cetyl trimethyl ammonium bromide (CTAB) was supplied by Amresco, LLC (Solon, OH, USA). CytoGuard LA 2X was kindly provided by A&B Ingredients Inc. (Fairfield, NJ, USA).

4.2.2. Production of Bacterial Cellulose Nanofibers/Nanocrystals

Bacterial cellulose nanofibers (BCNFs) weres prepared from *Gluconacetobacter xylinus* mats. Bacterial cellulose pellices were treated with NaOH and disintegrated with blender followed by neutralized with diluted acids, and freeze-dried. Bacterial cellulose nanocrystals (BCNCs) were produced from bacterial cellulose fibers by sulfuric acid hydrolysis according to a method previously described in Chapter 3. Briefly, BCNCs fibers were subjected to sulfuric acid (35 w/w %) at 70 ^{o}C at 240 min hydrolysis. Followed by hydrolysis BCNCs suspension was washed by several centrifugations and neutralized with NaOH until pH reached neutrality. The final suspension was freeze-dried.

4.2.3. Emulsion Preparation with BCNFs

The bacterial cellulose nanofibers were used to stabilize oil-in-water (O/W) Pickering emulsions mixed with eugenol and sodium dodecyl sulfate (SDS). Powder of freeze-dried BCNFs was redispersed in water and concentrated to 0.1 %(w/w). In all emulsions, the oil and BCNCs concentration was the same (3%-0.1% (w/w)). Six different SDS concentrations in the aqueous phase were used in the emulsion formulation, 8, 10, 12, 14, 16 and 20% (w/v), (0.277, 0.347, 0.416, 0.485, 0.555 and 0.694M), respectively. The 0.1% suspension of BCNFs were dispersed using a high-pressure homogenizer (IKA T10 Ultra-Turrax, NC, USA) at 30,000 rpm for 4 min. After the

dispersion of cellulose fibers, eugenol oil was added to the aqueous phase followed by emulsified for 4 min. Tween 20 was added to the 0.347M concentrated emulsion for stearic stabilization according to SDS concentrations (0.1 to 1.2 %).

4.2.4. Emulsion Preparation with BCNCs

Sulfuric acid treated bacterial cellulose nanocrystals aqueous suspension were used to stabilize oil-in-water (O/W) Pickering emulsions mixed with eugenol and cetyl trimethyl ammonium bromide (CTAB). In all emulsions, the oil and BCNCs concentration was the same (0.3%-0.1% (w/w)). Six different CTAB concentrations in the aqueous phase were used in the emulsion formulations; 10.11, 12.64, 15.17, 17.69, 20.22 and 25.28% (w/v), and (0.277, 0.347, 0.416, 0.485, 0.555 and 0.694M), respectively. The 0.1% suspension of BCNCs were dispersed using a homogenizer (IKA T10 Ultra-Turrax, NC, USA) at 30,000 rpm for 4 min. After the dispersion of cellulose crystals, different CTAB concentrations and the same eugenol oil concentration were added into the aqueous phase and emulsified including cycles of 4 min homogenizations.

4.2.5. Emulsion Preparation with BCNCs Reformulated with LA Surfactant

Oil-in-water (O/W) Pickering emulsions were prepared with a sulfuric acid treated bacterial cellulose nanocrystals aqueous suspension, eugenol oil and lauric arginate (LA) via ultrasound dispersion method. In all emulsions, the oil and BCNCs concentration was the same (3%-0.1% (w/w)). Six different LA concentrations in the aqueous phase were used in the emulsion formulation; 8, 10, 12, 14, 16 and 20% (w/v), respectively. The 0.1% suspension of BCNCs were sonicated with a probe sonicator (Cole-Parmer, 6mm probe, IL, USA) at 1min, followed by adding 8-20% (w/v) LA and 3% (w/w) eugenol sonicated for 30 seconds in an ice bath. Emulsion samples were dried at -35 °C and 135 militor with freeze drier (VerTis, NY, USA) for 24 h.

4.2.6. Particle Size Measurements of Emulsions

The particle size distribution of emulsion samples was conducted by a dynamic light scattering (DLS) technique with a Delsa^{TM}Nano C Particle analyzer (Beckman Coulter, CA, USA). Emulsion samples were diluted with 1:10 with water and analyzed. The mean particle diameters of all samples was an average of 70 runs and 3 measurements for each sample.

4.2.7. Zeta potential Measurements of Emulsions

BCNFs and BCNCs emulsions samples zeta experiments were performed on a Delsa Nano™ C (Beckman Coulter, CA, USA) using a flow cell. Emulsion samples were diluted with 1:10 water and analyzed. Reported values are the mean of three measurements. The zeta potential of BCNCS reformulation of LA Surfactant emulsions was measured before and after freeze-drying with a Malvern Zetasizer Nano (Malvern Instruments Ltd. WOR, UK). Folded capillary cells were used for the measurements. Each emulsion diluted 1:10 dilution and was measured at 25 °C for triplicate readings.

4.2.8. Scanning Electron Microscopy of Emulsions

Each emulsion and freeze-dried emulsions diluted 1:100 dilution and 20 μL drop of emulsions were allowed to dry on a glass coverslip at room temperature. Samples were mounted on a SEM stub with double-sided adhesive carbon tape before coated with gold. Samples were coated with gold for 30 seconds (EMS 150R ES Sputter Coater, EM Sciences, Hatfield, PA). Coated emulsion samples morphology were then observed with Scanning Electron Microscope, FEI Quanta 200 F, (Hillsboro, OR, USA) with an accelerating voltage of 5-10KV in high vacuum mode. ‘’ImageJ’’ software was used to measure the size of emulsions.

4.2.9. Electrical Conductivity and pH Measurements of LA Emulsions

The electrical conductivity of emulsions was measured before and after freeze-drying with an EC 215 conductivity meter (Hanna, RI, USA). The pH of emulsions was conducted before and after freeze-drying using a pH meter (Onolab, Weilheim, Germany).

4.2.10. Fluorescence Microscopy Images of LA Emulsions

Bacterial cellulose emulsions fluorescent images were acquired using a fluorescence microscope (Carl Zeiss Microscope, GmbH, Germany) using a modified method given by Carillo, Nypelö and Rojas (2015). To examine the cellulose and eugenol oil in samples, cellulose was stained with Calcofluor white stain and eugenol was stained using a Nile red. Bacterial cellulose and eugenol were stained according to the order of the emulsion formulation procedure separately. Freshly prepared 20µL drop of emulsion samples were placed on the glass slide, and the samples were covered with the glass slides. They were examined after 20 min incubation under a fluorescence microscope.

4.2.11. Stability Test of Emulsions

To evaluate the stability of the emulsions, 2 ml of each fabricated cellulose emulsion were put into the test tube, and the digital camera recorded the images of cellulose emulsions.

4.3. Results and Discussions

4.3.1. Particle Size and Zeta Potential Measurements of BCNFs Emulsions Screening Experiment

This part of the research has focused on the effect of ionic and nonionic surfactants interactions between bacterial cellulose fibers and crystals on the formation of oil–in-water Pickering emulsions formations. The hypothesis of this chapter was that BCNFs/

BCNCs would stabilize the eugenol oil emulsion formulations as Pickering emulsions (emulsions stabilized by solid particles) in the presence of surfactants.

From this viewpoint, first, the screening experiments of BCNFs were conducted to test this hypothesis with particle size and zeta analysis experiment in the presence of water, ionic surfactants; SDS and CTAB and a nonionic surfactant; Tween 20 and volatile eugenol essential oil. The bacterial cellulose fibers used in this study were produced from *A.xylinum,* and bacterial cellulose nanocrystals were hydrolyzed by sulfuric acid. The zeta potential of produced fibers and crystals were given in Table 4.1.

Table 4.1. Zeta potential measurements of emulsions with SDS, Tween 20 and CTAB at critical micelle concentrations for screening experiments

Sample	Zeta Potential	Water	SDS	Tween 20	CTAP
BCNFs	(mV)	-0.467 ±0.076	-2.15 ±0.086	-8.11 ±4.24	-
BCNCs	(mV)	-8.050±0.69	-4.413±0.318	4.323±0.30	2.94±0.49

In order to determine the interactions between the cellulose crystals and cellulose fibers with ionic and nonionic surfactants, which were used in this study, the first zeta potential of the cellulose samples were measured (Table 4.1). BCNFs had very low surface negative charges compared to BCNCs. The interaction of BCNFs with SDS and Tween 20 showed negative zeta potential. BCNCs have a high negative surface charge due to the surface modification of BCNCs with sulphuric acid. The interaction between the BCNCs and SDS showed negative zeta potential, while the interaction of BCNCs with the Tween 20 and CTAP showed positive zeta potential value (Table 4.1).

Table 4.2. Zeta potential measurements of BCNFs emulsions with different concentrations of SDS

SDS	0.277M	0.347M	0.416M	0.485M	0.555M	0.694M
(Molar/w/v %)	8%	10%	12%	14%	16%	20%
Zeta(mV)	-26.716±1.7	-31.693±1.88	-22.96±15.51	-7.133±0.28	-26.51±1.44	-6.046±1.48

According to the first screening experiments of BCNFs with an anionic surfactant, SDS was used in the BCNFs-eugenol emulsion formulations. Surfactants are widely used to stabilize the emulsions by reducing the interfacial tension of emulsion systems (Chevalier & Bolzinger, 2013). BCNFs were formulated with the first dispersion of

BCNFs in water and then emulsified with eugenol essential oil followed by the addition of different anionic SDS surfactant concentration into the mixture. Here in, to determine the effect of surfactant concentration on the emulsion formulations, increasing concertation of SDS 0.277M to 0.694M was used (Table 4.2). Increasing surfactant concentration did not increase the zeta potential of each BCNFs emulsions. Bacterial cellulose fibers entanglement and BCNFs disorder amorphous structure may prevent the proper adsorption of surfactants at the surface of cellulose.

BCNFs, due to its amphiphilic character, can easily adsorb at the solid-liquid interface and formed the oil-in-water Pickering emulsions. The adsorption ability of anionic surfactants onto the cellulosic materials; was discussed in the review of Tardy et al. (2017) and the adsorption phenomena could be the interaction between BCNFs and SDS anionic surfactant due to the affinity of hydrophobic head groups of surfactant and a BCNFs hydrophobic site that induced the stabilization of the oil-in-water emulsion.

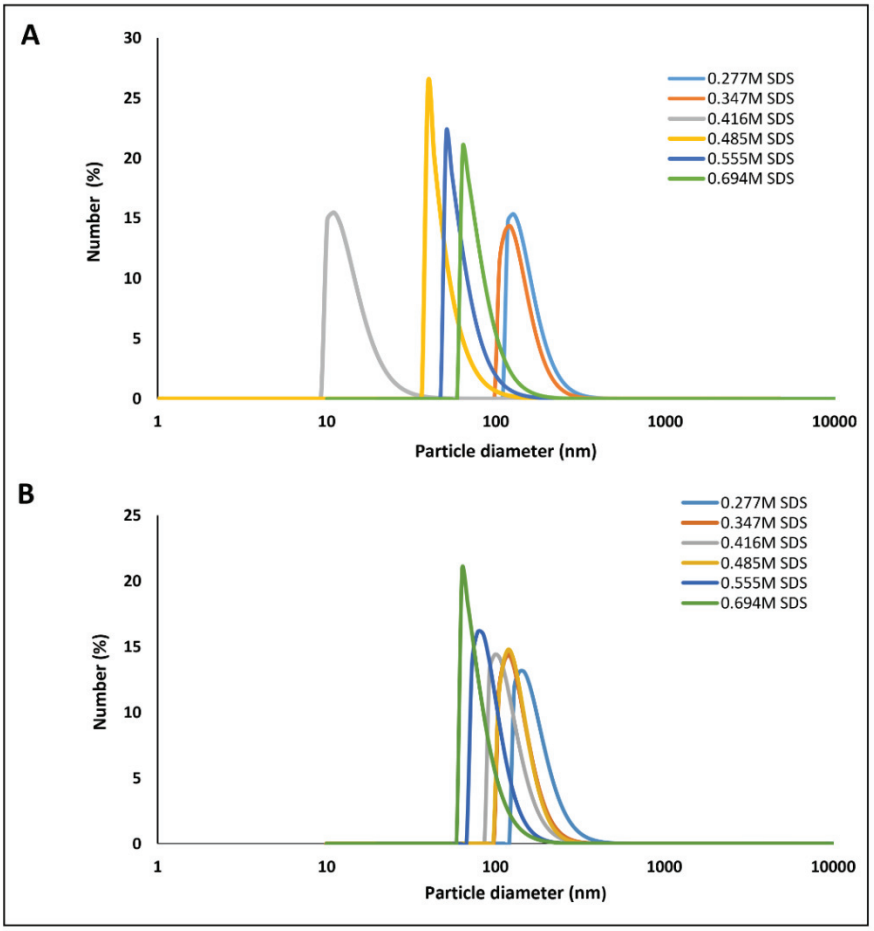

Figure 4.1. Particle size of a) BCNFs with SDS b) BCNFs emulsions with eugenol and SDS

Droplet size differences were monitored by the percentage of number distribution at varying concentration of SDS surfactant (Figure 4.1). The particle size of all the BCNFs emulsions samples decreased with increasing surfactant concentration.

The advantage of using bacterial cellulose and crystals in emulsion formulation is its unique properties such as high aspect ratio; the high surface to the volume ratio, low density, high crystallinity and thermal stability. Bacterial cellulose nature is more hydrophilic, and also it considered as amphiphilic (Gama et al., 2013) A few study have been focused on cellulose amphiphilic properties and used this unique property in the oil-in-water surfactant free Pickering emulsions stabilizations with bacterial cellulose crystals emulsions so far (Fu et al., 2015; Kalashnikova et al., 2011; Kalashnikova, 2012; Xhanari et al., 2011). Quite recently, considerable attention has been paid to the cellulose fibers combination with different kinds of surfactants and polymers to enhance the emulsion stabilization (Hu et al., 2015; Kedzior et al., 2017). The mechanism of emulsion stability with cellulose particles can relate to many factors such as particle surface charge, particle characteristics (hydrophobicity/hydrophilicity), wettability at interphase, nature of oil phase, the presence of a surfactant and pH (Hu et al., 2015; Xhanari et al., 2011).

Wettability of cellulose and cellulose derivatives at solid-liquid phase is one of the important factors, the contact angle of microcrystalline cellulose in water was 30 (Bilia et al., 2014), and bacterial cellulose contact angle was approximately 50 (Gama et al., 2013). The wettability of microcrystalline cellulose is higher than the bacterial cellulose. Pickering stabilization of particles was based on the irreversible adsorption at the interface and partial wetting properties of particles absorption (Kalashnikova et al., 2011). The other important factor for the Pickering emulsion stabilization is the polymer concentration. An example would be the Fu et al. (2015) study they observed that the concentration of bacterial cellulose fibers and stability of emulsions had a positive correlation, and fabricated emulsions were more stable even at alkaline conditions. In the Carrillo et al. (2015) work, when 3.0 wt % cellulose fibers were in the aqueous phase, the kinetically stable emulsions were obtained. Another important factor is the source of cellulose. As an example, Kalashnikova et al. (2012) produced oil in water Pickering emulsions with a different source of cellulose; cotton, bacterial cellulose and green algae (*Cladophora)* and concluded that the aspect ratio of different crystals had an impact on the emulsion surface coverage ratio, but both crystals used showed almost the same wetting properties and crystals flexibility. All factors discussed above should be taken into consideration during the emulsion formulations.

SEM examination was used to observe the shape and surface morphology of the eugenol-BCNFs emulsions. As can be seen from SEM images in Figure 4.2 BCNFs emulsions were successfully obtained from bacterial cellulose fibers in the presence of SDS and Tween 20. As can be seen from Figure 4.2. a) bacterial cellulose covered the surface as macroemulsion and also in Figure 4.2. b**)** as nanoemulsion.

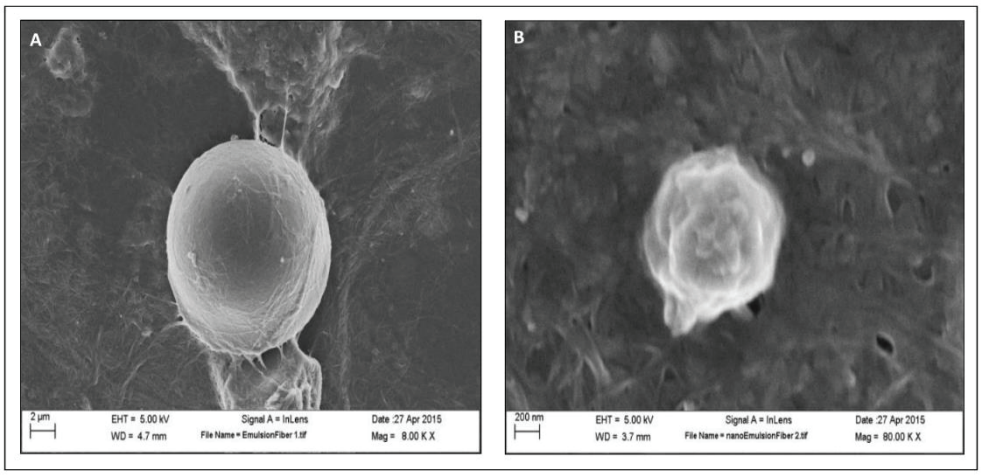

Figure 4.2. SEM images of a) BCNFs eugenol macroemulsions b) BCNFs eugenol nanoemulsions

4.3.2. Emulsion Stability of BCNFs Emulsions

In order to evaluate the stability and the phase separation of the emulsion during storage, stability test was performed on produced emulsions. The stability of BCNFs emulsions with different concentrations of SDS was determined visually for 8 days of the period, and they were presented in Figure 4.3 and Figure 4.4. It can be concluded from the images that when the concentration of SDS increased the BCNFs and emulsions became more stable, SDS adsorbed more on cellulose fibers and prevented phase separation, but SDS itself was not enough to stabilize the BCNFs emulsions. Phase separation at low surfactant concentrations could be due to coalescence and flocculation of droplets; low surfactant concentrations were not sufficient to fully cover the interface (Dickinson, 2009). BCNFs disorder amorphous structure and high aspect ratio may prevent the proper adsorption of enough surfactants at the interface.

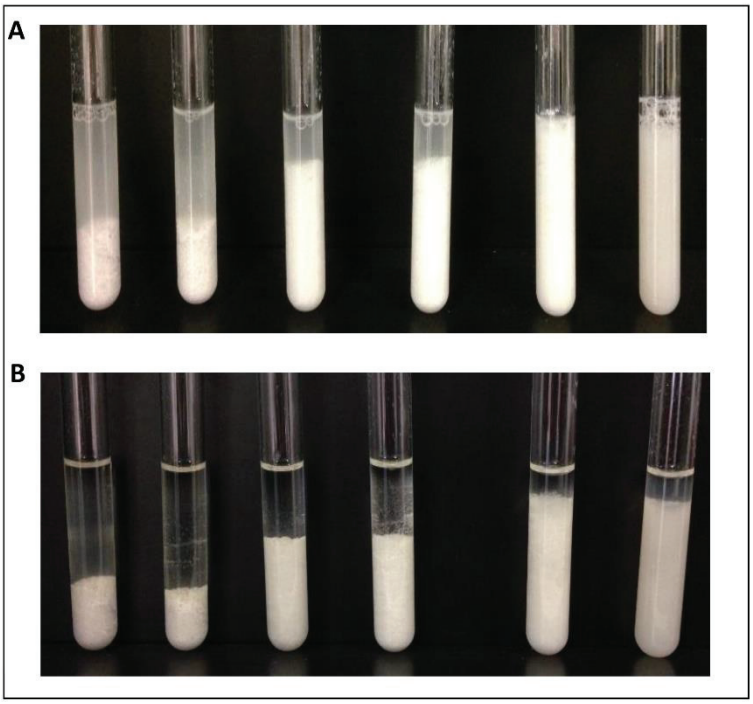

Figure 4.3. Photographic images of a stability test of eugenol emulsions formulated with BCNFs with increasing concentration of surfactant (0.277, 0.347, 0.416, 0.485, 0.555, and 0.694M SDS) a) at the first day and b) after the eight days of storage at room temperature

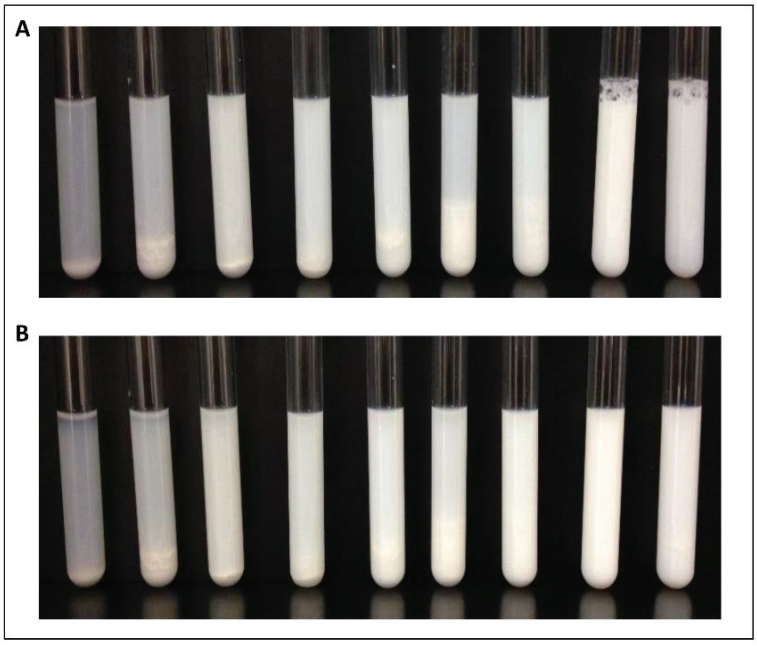

Figure 4.4. Photographic images of eugenol emulsions formulated with BCNFs and 10% (0.347M) SDS stability test with increased concentration of 20% Tween 20 (0.1, 0.2, 0.4, 0.6, 0.8, 1, 1.2 %) a) at first day and b) after the eight days of storage at room temperature

For the stabilization of BCNFs emulsions, 2 ml of 0.374M SDS containing emulsion was put into the glass jars, and increasing concentrations of Tween 20 was added into the emulsions. Stearic stabilization was achieved by Tween 20 and prevented the emulsion droplets against flocculation and coalescence. The stability of these tests indicated that the combination of two surfactants in the mixture led to more stable emulsions as shown in Figure 4.4. The stability tests are consistent with SEM results in Figure 4.2.

Increasing the anionic surfactant SDS concentration in the mixture decreased the interfacial tension between the oil and water. It also reduced the particle size of emulsions. However, the results of the stability tests and zeta measurements indicated that not all BCNFs were at the interface and able to adsorb the same amount of surfactant at the interface. This may be due to some irregular shape, size of crystals, which prevent the homogenous adsorption of the surfactant at the interface. These results are in good agreement with the work of Hu et al. (2015).

4.3.3. Particle Size and Zeta Measurements of BCNCs Emulsions (Eugenol Emulsion Formulated with H_2SO_4 Treated Fiber: A Macro/Nano Emulsions Coated with Bacterial Cellulose Nanocrystal)

BCNCs used in this study were produced by sulfuric acid hydrolysis from bacterial cellulose fibers. Crystal production and characterization were discussed in Chapter 3. Sulfuric acid provides the negatively charged surface anionic sulfate ester groups on the surface of nanocrystals. Negatively charged BCNCs due to the electrostatic repulsions formed the stable aqueous suspensions (De Souza Lima & Borsali, 2004). In literature, many surface modification methods were used to change the surface properties of cellulose as described in the introduction section (4.1). Surfactant modification is one of these methods. A few studies in the literature have been conducted so far on the combination of cellulose crystals with different kind of surfactants and other polymers to enhance the emulsion stabilization (Hu et al., 2015; Kedzior et al., 2017). This part of research hypothesis is that BCNCs could form and enhance the stability of eugenol-in-water emulsions with a combination of CTAB surfactant.

Table 4.3. Zeta potential of BCNCs and BCNCs emulsions with eugenol and with different concentrations of CTAB

Sample Name	CTAB (Molar/ w/v %)	0.277M 8%	0.347M 10%	0.416M 12%	0.485M 14%	0.555M 16%	0.694M 20%
BCNCs-CTAB	Zeta(mV)	2.97±0.49	7.10±0.41	6.14±1.04	3.54 ±0.282	3.12±0.34	14.90±6.73
BCNCs-CTAB Emulsions	Zeta(mV)	24.42±3.65	24.60±2.92	27.46±1.79	22.47±2.97	27.46±1.7	64.76±1.90

Zeta potential of BCNCs was -8.05±0.69 mV (Table 4.1). BCNCs would be repelling each other in water suspension due to the negatively charged surface of the BCNCs. BCNCs water suspension was mixed with CTAB before being emulsified with oil and homogenized with CTAB to produce the electrostatic interactions between negatively charged BCNCs particles and positively charged CTAB molecules. Positively charged CTAB molecule hydrophobic tail would possibly interact with oil, and hydrophilic head would attract with BCNCs, and CTAB may increase the hydrophobicity of the crystals in water suspension. Moreover, CTAB would attach to the oil-water interface to form the Pickering emulsions. Surfactants can change the colloidal surface properties. Hu et al. (2015) found that colloidal particles in the presence of surfactants can form the stable Pickering emulsions. At low cationic surfactant concentrations, surfactants adsorb onto the cellulose crystals and this lead to an increase in the surface hydrophobicity of crystals. However, at high surfactant concentrations, especially above critical micelle concentration, crystals adsorbed more surfactant and this lead to aggregation and formed hydrophilic cationic crystals. However, when these crystals were compared to the initial one they are still more hydrophilic. These surface changes of crystals will affect the wettability of the formed crystals.

Particle size measurements were monitored by the percentage of the number distribution of varying concentrations of CTAB as illustrated in Figure 4.5. The graph indicates that increasing the CTAB surfactant concentration in the formulation decreased the particle size of emulsions, and increased the zeta potential at 64.76 mV. From these results, it may be concluded that CTAB decreased the interfacial tension between the oil and water and this lead to a decrease in particle size and an increase in zeta potential. However, 0.485 M CTAB concentration zeta potential was lower than 0.347M CTAB concentration emulsion formulation (Table 4.3). These results indicated that not all BCNCs were able to absorb the same amount of surfactant and oil at the interface due to the morphology and the shape differences regarding the particle size measurements

mentioned in Chapter 3, the standard deviation of particle size measurements was high, and they do not have a uniform particle size distribution. These findings are agreement with the previous studies (Hu et al., 2015). 0.22M CTAB concentrations in the emulsion formulations showed the monodisperse and mean particle size was 20 nm. The results of SEM images revealed that oil-in-water Pickering emulsions formulations were successfully formulated and stabilized by BCNCs in the presence of CTAB surfactant. Hydrophobic, stearic, and electrostatic interactions between the bacterial cellulose nanocrystals and CTAB may play an impact on the formation of Pickering emulsions.

The mechanism of emulsion stability with cellulose particles can relate to many factors. Previous research has demonstrated the production of Pickering emulsions with low charged bacterial cellulose nanoparticles by hydrochloric acid treatment from bacterial cellulose fibers without any modifications. BCNs stabilized the hexadecane oil-water interface and obtained high stable surfactant free Pickering emulsions (Kalashnikova et al., 2011). In another study, the importance of the surface charge density on the formation of stable emulsions on the cellulose, cotton linters hexadecane emulsion formations has been described. Cellulose crystals with high charge density (above 0.03 e/nm^2) formed unstable emulsions with hexadecane. However, low surface charged crystals produced the stable emulsions with smaller drop size by stabilizing the large surface area at the interface (Kalashnikova et al. , 2012).

Capron (2013) reported the gel-like high internal phase emulsion formation with sulfated cotton cellulose crystals. Cunha et al. (2014) produced less hydrophilic cellulose nanofibers and cellulose nanocrystals from the chemical modification of lauroyl chloride and obtained surfactant free O/W/O double emulsions from produced cellulose.

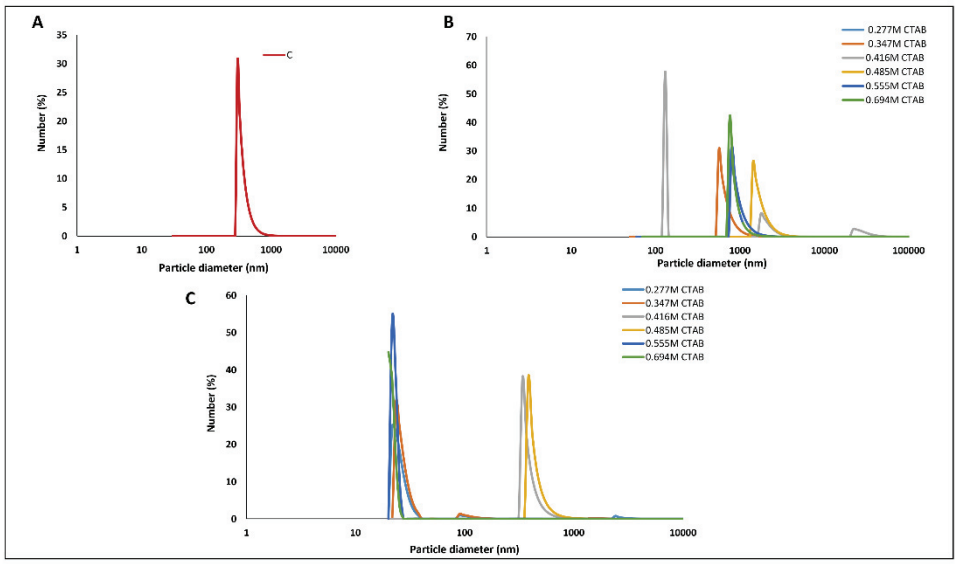

Figure 4.5. Particle size of a) BCNCs b) BCNCs with different concentrations of CTAB c) BCNCs emulsions with eugenol and different concentrations of CTAB

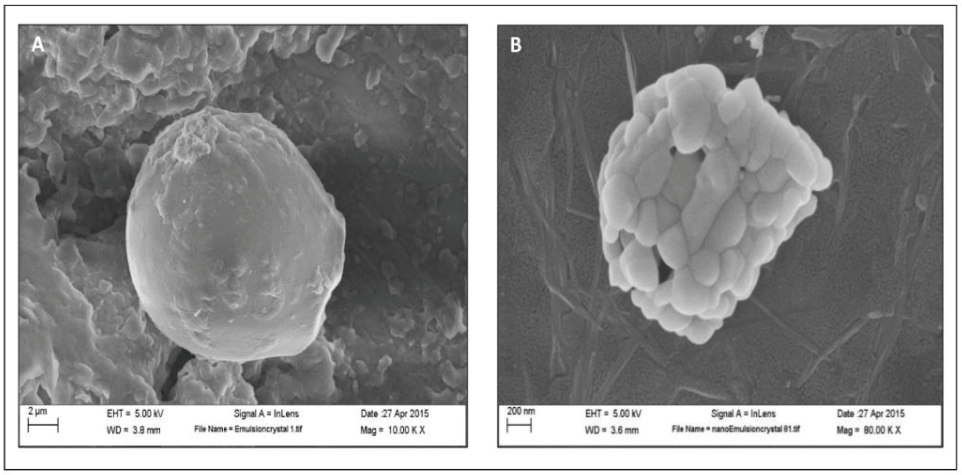

Figure 4.6. SEM images of a) BCNCs eugenol macroemulsion b) BCNCs eugenol nanoemulsion

The shape and surface morphology of BCNCs eugenol emulsions were determined by SEM analysis. As can be seen from SEM images in Figure 4.6, BCNCs emulsions were successfully obtained from sulfuric acid hydrolyzed bacterial cellulose crystals in the presence of CTAB. From Figure 4.6. a) it can be seen that BCNCs covered the surface as macroemulsion and also in Figure 4.6. b) as nanoemulsion.

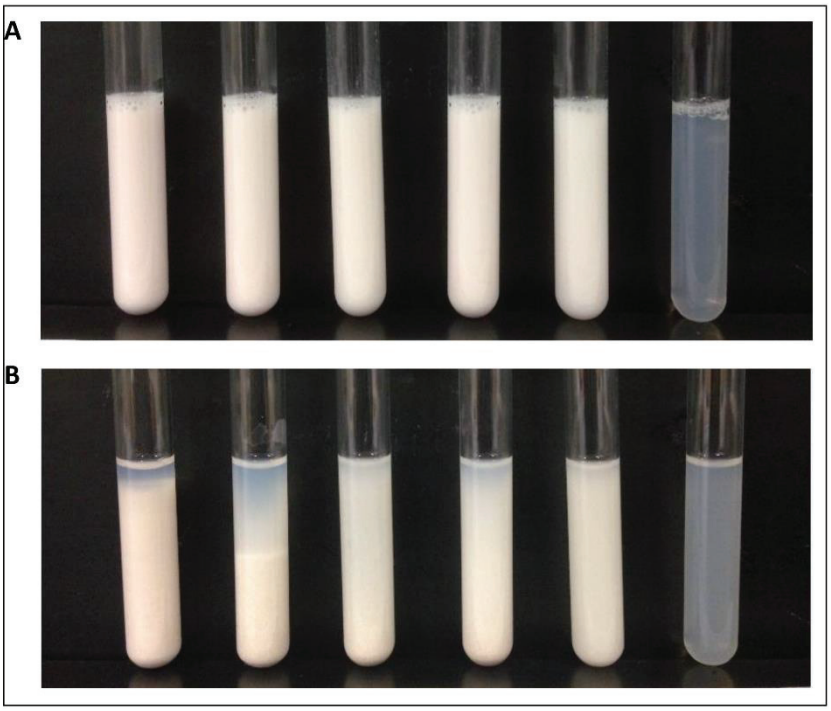

Figure 4.7. Photographic images of a stability test of eugenol BCNCs emulsions formulated with increasing concentration of CTAB surfactant (0.277, 0.347, 0.416, 0.485, 0.555, and 0.694M CTAB) a) at first day and b) the eight days of storage at room temperature

Pickering emulsions were formulated with negatively charged BCNCs, volatile eugenol oil and different concentration of CTAB. Stability tests showed that BCNCs CTAB surfactant emulsions were stable after the 8th day of storage (Figure 4.7). BCNCs Pickering emulsion showed the specific stability characteristics. Phase separation and flocculation have never been observed during the storage. It can be concluded that cellulose crystals adsorbed on the surface of emulsions irreversibly and the stability of emulsions were surfactant concentration dependent. The electrostatic, stearic and hydrophobic interactions between the cationic surfactant and the negatively charged cellulose crystals could be the critical key point for the emulsion formulations.

4.3.4. Reformulation of BCNCs Emulsions with LA

This part of the research hypothesis is that BCNCs could be reformulated and could enhance the stability of eugenol-in-water emulsions with a combination of food grade surfactant LA (Lauric Arginate). This chapter hypothesized that BCNCs and BCNFs could encapsulate the eugenol essential oil in the presence of surfactants.

The results of SEM images support this hypothesis, and Pickering emulsions formulations were successfully stabilized by BCNFs with SDS and BCNCs in the presence of CTAB surfactants. The concept was proved by SDS and CTAB surfactants.

The ability of BCNCs to stabilize Pickering emulsions in the presence of food grade LA surfactant were tested. The dispersion of BCNCs in water was carried out by using the ultrasonic probe in an ice bath. Emulsions were prepared by varying percentages of LA surfactant introduced emulsions, and weight of nanocrystals and oil phase was the same in all emulsion formulations.

The concept was first proved by CTAB surfactant, but CTAB surfactant was not green and food grade surfactant. At the preparation step, CTAB must be heated and kept below its crystallization temperature. Due to these challenges, it would be inconvenient to use in our further experimental setup. Therefore, LA food grade surfactant was used instead of CTAB. In this part of the research, the formulation of BCNCs emulsions was reformulated with eugenol and food grade surfactant LA. BCNCs emulsions would be freeze-dried for further use in the electrospinning process and also the dichloromethane (DCM) which would be used in the spinning process, was not miscible with water. Freeze dried LA (FDLA) emulsions will be used in our next experimental design in electrospinning process. Also in this part of the research, both the freeze dried emulsions (FDLA) and non-freeze dried emulsions (LA) were characterized**.** As it has been mentioned previously, for CTAB surfactant mechanism is the same for LAE emulsions, both are positively charged, but the stabilization mechanism could be slightly different due to the surfactant chemical structure. Therefore, the mechanism is not explained in that part again.

Sulfuric acid hydrolyzed crystals zeta potential was -8.05±0.69 mV (Table 4.1) and crystals with zeta potential with LA at critic micelle concentration were -1.22±3.04 mV. This result indicated that electrostatic interaction between negatively charged crystals and positively charged LA and adsorption of surfactant on the cellulose crystals occurred.

Zeta potential value was slightly different for both 10, 12% LA surfactant concentrations for (FDLA) and (LA) emulsions. At 20%, FDLA concentration zeta potential decreased the approximately half value, which could be due to the freeze-drying effect and aggregation of excess surfactant (Table 4.4, 4.5, 4.6). As can be observed from the SEM images (Figure 4.9), FDLA at 20 % LA concentration aggregation occurred at this concentration, but zeta potential was still above 30. For physical stability, zeta

potential should be greater than ± 30 mV (Honary & Zahir, 2013). These results demonstrated that the Pickering emulsions formulations with lauric arginate were feasible for, in FDLA and LA emulsions. The stability of the emulsions may be probably related to the presence of an LA surfactant at the interface which decreased the interfacial tension.

Table 4.4. Zeta potential of BCNCs at different LA concentrations

LA (w/v %)	10%	12%	14%	16%	20%
Zeta(mV)	10.7±4.02	6.01±4.69	10.9±3.24	9.84±3.11	8.57±4.36

Table 4.5. Zeta potential, Conductivity and pH of BCNCs emulsion at different LA concentrations

LA (w/v %)	10%	12%	14%	16%	20%
Zeta(mV)	47.4±10.8	57.4±6.12	55.2±7.13	53±10.8	58.9±7.92
Conductivity (mS/cm)	3.42±0.005	3.22±0.005	3.12±0.005	2.84±0.005	2.37±0.005
pH	2.50±0.005	2.44±0.005	2.35±0.005	2.34±0.005	2.46±0.005

Table 4.6. Zeta potential, Conductivity, and pH of freeze-dried BCNCs emulsion at different LA concentrations

FDLA (w/v %)	10%	12%	14%	16%	20%
Zeta(mV)	45.12±9.33	53.12±11.21	36.3±9.735	41±15.25	32.05±3.99
Conductivity (mS/cm)	2.74±0.005	2.52±0.005	2.63±0.005	2.57±0.005	2.73±0.005
pH	2.76±0.005	2.62±0.005	2.55±0.005	2.52±0.005	2.4±0.005

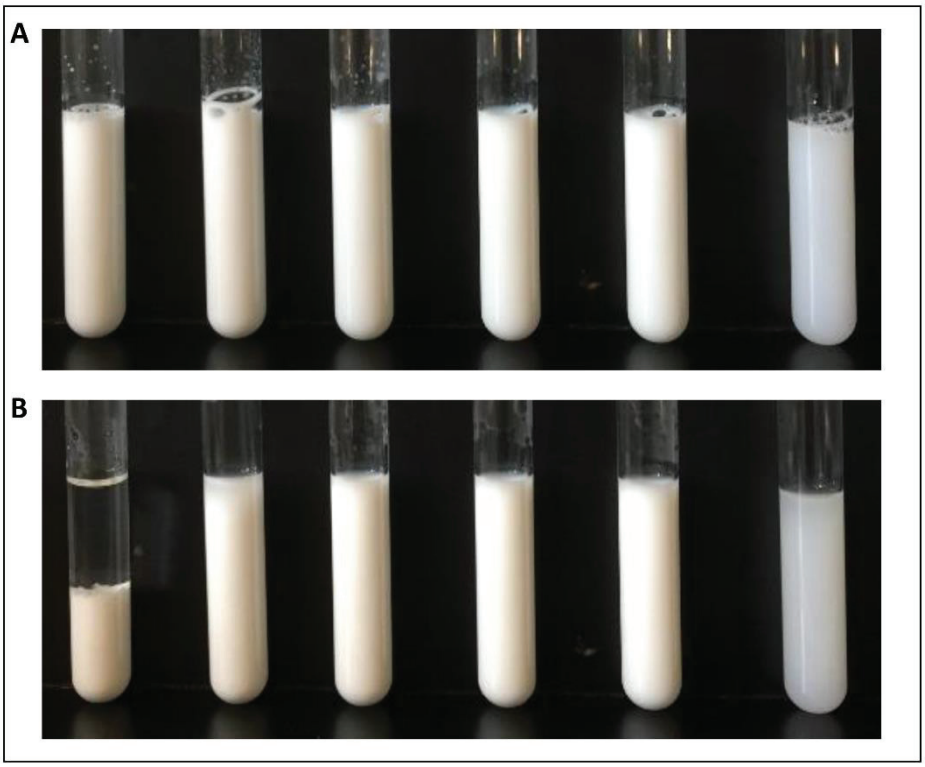

Figure 4.8. Photographic images of eugenol emulsion formulated with BCNCs with LA different concentration (8, 10, 12, 14, 16 and 20%) a) at the first day and b) after the eight days of storage at room temperature

As can be seen from Figure 4.8 and Table 4.5. Increasing the lauric arginate surfactant in BCNCs emulsions lead to an increasein the stability of cellulose emulsions. Hydrophilic-hydrophobic balance and wettability of the cellulose nanocrystals at the interface may have affected the surfactant adsorption (Hu et al., 2015).

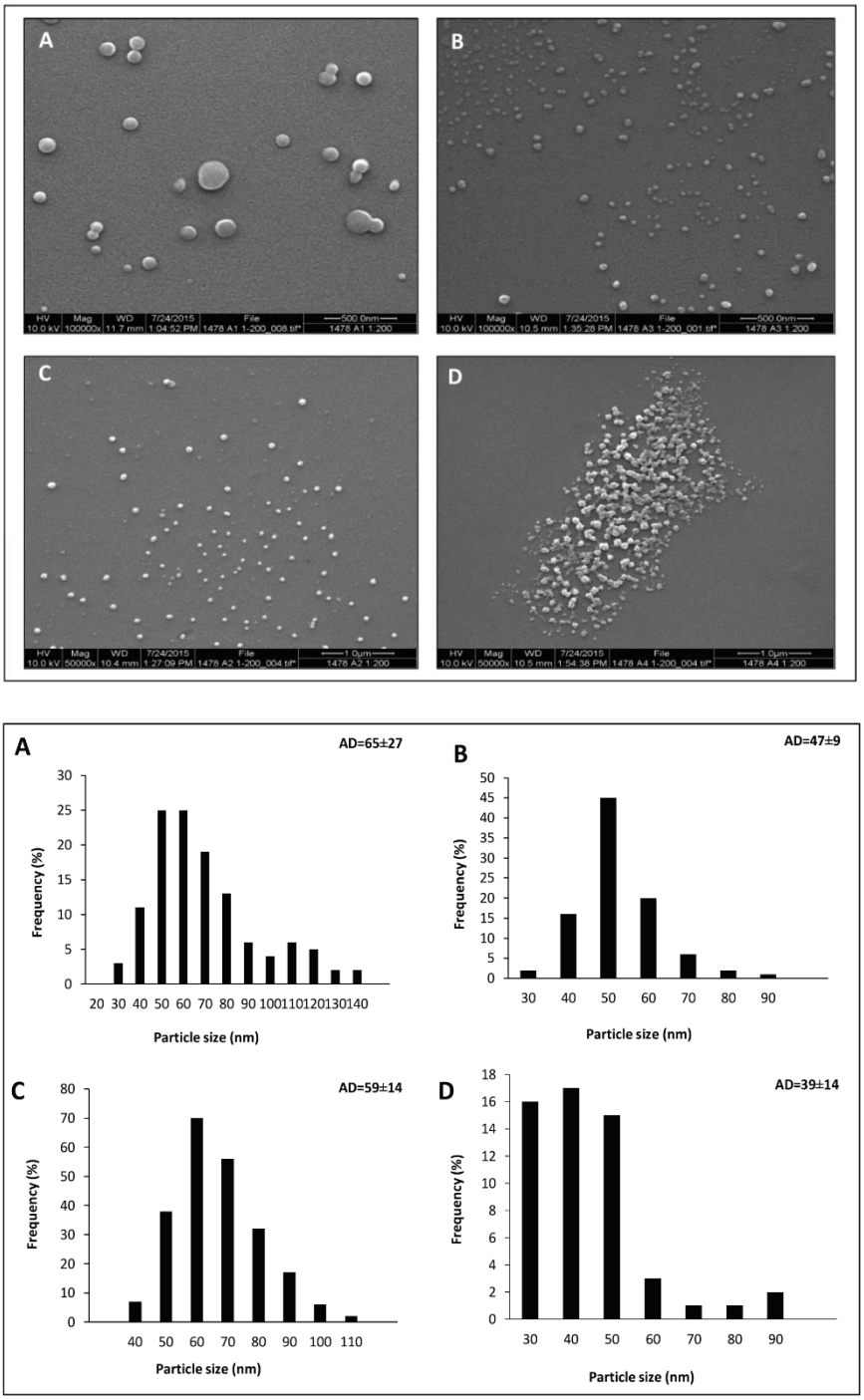

Figure 4.9. SEM images and average diameter (AD) measurements from SEM of BCNCs emulsion with a) 12 % LA and b) Freeze-dried 12% LA c) 20% LA and d) Freeze-dried 20% LA

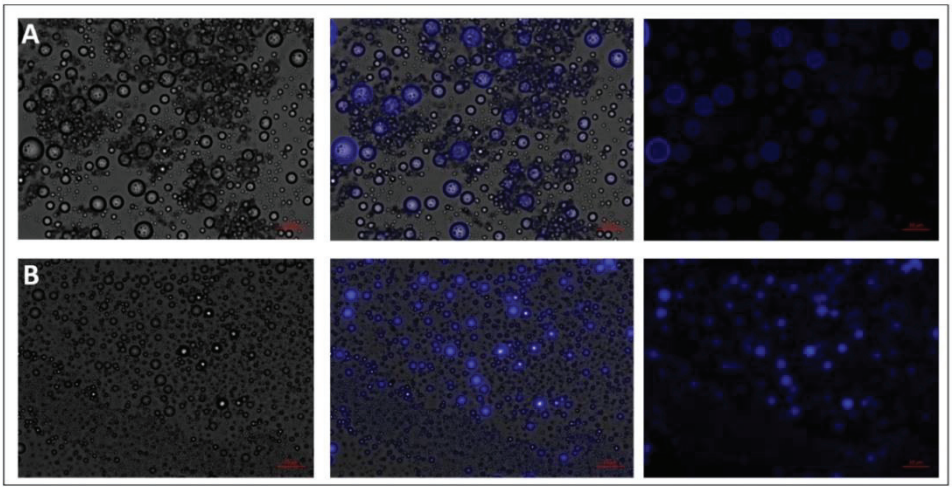

Figure 4.10. Fluorescence microscopy images of BCNCs emulsion with a) 12% LA and b) Freeze dried 12% LA stained with Calcofluor. Scale bars correspond to 10 μm

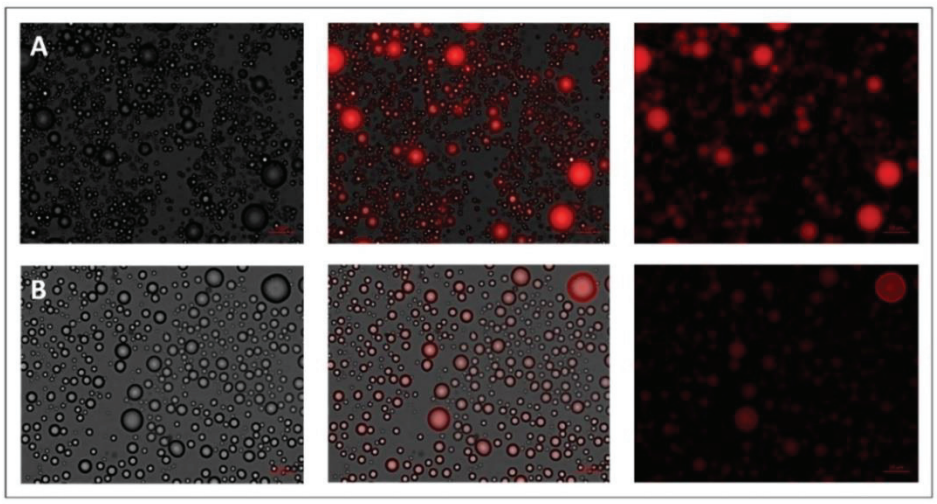

Figure 4.11. Fluorescence microscopy images of BCNCs emulsion with a) 12% LA and b) Freeze dried 12% LA stained with Nile Red. Scale bars correspond to 10 μm

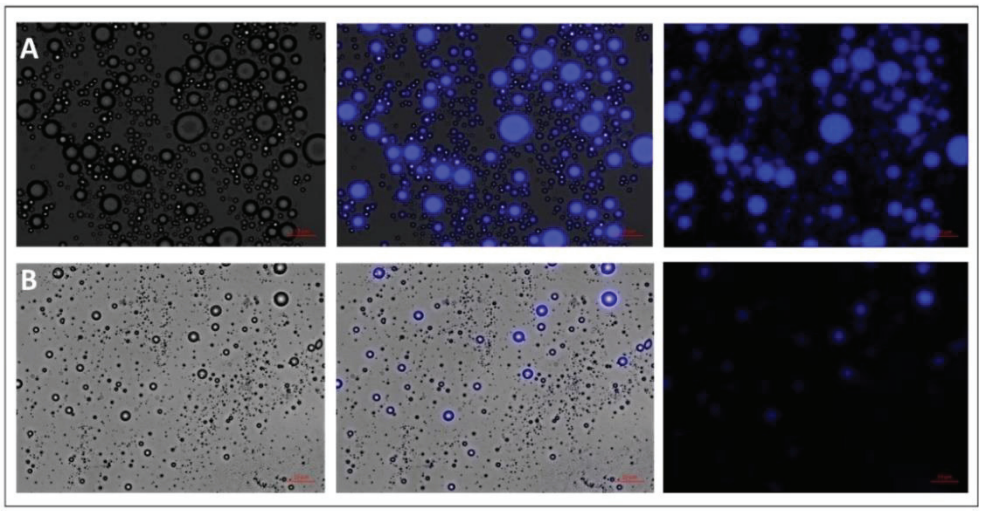

Figure 4.12. Fluorescence microscopy images of BCNCs emulsion with a) 20% LA and b) Freeze-dried, 20% LA, stained with Calcofluor. Scale bars correspond to 10 µm

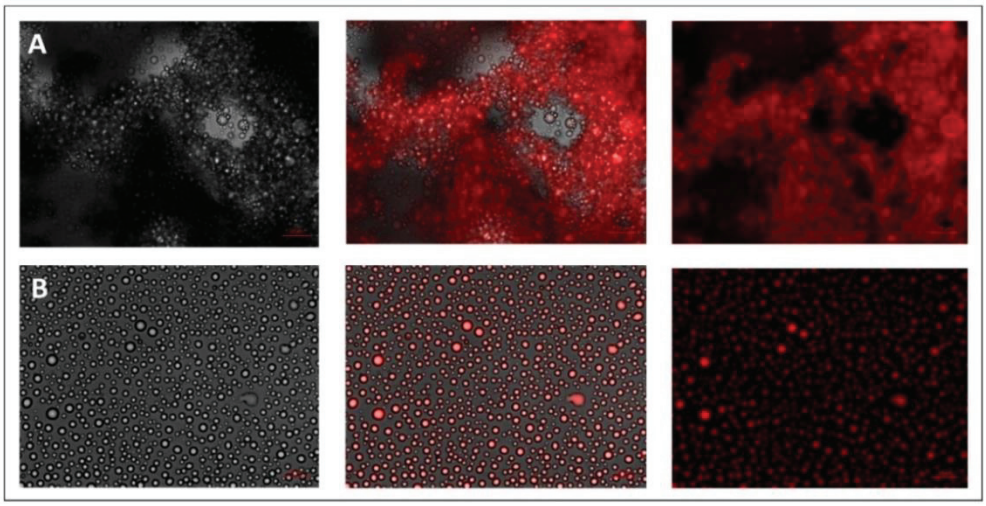

Figure 4.13. Fluorescence microscopy images of BCNCs emulsion with a) 20% LA and b) Freeze-dried 20% LA stained with Nile Red. Scale bars correspond to 10 µm.

Fluorescence microscopy was used to visualize the cellulose particles in the formation of Pickering emulsions (Figure 4.10, 4.11, 4.12, 4.13). The hydrophobic phase (eugenol oil) was stained with Nile red and cellulose was stained with Calcofluor. Fluorescence microscopy results confirmed the formation of LA-BCNCs stabilized emulsions. As can be concluded from the SEM and fluorescence microscopy results, the particle size and also conductivity of the BCNCs emulsions with LA decreased when emulsions were freeze-dried (FDLA) (Figure 4.10-b, 4.11-b, 4.12-b, 4.13-b). However,

the pH value of freeze-dried emulsions was higher than the non-freeze-dried BCNCs emulsions. This may be due to the aggregation phenomena of LA emulsion.

The formulation and stability of emulsions with cellulose and surfactants are a complex phenomena, and many critical factors such as the adsorption of surfactant on the surface of cellulose crystals, the size, shape and concentration of cellulose, self-assembly of cellulose structure, intermediate wettability of cellulose, cellulose surface properties according to modification, and concentration of surfactants, surfactant chemical structure and concentration of oil may play a role in the formulation and stabilization of Pickering emulsions. The adsorption of surfactants on the surface of cellulose depends on many factors such as surfactant chemical structure and the '' Hydropile-Lipophile Balance'' (HLB) value, the cellulose charge and ionic strength of the emulsion solution (Alila et al., 2005; Hu et al., 2015).

Recently, researchers have shown an increased interest in colloidal particles stabilized emulsions. The mechanism of emulsion stability with colloidal particles such as cellulose is a complex phenomenon and can be related to many factors. Previous research has demonstrated that colloidal particles like rod-like cellulose crystals can adsorb at the oil-water interface and form the stable Pickering emulsions (Capron, 2013; Kalashnikova et al., 2011, Kalashnikova et al., 2012). The most interesting approach supported by Kalashnikova et al. (2013) is that cellulose has a mainly hydrophilic character, and it shows homogenous dispersion in the aqueous phase to form the oil in water Pickering emulsions. Neither crystalline lattice nor morphology effects the emulsion stability; the surface charge density is a critical key point on the formation of stable emulsions. Also, the amphiphilic character of cellulose and wetting ability of cellulose at interface impact the production of stable emulsions (Kalashnikova et al., 2012). The surface modification also influenced the stability of the produced emulsions. Tempo-oxidized bacterial cellulose is superior to the native bacterial cellulose to stabilize oil-in-water interface due to the wetting ability of interface and smaller particle size (Jia et al., 2016). Another chemical surface modification has been done via non-covalent surface modifications of cellulose with adsorption of surfactants. Adsorptions between cellulose and surfactants might be due to the hydrogen bonds, van der walls forces, hydrophilic affinity and electrostatic interactions (Habibi et al., 2014; Heux, Chauve, & Bonini, 2000).

However, Cherhal, Cousin, and Capron (2016) emphasize the differences of the crystalline plane of the cellulose and state that the structure of cellulose had an impact on

the drop size and coverage. The hydrophilic (200) crystalline plane was able to interact with the interface and influenced the emulsion stability. The detail crystalline structure of sulfuric acid treated BCNCs was given in Chapter 3.

The results of this chapter indicated that emulsion formulation with BCNFs needs to be mixed with two surfactants and bacterial cellulose fibers stabilized emulsion systems in the presence of two surfactants will be more complex systems for further studies of this research. Also, emulsion particle size is big for electrospinning process compared to emulsion formulated with BCNCs. Reformulated BCNCs with LA emulsions had a low particle size and high zeta potential, and these emulsions can be used in spinning solution to form the functional fibers. The knowledge from this chapter will be helpful for the rational design of the electrospinning process.

4.4. Conclusion

The formulation and stability of eugenol essential oil with BCNFs and BCNCs cellulose in the presence of different surfactants was achieved. However, the stability of emulsions with BCNFs and BCNCs is very complex, and many critical factors may play in the formulation and stabilization of Pickering emulsion formulations. To understand the detailed mechanism of bacterial cellulose stabilized emulsions in the presence of LA, CTAP and SDS surfactants, further research is required. Surfactant chemical structure and concentration would be the most critical parameter for the stability of emulsions. BCNCs have a negative charge, and BCNFs have no charge. Pickering emulsions stabilized by BCNFs and BCNCs, and successfully produced BCNFs Pickering emulsions with eugenol essential oil in the presence of negatively charged emulsifier SDS and BCNCs Pickering emulsions with a positively charged emulsifier CTAB and LA. Bacterial cellulose based emulsions systems could be a potential carrier for bioactive volatile compounds. Developed Pickering emulsions can be used in bioactive food packaging applications. Edible, non-digestible bacterial cellulose carriers may be considered as prebiotic for human health benefits.

CHAPTER 5

ELECTROSPINNING OF POLY(LACTIC ACID) (PLA) WITH EUGENOL BCNCs EMULSIONS

5.1. Introduction

There has been growing interest in using natural volatile compounds in the active food packaging recently. Volatile compounds such as essential oils (EOs) and plant extracts can be directly added to the packaging, and vapor phase of volatile compounds can be released into the headspace of the package and adsorbed on the food surface inside the package system (Robertson, 2014). Some researchers have suggested the use of essential oil vapors as using antimicrobial compounds against food spoilage microorganisms is a promising way to create a protective atmosphere between the food and package (Peretto et al., 2014; Kara et al., 2016).

Essential oils (EOs) are categorized as generally recognized as safe (GRAS) by U.S. Food and Drug Administration (FDA, 1973). EOs are widely used in many foods as a preservative and flavoring substance. Antibacterial properties of EOs are related to their lipophilic character (Helander et al., 1998). Eugenol (2-methoxy-4-allylphenol) is, an allyl chain substituted guaiacol and phenylpropanoid group chemical agents, the major component of clove oil (Farag, Daw, Hewedi, & El-Baroty, 1989; Jirovetz et al., 2006; Seo et al., 2010). Eugenol has antimicrobial activity against pathogenic and spoilage bacteria (Sanla-Ead, Jangchud, Chonhenchob & Suppakul, 2012) and eugenol exhibit an excellent antioxidant activity (Cui et al., 2017). Volatile essential oils have been used for food preservation applications, such as cinnamon and eucalyptus were used for the preservation of postharvest quality of strawberry (Tzortzakis, 2007) and ally isothiocyanate vapor for grape and meat preservation (Kara et al., 2016). Another study was carried out based on the incorporation of carvacrol and methyl cinnamate vapor into strawberry pure edible films (Peretto et al., 2014). Other researchers investigated the antimicrobial activity of cinnamon and clove oil with a combination of the modified atmosphere (Rodriguez-Lafuente, Nerin, & Batlle, 2010).

The challenge of using essential oils in food packaging application is that they are sensitive to the environmental factors, and they are chemically unstable compounds. Eugenol essential oil is highly volatile essential oil, and it is hard to protect eugenol from environmental factors (moisture, heat, oxygen, and light) during processing and handling (Bakry et al., 2016). To enhance its stability, volatile eugenol can be encapsulated in emulsion formulation such as via cyclic oligosaccharides cyclodextrin (Seo, Min, & Choi, 2010) and biopolymer based electrospun fibers (Kayaci et al., 2013).

Electrospinning is a convenient technique for encapsulating the heat-sensitive active agents such as essential oils (Vega-Lugo & Lim, 2009). During electrospinning, high voltage is applied to a polymer solution and fibers are formed after solvent evaporation (Sousa et al., 2015). The significant challenge with active agents in electrospinning is that an organic solvent is used for dissolving the polymer may decrease the bioavailability of the active compound. Emulsion and coaxial electrospinning are more convenient to form the core-shell structure to prevent the bioactivity. The idea behind the electrospinning of polymer with emulsions is to produce fibers with sustain release, high encapsulation efficiency and high thermal stability for active agents compared to conventional spinning (Kayaci et al., 2013; Wang, Tong, Tse, & Wang, 2011). In the conventional electrospinning technique, compound encapsulated nanofibers have a porous structure, and high surface area allows for a rapid release of the active compound (Kriegel, Kit, McClements, & Weiss, 2009). There are few examples of volatile compounds encapsulated fibers. For instance, Mascheroni et al. (2013) obtained the nanofibers with encapsulating the volatile perillaldehyde in the β-cyclodextrin complex and pullulan and Kayaci et al. (2013) encapsulated the eugenol cyclodextrin inclusion complex in polyvinyl alcohol (PVA) electrospun nanofibers.

Poly(lactide) (PLA) is derived from fermentation of lactic acid (2-hydroxy propionic acid), and as an alternative to petroleum-based materials, it is commonly used for food packagings such as drinking and salad cups, since it is compatible with many foods (Auras et al., 2004; Munteanu et al., 2014). Lauric arginate (LA) is a cationic, food grade surfactant and derived from lauric acid, L-arginine, and ethanol (Nair, Nannapaneni, Kiess, Mahmoud, & Sharma, 2014) and LA was approved by Food and Drug Administration of United states in 2005 as generally recognized as safe (GRAS) antimicrobial (USDA, 2005).

Contaminated fresh food consumption cause the foodborne illness. Tomatoes as fresh produce are the second largest consumed vegetable in the world (FAO, 2011).

Tomatoes can be contaminated by pathogenic, and spoilage microorganisms by pre-and post-harvest factors. Due to its porosity structure, tomatoes stem scars are subjected to bacterial contamination (Jin & Gurtler, 2012). Recent research has indicated that volatile antimicrobials in the vapor phase may significantly decrease the pathogen population on tomatoes. Methyl jasmonate and ethanol may increase the shelf life of fresh cut tomatoes (Ayala-Zavala et al., 2008a) and allyl isothiocyanate, carvacrol, and cinnamaldehyde in the vapor phase are used on the whole and sliced tomatoes for inactivation of *E.coli* O157: H7 and *Salmonella* (Obaidat & Frank, 2009). Another research has tested the effectiveness of hexanal vapor into the headspace of the package for controlling the *Botrytis cinerea* to extend the shelf life of tomatoes (Utto, Mawson, & Bronlund, 2008). *E.coli* is the second bacterium that causes the foodborne outbreaks to tomatoes after *Salmonella enterica*, *E. coli* and *Listeria* are indicators of contamination in post-harvest processes (Beuchat & Brackett, 1991; Forslund et al., 2012).

We hypothesize that cellulose emulsions could be spun with PLA polymer to fabricate the antimicrobial electrospun fibers for food packaging applications. Active fibers/films could deliver the volatile eugenol vapors from the electrospun fibers to the headspace of the package. To test this hypothesis, PLA, eugenol, LA and Pickering emulsions of BCNCs were used in the spinning solution formulations to fabricate the beaded free active PLA-composite films.

As far as we know, no studies have been reported on electrospun PLA/cellulose emulsion formulations with eugenol for food applications. In literature, limited information is available about eugenol efficacy in vapor phase for food application, and this is the first research study using eugenol formulated emulsion fibers at headspace to improve the safety of packed grape tomatoes.

5.2. Experimental

5.2.1. Materials

Poly(lactic acid) (PLA) with a weight-average molecular weight of 148 kDa and a number-average molecular weight of 110 kDa (product No. 4060D) was obtained from NatureWorks LLC (Minnetonka, MN, USA). Dichloromethane (DCM) was purchased from Fisher Scientific (Fair Lawn, NJ, USA). *Gluconacetobacter xylinus* (ATCC® 700178™) freeze-dried culture, *Listeria innocua* (ATCC 51742) and *Escherichia coli* K12 (ATCC 23716) were purchased from American Type Culture Collection (Manassas, VA, USA). Sulfuric acid (H_2SO_4, 95.0 to 98.0 w/w %) was purchased from Thermo Fisher Scientific Inc. (Waltham, MA, USA). Eugenol oil (Natural, ≥98 % W246719) was purchased from Sigma-Aldrich (St. Louis, MO, USA). CytoGuard lauric arginate LA 2X was kindly provided by A&B Ingredients (Fairfield, NJ, USA). Tryptic Soy Agar was purchased from BBL/Difco Laboratories (Sparks, MD, USA) and Palcam Agar was obtained from Oxoid™ (Basingstoke, Hampshire, England, UK).

5.2.2. Emulsion Preparation of BCNCs with LA Surfactant

Bacterial cellulose nanocrystals (BCNCs) were produced from bacterial cellulose fibers by sulfuric acid hydrolysis according to a method previously described in chapter 3. BCNCs Pickering emulsions were stabilized by BCNCs with a positively charged emulsifier lauric arginate according to the method as previously described in chapter 3 in Section 4.3.4. Briefly, oil-in-water (O/W) emulsions were prepared with a sulfuric acid treated bacterial cellulose nanocrystals aqueous suspension, eugenol oil and lauric arginate (LA) via ultrasound dispersion method. In all emulsions, the oil and BCNCs concentration was the same (3%-0.1% (w/w)). Six different LA concentrations in the aqueous phase were used in the emulsion formulation, 8, 10, 12, 14, 16 and 20% (w/v), respectively. The 0.1 wt % of BCNCs suspensions were sonicated with a probe sonicator (Cole-Parmer, 6mm probe, IL, USA) at 1min for the proper dispersion, followed by adding 8-20% (w/v) LA and 3% (w/w) eugenol sonicated for 30 seconds in an ice bath. Emulsion samples were dried at -35°C and 135 millitorr with freeze drier (VerTis, NY, USA) for 24 h.

5.2.3. PLA Films Fabrication by Casting

PLA pellets were dissolved in dichloromethane (DCM) to a final PLA/DCM concentration of 5 wt % using a method given by Kara et al. (2016). The electrospinning solutions were prepared in closed borosilicate glass to avoid solvent evaporation and stirred overnight at room temperature. Ten milliliters of each film-forming solution was spread at room temperature over a glass plate using a K-101 Control Coater apparatus with a spiral wound meter bar (RK Print-Coat Instrument Ltd., Royston, UK). The spread solution was dried in a hood at room temperature. Finally, the films were peeled off from the supports and cut into 10x18 cm dimensions. Films with a final thickness of 0.011-0.013 mm were stored in a refrigerator until it's use.

5.2.4. Spinning Operation Conditions of PLA Fibers

Electrospun PLA/emulsion fibers were produced at room temperature by electrospinning technique using a NaBond NEU-PRO unit (NaBond Technologies Co., Limited, China). A tubeless spinneret was placed inside the spinning chamber and connected to an external syringe pump (Veryark, model TCI-IV). The spinning solutions were loaded into a 5 mL syringe with a metallic needle (outer diameter/ length=0.6 mm x30 mm and inner diameter =0.560 mm) and placed in the tubeless spinneret. Preliminary trials showed that best electrospinning conditions for fiber formation were, a flow rate of 3 mL/h, an applied voltage of 22 kV and a distance from the needle tip to the collector of 12 cm, with the spinneret moving at constant x-axial sliding speed (60 mm/s for a 3.8 rps in the tachometer) and the drum motor set to zero speed. Each spinning solution was mixed with freeze-dried emulsion and vortexed before spinning. Five milliliter of solution was electrospun onto the PLA cast films (10x18 cm) by placing the films on drum collector covered with aluminum foil. The amount of loaded fibers was checked by weighing the PLA films before and after fiber loading. All experiments were carried out in triplicate.

5.2.5. Electrical Conductivity Measurements PLA Films

The electrical conductivity of PLA-emulsions spinning solutions was measured using an EC 215 conductivity meter (Hanna, RI, USA).

5.2.6. Scanning Electron Microscopy of PLA Films

The surface morphology of the electrospun fibers was performed with scanning electron microscopy (SEM), FEI Quanta 200 F, (Hillsboro, OR, USA) using an accelerating voltage of 10KV in high vacuum mode. Before observation, each sample was mounted on a SEM stub with double-sided adhesive carbon tape. The PLA fibers were coated with gold for 30 seconds with EMS 150R ES Sputter Coater (EM Sciences, Hatfield, PA) and analyzed. The diameters of PLA films were measured using ImageJ software and, at least 100 measurements for each sample were taken to determine the mean fiber diameter. Images were collected at 2500 magnification.

5.2.7. Fluorescence Microscopy Images of Electrospun PLA/Emulsion Fibers-Grafted to PLA Films

The composite electrospun PLA/emulsion fibers-grafted to PLA films fluorescent images were acquired using a method given by Gu and Catchmark (2013). Electrospun PLA/emulsion fibers-grafted to PLA films were stained with Calcofluor white stain, and one drop of 10% sodium hydroxide was added to the fibers to dissolve the PLA and leave the cellulose. Samples were cover with the glass slides, and they were examined under a fluorescence microscope after 20 min incubation.

5.2.8. Mechanical Properties of PLA Films

The thickness of each film was measured at eight different points using a Mitutoyo Absolute thickness gauge (Mitutoyo, Kanagawa, Japan). Elongation, tensile strength and tensile modulus of films were determined using a Texture Analyzer TA-XT2-Texture analyzer (Texture Technologies Corp., NewYork, USA). Samples of films were cut into

strips with dimensions of 4x1 mm. Five kg load cell was used during measurements. The initial distance between grip was 50 mm, and crosshead was 50mm/60 second according to ASTM Standard Method D 882-02 (ASTM, 2002). The films were conditioned at 50±5 % relative humidity and 25 °C for 7 days before testing. At least six replicates were performed, and averages of measurements were taken.

5.2.9. Antimicrobial Properties of Electrospun PLA/Emulsion Fibers-Grafted PLA Films

The antimicrobial efficacy of the produced films, that is, EE, EF and EG Films containing 1.3, 3.0, 6.0 mg/cm^2 eugenol (Table 5.2) in headspace was tested on *Listeria innocua* and *Escherichia coli* K12 as model microorganisms on agar media. Tryptic soy agar (TSA) plates for *Escherichia coli* K12 and Palcam agar plates for *Listeria innocua* were surface-inoculated (100 µl, approximately 10^5 cells for EF film and100 µl, approximately 10^7 cells for EG film). The inoculated plates were placed in a clamshell PET box (250 ml) with a piece of antimicrobial film stuck on the lid of the box. Boxes without films were used as controls. The boxes with TSA and Palcam plates were incubated at 35˚C for 24 h and 48 h, respectively. The bacterial populations were enumerated by counting the colony forming units (CFU).

5.2.10. Antibacterial Activity of Electrospun PLA/Emulsion Fibers-Grafted to PLA Films on Grape Tomatoes Stem Scar

The antimicrobial activity of the produced films in headspace was tested on grape tomatoes as real food application. Grape tomatoes were purchased from the local supermarket and stored at 4˚C until used. Grape tomatoes were washed with tap water and then rinsed with 70% ethanol. Samples were dried under the biohood for 2 hours. Each stem scar spot was inoculated with 50 µl of inoculum (*L. innocua* or *E. coli* K12). Non-inoculated tomatoes were used as a control. The inoculated tomatoes were dried under the hood for 1 hour, and then tomatoes were placed in clamshell PET box (250 mL) with antimicrobial film stuck on the lid of the box, and tomatoes placed in plastic PET box without film served as a control. All boxes were placed in 10 ˚C for 24 h and 48 h before microbiological analysis. Two tomatoes were randomly selected from a box; each stem scar was removed with sterile scissors, placed in a stomacher bag with 10 ml of

0.1% Peptone water, and stomached for 2 min at 230 rpm. Serial dilutions of the suspensions were plated (100 µl) onto TSA and Palcam plates and incubated for 24 h/48 h at 35˚C. Colony forming units (CFU) were used for the enumeration of the bacterial populations counting.

5.2.11. Statistical Analysis

The statistical significance of differences was determined by analysis of variance (ANOVA). The mean values were compared by a Tukey's test. Differences were considered significant if $p<0.05$.

5.3. Results and Discussions

5.3.1. Composition and Morphology of PLA Films

The cellulose nanocrystals were produced from *Acetobacter xylinum* by sulfuric acid hydrolysis according to a previously reported procedure in Chapter 3. Morphological, particle and surface analysis of sulfuric acid hydrolyzed bacterial cellulose nanocrystals (BCNCs), and production of freeze dried BCNCs-eugenol lauric arginate emulsion were explained in Chapter 4. Freeze dried BCNCs-eugenol emulsions with 12% LA surfactant, which was used in this chapter in the spinning solution formulations, the average particle size was 47±90 nm, and zeta potential was 53.12±11.21 mV.

In the electrospinning part of this study, the poly(lactic acid)(PLA) fiber mats supported by PLA solution cast film were produced for headspace food packaging applications.The grafting was implemented by the method described by Kara and co-workers (Kara et al., 2016). This chapter aimed to fabricate the nanofibers containing volatile eugenol oil encapsulated nanostructures for delivering the eugenol vapor to the headspace of the package. For the screening experiments, first 5-8-10-12 % PLA concentrations were dissolved in dichloromethane (DCM) as a spinning solution and spun onto the PLA solution cast film. The thickness of the PLA solution cast film was 12±2 µm. It was observed from trial experiments that PLA solution concentration above 8 % was very viscous and blocked the needle, even at PLA 8 % concentration, it is hard to

observe the spinning jet formation, and the needle was sometimes blocked, and the solution did not come down. The high solution viscosity and concentration may result in the formation of a localized gel; therefore high concentration of the solution may prevent the proper formation of Taylor cone for the producing of the fibers (Kriegel et al., 2008).

In electrospinning process, the polymer concentration is one of the key factors that affect the fiber morphology and its properties. The results of Xu and Hanna's (2006) study showed that the effects of the solvent type on the physical properties of PLA solution and at 3 % PLA solution in dichloromethane conductivity was 0.039 (μScm^{-1}).

They observed that the conductivity of PLA solution was changed by changing the solvent type; 0.039 μScm^{-1} PLA in DCM, 0.058 μScm^{-1} in 1,2-dichloromethane, 0.412 μScm^{-1} in 1,2-dichloromethane/acetone and 2.26 μScm^{-1}1,2-dichloromethane/N,N-dimethylformamide. In our case, the electrical conductivity of 5 % wt PLA/DCM was too low to measure (Table 5.1). The addition of BCNCs-eugenol-LA emulsions to the PLA solutions increased conductivity values to 2.52±0.0054 ($mScm^{-1}$). The combination of all emulsion formulation compositions electrical conductivity measurements were given in Table 5.1. It was interestingly observed that the electrical conductivity of 5 % wt PLA/DCM solution was increased with the addition of each emulsion compositions materials; LA surfactant, eugenol essential oil and BCNCs; 0.3, 0.4, and 0.5 (μScm^{-1}), respectively. Spinning experiments were carried out with 5 % PLA-DCM solution and spun onto the PLA solution cast film. In this part of the study, PLA solutions first prepared in various combinations of emulsion compositions materials and with freeze dried emulsions (Table 5.2) to investigate the effect of each different emulsions compositions and the properties of freeze dried emulsions solutions on fiber morphology and diameter. The structure of fiber mats was examined by a SEM analysis. The best electrospinning conditions were optimized according to the SEM results. Regarding the SEM results in PLA cast film prepared at 5 % PLA-DCM solution had smooth and crack defects free surface (Figure 5.1 A). Kara et al. (2016) described the grafting fibers as'' horticulture-to insert the scion (the PLA fibers) onto the rootstock (the PLA film) to form a new entity''. Electrospun PLA fibers grafted PLA films and electrospun PLA-eugenol fibers grafted PLA films showed beaded morphology (Figure 5.1 B and 5.1 C). Electrospun PLA-LA surfactant fibers grafted PLA films (Figure 5.1 D) formed smooth and beaded free fibers, but these ''puffy like cotton'' fibers were not able to stick to the PLA solution cast film. Addition of emulsion formulations to the spinning solutions formed perfect spinning jet and formed the bead free and homogenous

fibers (Figure 5.2 A-B-C). Increasing the emulsion concentration in the spinning solution increased the fiber diameter 648±193 in EE film, 781±400 EF film and 857±179 nm EG films. SEM results indicated that emulsions were homogenously dispersed throughout the fibers and formed bead free fibers structure. These results demonstrated that BCNCs-eugenol emulsions formulations were technically feasible for electrospinning applications. However the system had some challenges to overcome, for instance, the concentration of PLA and emulsion in the spinning is a critical key factor to prevent the phase separation of the spinning solution. During the spinning phase, separation and needle blocking were rarely observed; it might have been to the non-encapsulated big cellulose crystals in the emulsion formulations. Moreover, the sulfuric acid hydrolyzed crystals as the final material may have some fibrils. One of the drawbacks of cellulose crystals spinning with organic solvents is their poor dispersibility. The surface chemical modification can change the surface properties of cellulose, change the hydrophilicity and hydrophobicity of cellulose, and enhance the dispersibility in organic solvents (Habibi, 2014). Some researchers investigated the surfactant effect on the dispersion of cellulose for example in the study of Kim et al. (2009) nonionic surfactant sorbitan monostearate was used to enhance the dispersion of hydrophilic cellulose particles in the polystyrene matrix and the study of Bondeson and Oksman (2007) beycostat A B09 (an acid phosphate ester of an ethoxylated nonylphenol) was mixed with PLA to increase the crystals in the nanocomposite.

The electrospinning processing parameters that affect the fibers morphology were reported in the review of the Ghorani and Tucker (2015); these are the polymer solution concentration, conductivity, surface tension, applied voltage, feed rate and needle distance between the collector.

In literature, there are many examples of emulsions spinning research (Kriegel et al., 2009). However, there are few examples of PLA-cellulose with emulsions spinning research. One has been done by Li, Ko and Hamad (2013), they produced the PLA-cellulose fibers with water-in-oil emulsion. A few studies have been published on PLA and volatile essential oil containing fibers. Kara et al. (2016) and Vega-Lugo and Lim (2009) investigated the effect of ally isothiocyanate (AITC) concentration on the fiber morphology. Moreover, there are few examples of volatile compounds encapsulated fibers. In their study, Mascheroni et al. (2013) obtained the nanofibers with encapsulating the volatile perillaldehyde in the β- cyclodextrin complex and pullulan.

Table 5.1. Electric Conductivity of Film Composition Materials

Solutions	Conductivity (mS/cm)
PLA 5%	nd
PLA 5% + 0.01g BCNCs	nd
DCM	nd
PLA+ 12%LA	0.03
PLA+ 12%LA +EU	0.04
PLA+ 12% LA% + 0.01 BCNCs	0.05

nd: Not detectable

Table 5.2. Composition of the Films

PLA Films	Composition of tested Films
A	Solution cast neat PLA Film
B	Electrospun PLA fibers-grafted to PLA film
C	Electrospun PLA/Eugenol fibers-grafted to PLA film
D	Electrospun PLA/ LAE fibers-grafted to PLA film
EE	Electrospun PLA/emulsion fibers-grafted to PLA film (1.3 mg/cm^2 eugenol containing cellulose-emulsion)
EF	Electrospun PLA/emulsion fibers-grafted to PLA film (3.0 mg/cm^2 eugenol containing cellulose-emulsion)
EG	Electrospun PLA/emulsion fibers-grafted to PLA film (6.0 mg/cm^2 eugenol containing cellulose-emulsion)
CG	Electrospun PLA fibers-grafted to PLA film (6.0 mg/cm^2 eugenol containing film without cellulose)

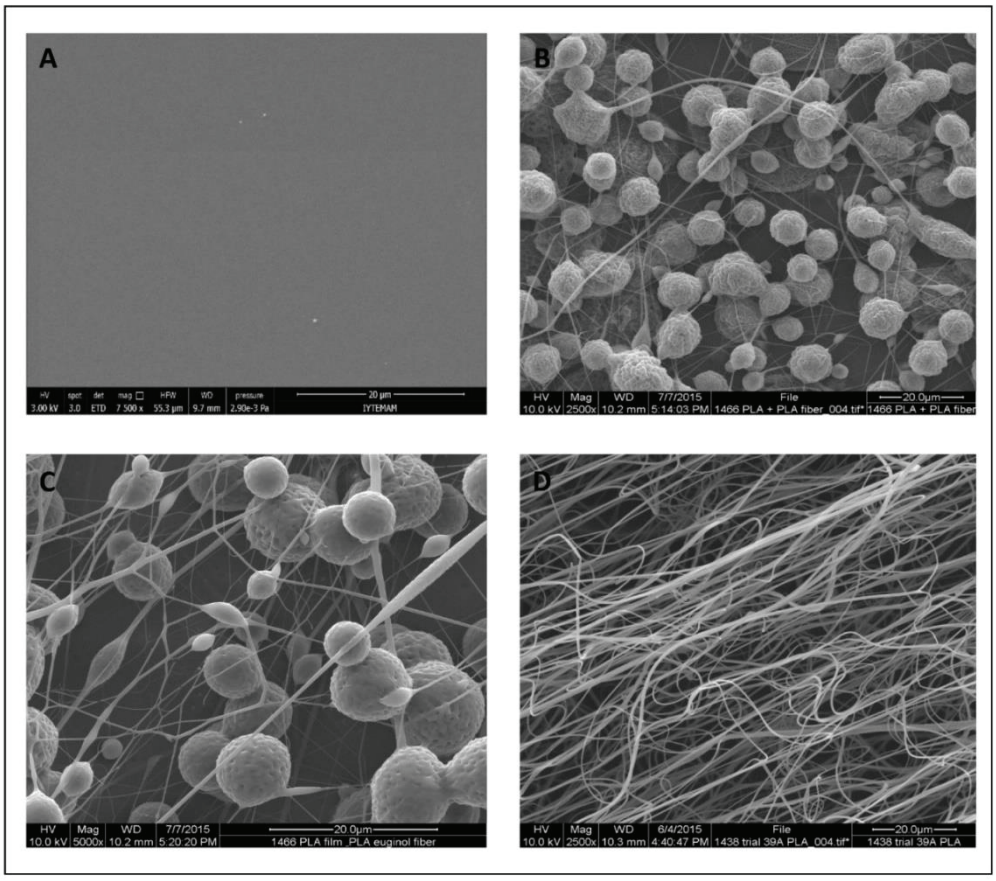

Figure 5.1. Scanning electron microscopy images of a) Solution cast neat PLA Film b) Electrospun PLA fibers-grafted to PLA film c) Electrospun PLA/eugenol essential oil fibers-grafted to PLA film d) Electrospun PLA/LA surfactant fibers-grafted to PLA film

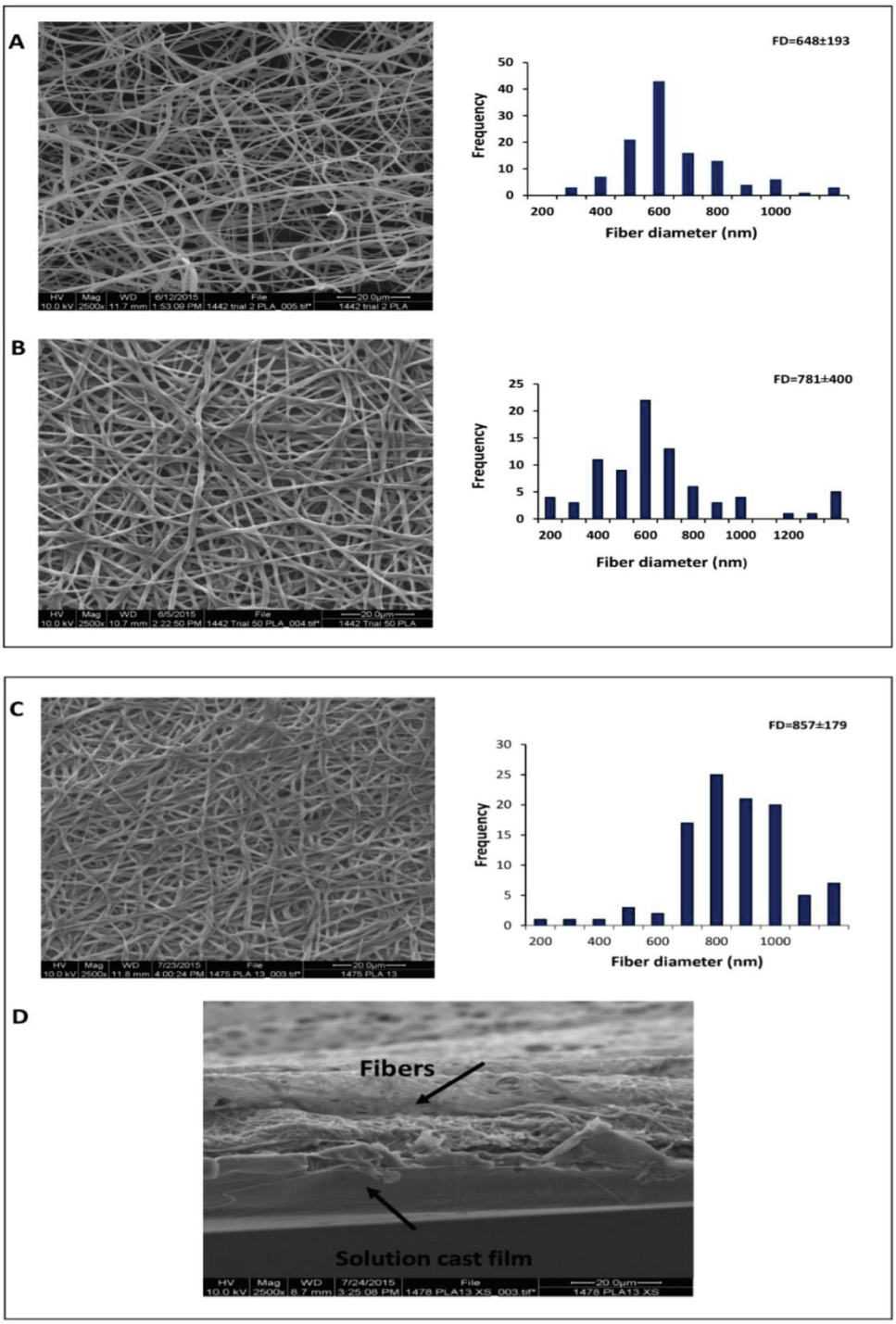

Figure 5.2. Scanning electron microscopy images of a) EE, b) EF, c) EG Electrospun PLA/emulsion fibers-grafted to PLA film d) Cross-section images of EG-Electrospun PLA fibers-grafted to PLA film

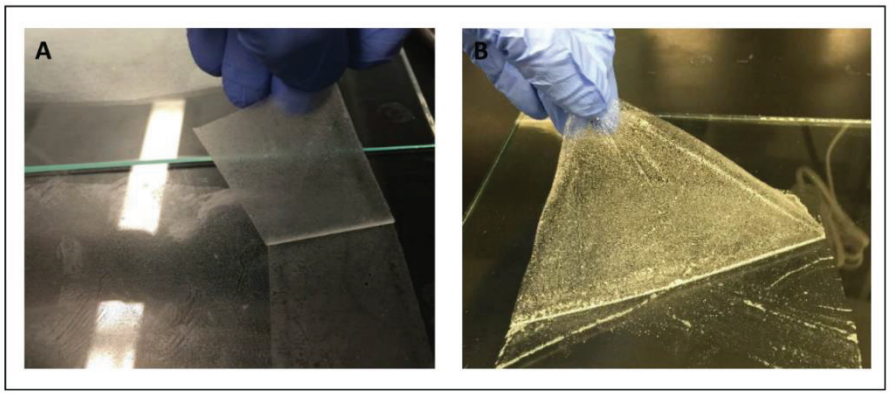

Figure 5.3. Visual comparison of PLA composite films produced by solution casting method with emulsions. Photographic pictures of a) EE Film 1.3 mg/cm^2, b) EF films 3 mg/cm^2 eugenol containing cellulose-emulsions

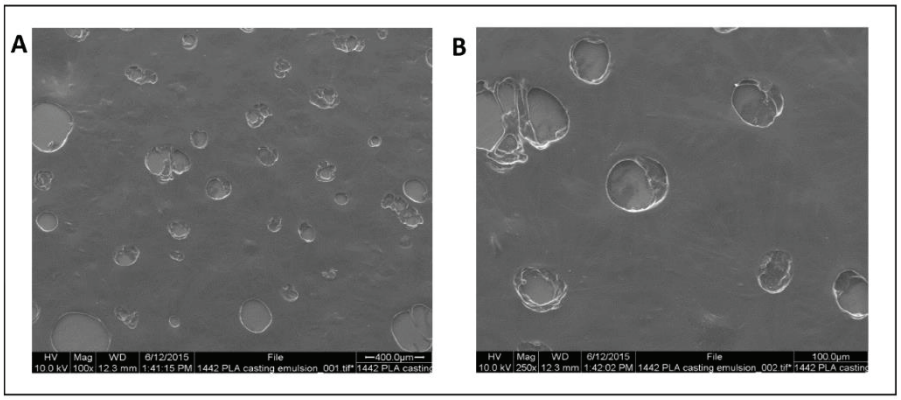

Figure 5.4. Scanning electron microscopy images of a) EE Film 1.3 mg/cm^2, b) EF films 3 mg/cm^2 eugenol containing cellulose-emulsions

As reported in the literature, high loading is possible with electrospinning processes (Agarwal et al., 2008). The film produced by casting method EF film, (Figure 5.3 b) with the same film formulation that was used in electrospinning process has a porous structure with the big size of cracks. As it can be seen visually and in the SEM images from Figure 5.4, films have a porous structure and cannot be used as a self-standing film. High loading is possible with the electrospinning technique and eliminates the structural defects of the film. Therefore, this is the superiority of the electrospinning technique to compare with the films produced via the solution casting method.

5.3.2. Fluorescence Microscopy Images of LA Emulsions in PLA/Emulsion Fibers-Grafted to PLA Films

The fabricated composite fibers were characterized using a fluorescence microscope. First sodium hydroxide was used to dissolve the PLA fibers to enable the adsorption of Calcofluor stain on the cellulose and become the fluorescent under a microscope. The fluorescence microscope images of composite fibers were obtained as shown in Figure 5.5. The existence and distribution of cellulose emulsion into the PLA fibers were confirmed under the fluorescence microscopy by staining the PLA fibers-grafted to PLA films by Calcofluor stain.

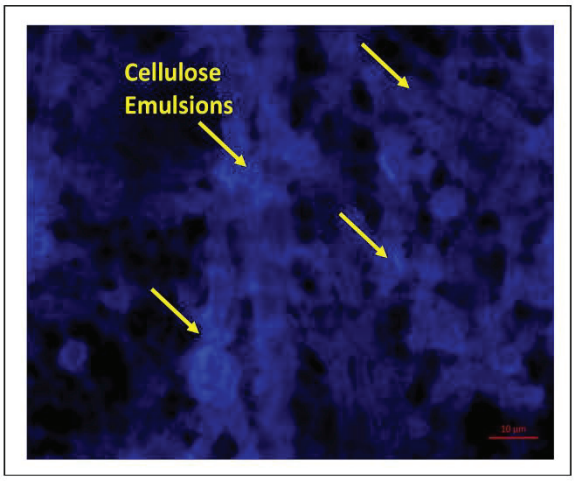

Figure 5.5. Fluorescence microscopy images of electrospun EG-PLA/emulsion fibers-grafted to PLA films stained with Calcofluor stain. Scale bars correspond to 10 µm

5.3.3. Antimicrobial Properties of Electrospun PLA/Emulsion Fibers-Grafted PLA Films at Headspace

Antibacterial activity of fabricated PLA fibers-grafted to PLA films, that is, EE, EF and EG Films containing 1.3, 3.0, 6.0 mg/cm^2 eugenol (Table 5.2) were used to test *Listeria innocua* and *Escherichia coli* K12 on agar media. EE film containing 1.3 mg/cm^2 eugenol did not show any antimicrobial activity on both tested microorganisms (data were not shown). The EF film containing 3 mg/cm^2 eugenol was able to completely inhibit the *Listeria innocua* growth (Figure 5.6 A) but did not show any potent antimicrobial activity on *Escherichia coli* K12 at this concentration and (Figure 5.6 B). The increasing the fiber

mats with 6 mg/cm^2 eugenol in the film (EG) completely prevented the growth of the *Listeria innocua* (Figure 5.6 C), and decreased the microbial growth of *E.coli* K12 (Figure 5.6 D), but compared to *Listeria innocua* the antimicrobial efficacy of eugenol in headspace was very low on inhibition of *E.coli* K12 growth (Fig 5.6 B and 5.6 D). Antimicrobial activity of volatile eugenol was depended on the eugenol vapor concentration in the headspace. Antimicrobial results of this study demonstrated that natural volatile eugenol vapors could be successfully delivered by emulsion-based electrospun fibers into the headspace of the package and retain its inhibitory effect against microbial growth for 48 h.

Listeria innocua is more sensitive against the eugenol vapor than *E.coli* K12 this could be due to the difference in the outer membrane structure of Gram-positive and Gram-negative bacteria (Friedman, Henika, & Mandrell, 2002). The inhibition efficacy of essential oils in the vapor phase is still a complex phenomenon, the mode of cation has not been determined yet and can be related to many factors. The antimicrobial efficacy is totally related to the amount of released vapors in the headspace of the packaging. Laird and Phillips (2012) explained the potential use of the antimicrobial activity of the vapor phase of many essential oils for future applications. In another study, the antimicrobial properties of thirteen essential oils in vapor phase against food borne bacteria has been investigated (Nedorostova, Kloucek, Kokoska, Stolcova, & Pulkrabek, 2009).

The difference in the outer membrane structure bacteria may not be the case factor in vapor phase inhibition for all essential oils. In the research of López, Sánchez, Batlle and Nerín (2005) the antimicrobial activity of clove and cinnamon essential oils at headspace against some Gram-positive, Gram-negative, yeast and molds have been investigated. The MIC value of clove for *L.monocytogenes* (Gram-positive) and *E.coli* (Gram-negative) was 17.5 and 26.2 (MIC $\mu L_{EO}/L_{headspace}$), respectively and for cinnamon MIC value was 34.9 and 17.5 (MIC $\mu L_{EO}/L_{headspace}$), for *L.monocytogenes* and *E.coli,* respectively.

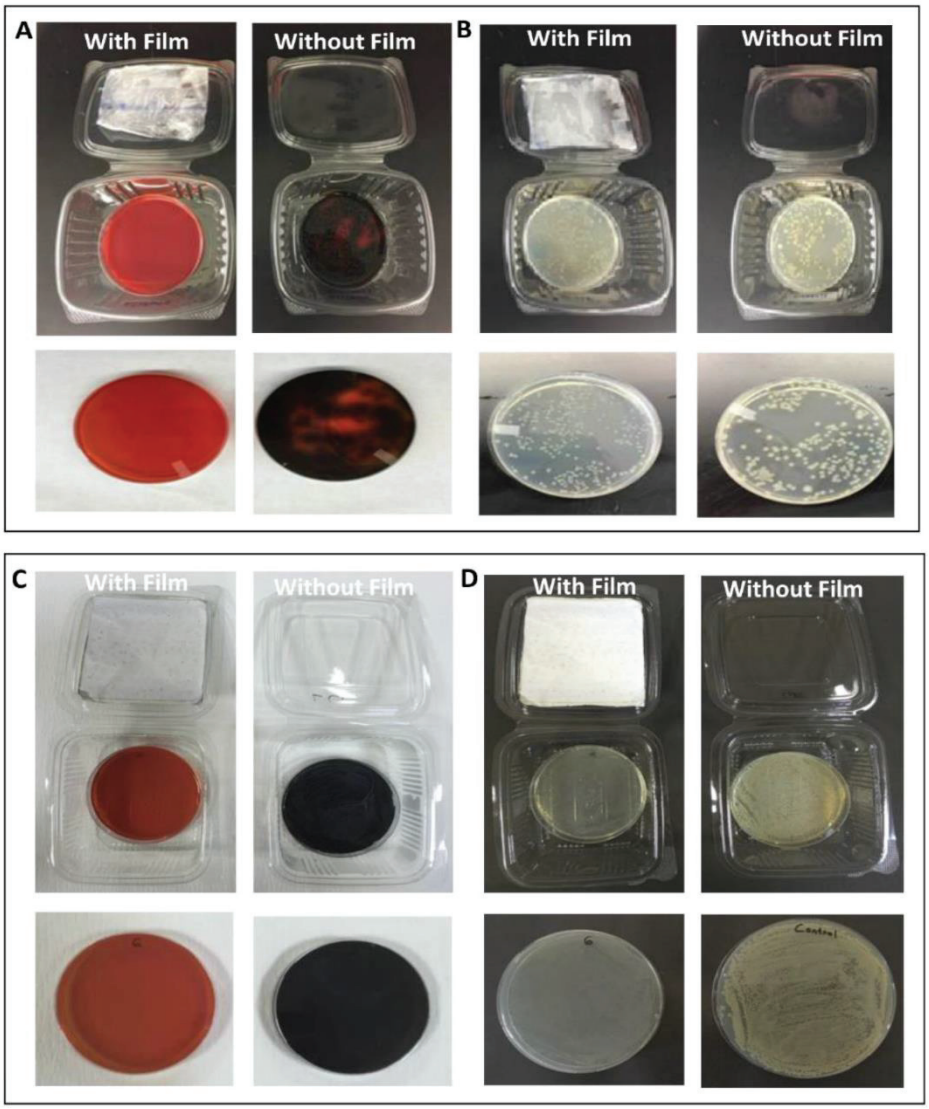

Figure 5.6. Photographs of antimicrobial activity of electrospun a-b) EF-PLA fibers-grafted to PLA films against *L. innocua* and *E. coli* K12 with film and without film at headspace c-d) EG-PLA fibers-grafted to PLA films against *L. innocua* and *E. coli* K12 with film and without film at headspace.

5.3.4. Antibacterial Activity of PLA/Emulsion Fibers-Grafted PLA Films on Grape Tomatoes Stem Scar

Antibacterial efficacy of fabricated electrospun EG-PLA fibers-grafted to PLA films in headspace containing 6 mg/cm^2 eugenol were tested on artificially inoculated *Listeria innocua* and *Escherichia coli* K12 as model microorganisms on grape tomatoes stem scar as real food model. The bacterial populations were enumerated by plate counting method. Approximately 1.5 log CFU per stem scar reduction was achieved on contaminated tomatoes stem scar after 48 h. The populations of *E. coli and L. innocua* on

tomatoes stem scar after 48 h were 1.65 and 1.4 log CFU per stem scar, respectively (Figure 5.7). These results demonstrated the active release of encapsulated eugenol vapors from the fibers to the headspace. Eugenol vapor at headspace was statistically significant ($p< 0.05$) to decrease the microbial load of both microorganisms. The antimicrobial activity of essential oils in vapor phase was related to volatile components chemical compositions (Goñi et al., 2009).

Due to the porous structure of tomato stem scars, pathogen microorganisms are able to penetrate and survive in the stem scar (Jin & Gurtler, 2012). The consumption of contaminated raw tomatoes or tomatoes in salads caused the outbreaks (Deza et al., 2003). Antimicrobial treatment of fresh produce surface can be a potential application for preventing the microbial contamination. Another study also showed the antimicrobial efficacy of the allyl isothiocyanate encapsulated PLA film on *Listeria innocua* and *Escherichia coli* K12 contaminated table grapes and meat (Kara et al., 2016).

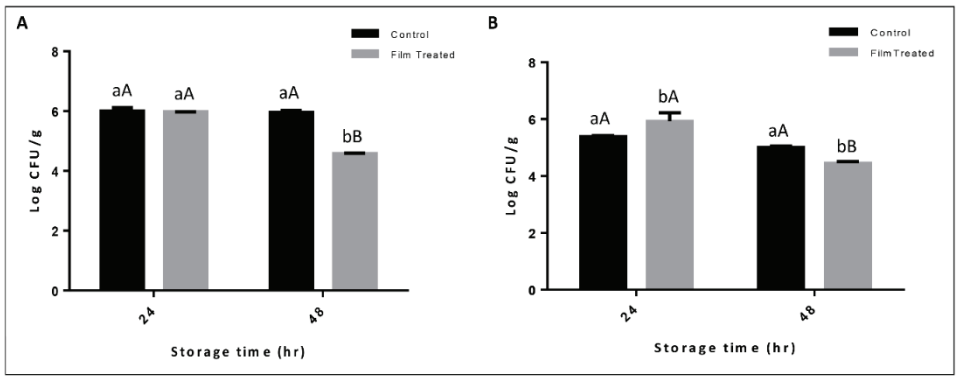

Figure 5.7. Survival of a) *L. innocua* b) *E. coli* K12 on contaminated grape tomatoes stem scar at 10°C storage. $^{a-b}$:Different letters within each treatment indicate a significant difference at $p<0.05$, $^{A-B}$:Different letters within each storage time indicate a significant difference at $p<0.05$

This study indicated that active layers of produced films showed statistically significant inhibition and sustained the eugenol vapor release up to 48 h in the packed food. The result of this study is promising in terms of using the gaseous antimicrobial compound to prevent the fresh produce loss. The idea behind the creating headspace in the food package is able to reach all the inaccessible sites and the surface of foods via free attachment of gaseous antimicrobial eugenol to the food surface. Foods like lettuce, spinach, clustered table grapes and grape tomatoes have porous or inaccessible areas.

5.3.5. Mechanical Properties of PLA Films

Mechanical properties of PLA cast film, EG-electrospun PLA/emulsion fibers-grafted to PLA films (with containing 6 mg/cm^2 eugenol) and CG-electrospun PLA fibers-grafted to PLA films (without containing bacterial cellulose but containing same eugenol as EG film) were given in Table 5.3.

There were no statistically significant differences ($p<0.05$) between EG and CG films mechanical properties. The EG films with bacterial cellulose emulsions have a higher tensile strength, Young's modulus and also slightly higher elongation compared to CG films. The results have been compared between with and without cellulose electrospun PLA fibers-grafted to PLA films with the same amount of eugenol essential oil. The results indicated that the presence of bacterial cellulose slightly improved the mechanical properties of EG films. Li et al. (2013) reported the cellulose reinforcing effect on electrospun PLA fibers. The PLA cast film showed the characteristic properties, and similar results were reported for PLA solution cast method in the work of Kara et al. (2016).

Recently, several authors (Almasi, Ghanbarzadeh, Dehghannya, Entezami, & Asl, 2015), (Ambrosio-Martıin, Fabra, Lopez-Rubio, & Lagaron, 2015), (Graupner, Herrmann, & Müssig, 2009), (Iwatake, Nogi, & Yano, 2008) and (Jonoobi, Harun, Mathew, & Oksman, 2010) have reported the cellulose reinforcing effect on mechanical properties of PLA-cellulose composites films via different film processing methods.

Table 5.3. Mechanical properties of PLA solution cast film, CG and EG Electrospun PLA fibers-grafted to PLA films

Films Name	Young's modulus (MPa)	Tensile strength (MPa)	Elongation (%)
PLA Cast Film	2710.91±483^a	66.08±4.87^a	2.92±0.71^b
CG-Electrospun PLA fibers-grafted to PLA films	404±169^b	17.35±7.50^b	6.55±1.90^a
EG-Electrospun PLA/emulsion fibers-grafted to PLA films	523±87^b	19.54±3.36^b	5.30±0.86^a

$^{a-b}$: Different letters within each treatment indicate a significant difference at $p<0.05$

5.4. Conclusion

To conclude, the SEM results supported the hypothesis of that chapter, cellulose emulsion could be spun with PLA, and antimicrobial results on agar media and real food results supported the fabrication of the antimicrobial electrospun fibers. In this research, BCNCs Pickering emulsions with PLA polymer were electrospun on PLA solution cast film, and bead-free PLA composite fibers were fabricated. Regarding the SEM results, PLA solution with emulsions formed beaded free fibers compared to PLA fibers and PLA-eugenol containing fibers. The electrical conductivity of solution was increased with the addition of each emulsion formulation materials. PLA solution with emulsion formulations had the highest conductivity compared to other spinning formulations. These results proved the superiority of successfully developed BCNCs Pickering emulsions with high electrical conductivity. Moreover, these results demonstrated that the electrical conductivity of spinning solution was one of the important parameters in determining the morphology of the obtained fibers. The active release of encapsulated eugenol vapors was effective on agar media and tomato stem scars as real food model for the inhibition of *L. inocula* and *E. coli* K12. The fabricated nanocomposites have antibacterial activity, and these films can be used as a biodegradable active films/labels inside the food package similar to sachets or pouches to improve the food quality, safety, and the shelf life of fresh produce. Developed novel biodegradable-PLA cellulose composite films have a great potential for delivering bioactive gaseous compounds for intelligent food packaging applications. To sum up, the finding of this research support the technical feasibility of delivering eugenol gaseous in the packed food via electrospun fibers. Further research will be needed to prove the economic feasibility of eugenol in the food packaging systems in commercial applications.

CHAPTER 6

ANTIFUNGAL PROPERTIES AND CONTROLLED RELEASE STUDY OF ELECTROSPUN PLA FILMS

6.1. Introduction

The globalization of the markets and today's consumer demand for natural, safe and quality foods bring novel approaches in food packaging. Today food scientists make significant efforts to prevent foods from spoilage and increase the shelf life. Recently, active antimicrobial packaging with volatile compounds has increased the attention of the scientific community because these compounds can be vaporized and released in the headspace of the package easily (Peretto et al., 2014). Antimicrobial volatile compounds (AVC) can be delivered by encapsulation techniques and carriers such as adsorbent pads, natural, biodegradable films/fibers, sachets, punches and pads and can easily be combined with the packaging materials to increase the efficacy of volatile compounds (Kapetanakou & Skandamis, 2016).

Nanofibers can be produced by electrospinning, which is a simple and low-cost technique. Polymer carriers are dissolved in an organic solvent/water mixture to form a suspension with the active compounds to encapsulate active agents. Polymer nanofibers can be obtained by using a high electrical field between a grounded collector and a polymer solution that is pumped from a needle. Electrospun fibers can be directly spun onto the packaging film surface to produce multilayer films, with a good interfacial adhesion to the surface of the films (Kara et al., 2016) or can be produced as interlayers films for food packaging applications (Fabra, Lopez-Rubio, & Lagaron, 2013). One of the advantages of this technique is that it does not require the use of temperature. That is why it is convenient to encapsulate the heat-sensitive bioactive compounds. In this regard, electrospinning is generally considered as a suitable technique to deliver heat-sensitive bioactive compounds and to produce multifunctional electrospun fibers with the high specific surface area and porous structure for active food packaging applications (Aytac et al., 2014; Dai & Lim, 2015; Kara et al., 2016).

Poly (lactic acid) (PLA) is a suitable polymer for electrospinning applications, and PLA-based electrospun fibers have been used as carriers for bioactive compounds (Kara et al., 2016; Kayaci et al., 2013; Vega-Lugo & Lim, 2009). The conceptual framework that was developed by Yam and Lee (2012) showed the variables that affected the release of antimicrobial compounds are the polymer composition effects, processing effects, and structural effects.

‘’Controlled release packaging is a sophisticated form of controlled release, which uses the package as a delivery system to release the active compound in a controlled manner’’ (Yam & Lee, 2012). Controlled release packaging can enhance the quality and extend the shelf life of foods via allowing the releasing of antimicrobials and antioxidants at controlled manner to the food surface (Yam & Lee, 2012). A few number of reports have been published describing some essential oils volatile components release characteristic from electrospun fibers at headspace (Dai & Lim, 2015; Mascheroni et al., 2013; Kara et al., 2016; Vega-Lugo & Lim, 2009).

Volatile components of different sources of plants such as limonene, clove, lemongrass, citral, thymol, eugenol, cinnamaldehyde, trans-2-hexanal, acetaldehyde and perillaldehyde have proven to be efficient antimicrobials (Burt, 2004; Dorman & Deans, 2000; Goñi et al., 2009; Inouye, Uchida, Maruyama, Yamaguchi, & Abe, 2006; Kim et al., 2016; Mari, Bautista-Baños, & Sivakumar, 2016). In literature, few researchers have investigated the efficacy of those volatile components of food applications without direct contact with the fruit (Kara et al., 2016; Peretto et al., 2014).

Postharvest losses of fruits is a major problem during storage, handling, and marketing (Amiri, Dugas, Pichot, & Bompeix, 2008). The quality maintenance of ready to eat table grapes (Vitis vinifera L.) has been a challenge due to severe problems during postharvest mainly due to gray mold. *Botrytis cinerea*, gray mold, is the important pathogen that causes the grape decay even at low temperatures and result in economically significant post-harvest losses in marketing and storage (Parafati et al., 2015; Shin, Kim, Choi, Keum, & Chun, 2014). Sulfur dioxide (SO_2) a synthetic fungicide has been a currently used method for controlling the pre harvest and postharvest gray mold of table grapes (Romanazzi, Lichter, Gabler, & Smilanick, 2012). Natural volatile antimicrobial compounds could be an alternative to synthetic preservatives for controlling the food processing and post-harvest storage technology. The potential use of natural volatile antimicrobial compounds applications in preservation of fresh produce has been reported by a number of researchers (Chanjirakul, Wang, Wang, & Siriphanich, 2007; Melgarejo-

Flores et al., 2013; Peretto et al., 2014; Shin, Kim, Choi, Keum, & Chun, 2014; Tzortzakis, 2007; Ugolini, Martini, Lazzeri, D'Avino, & Mari, 2014). A few data have reported the effect of eugenol vapor treatment applications on maintaining the quality and safety of table grapes (Guillén et al., 2007; Valero et al., 2006; Valverde et al., 2005).

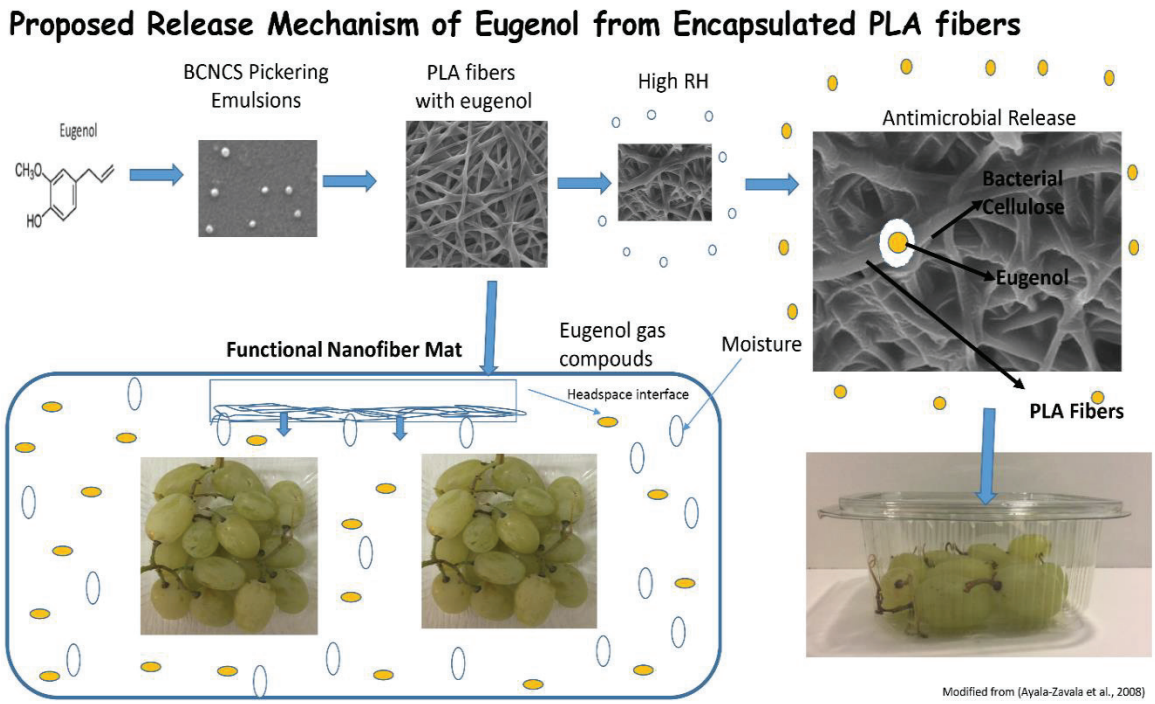

Figure 6.1. Proposed release mechanism of eugenol from encapsulated fibers to the interface

The objective of this chapter is to predict the release profile of volatile antimicrobial eugenol from electrospun PLA/emulsions fibers-grafted to PLA films to the headspace of the package. To achieve the objective, two hypotheses were proposed.

Hypothesis one: Water vapor and temperature could act as an external stimulus to trigger the release of eugenol vapor from the electrospun PLA/emulsions fibers-grafted to PLA films and vaporize into the headspace of the package in a controlled manner for food packaging applications. To test this hypothesis, electrospun PLA/emulsions fibers-grafted to PLA films with/without bacterial cellulose was used. To stimulate the fresh produce packaging conditions 4±1°C and 22±1°C temperature and low (60±2 %RH) and high (87±2 % RH) relative humidity were used.

Hypothesis two: Appropriate amount of eugenol could be released from electrospun PLA/emulsions fibers-grafted to PLA films into the headspace of the package for inhibition/retarding the growth of the food spoilage m/o. To test this hypothesis, the

efficacy of electrospun PLA/emulsions fibers-grafted to PLA films were tested on artificially *B.cinerea* contaminated table grapes without direct contact with the grapes.

6.2. Experimental

6.2.1. Materials

Poly(lactic acid) (PLA) with a weight-average molecular weight of 148 kDa and a number-average molecular weight of 110 kDa (product No. 4060D) were obtained from NatureWorks LLC (Minnetonka, MN, USA). Dichloromethane (DCM) was purchased from Fisher Scientific (Fair Lawn, NJ, USA). *Gluconacetobacter xylinus* (ATCC® 700178™) freeze-dried culture was purchased from American Type Culture Collection (Manassas, VA, USA). Sulfuric acid (H_2SO_4, 95.0 to 98.0 w/w %) was purchased from Thermo Fisher Scientific Inc. (Waltham, MA, USA). Eugenol oil (Natural, ≥98 % W246719) was purchased from Sigma-Aldrich (St. Louis, MO, USA). CytoGuard LA 2X was kindly provided by A&B Ingredients (Fairfield, NJ, USA). *Botrytis cinerea* was kindly provided by Prof.Dr. Figen Yıldız from Ege University (İzmir, Turkey). Potato dextrose agar (PDA) was obtained from BD: Difco (Sparks, MD, USA).

6.2.2. Spinning Operation Conditions of PLA Films

Due to the relocation electrospun PLA/emulsions fibers-grafted to PLA films were produced using the electrospinning equipment (Inovenso Ne300, Turkey). The equipment consists of a syringe attached to a syringe pump (New Era Pump System Inc., NE-300, USA), a single brass nozzle connected via a tube, an electrically ground collector, high voltage supplier and a coating homogeneity system. Preliminary trials showed that the best electrospinning conditions for fiber formation were; a flow rate of 4 mL/h, an applied voltage of 28 kV and distance from the needle tip to the collector of 12 cm, the drum with the coating homogeneity system. Ten milliliters of the spinning solution was mixed with freeze-dried cellulose emulsion and vortexed before spinning.

Eugenol and LA with PLA solution were used to produce the electrospun PLA fibers-grafted to PLA films. PLA cast film (10x27 cm) was placed on aluminum foil

covering the drum collector and the amount of loaded fibers were checked by weighing the PLA films before and after fiber loading. All experiments were carried out in triplicate at room temperature.

6.2.3. Scanning Microscopy of PLA Films

The methodology of the SEM is explained in section 5.2.6.

6.2.4. GC Operating Conditions

Headspace analysis of eugenol was carried out using Agilent Technologies 6890N Network GC System Gas Chromatograph (USA) was equipped with a flame ionization detector (hydrogen, 40 mL/min; air, 300 mL/min) and a HP-5 5% Phenyl Methyl Siloxane Capillary column (30 m x 0.25 mm, film thickness 0.25 µm Agilent 19091 J-433). Injections were done in splitless mode. The oven temperature was set at 50 to 290 ºC at 12 ºC/min. Inlet and detector temperatures were adjusted to 50 to 300º C respectively. Helium was used as a carrier at a flow rate of 1 mL/min column flow. Six concentrations of eugenol (Natural, ≥98 % (W246719) Sigma-Aldrich, St. Louis, MO, USA), namely 0.53 ppm, 1.16 ppm, 2.12 ppm, 5.30 ppm, 21.20 ppm and 53 ppm from the stock solution were used for preparing a eugenol headspace calibration curve. The standard calibration curve was plotted by the eugenol concentration against the area under the curve which was obtained from the GC software for each concentration (Appendix A). All experiments were carried out twice.

6.2.5. Eugenol Release Measurements

The release kinetics of eugenol from electrospun PLA fibers-grafted to PLA films with cellulose emulsions and without cellulose was studied by conducting Gas Chromatograph (Agilent Technologies 6890N Network Gas Chromatograph, USA) headspace analysis under both high (87±2 % RH) and low (60 ±2% RH) relative humidity conditions, and at refrigerated (4±1°C) and room temperature (22±1°C). To provide an 87±2 % RH in 250 mL, a glass jar at 4±1°C and 22±1ºC, 600 and 100 µL of distilled

water were injected into the 250 mL glass jars, respectively. For low RH (60 ±2%) no water was added. RH in 250 mL glass jars was controlled using a humidity probe set by Agilent Data Logger system (Appendix A). Release kinetics of eugenol from electrospun fibers was evaluated in sealed 250 mL glass jars sealed with airtight valve (Mininert®Valves, Supelco, Bellefonte, PA, USA) in order to monitor the eugenol release profile concentration in the headspace. Glass bottles were purged with dry N_2 gas for 1 min before the experiment set up. PLA films (9*10 cm) were cut into 1*9 cm^2 pieces and attached to the inside wall of the bottle via double sided tape. Headspace samples (0.5 mL) were taken at predetermined time intervals to measure the released eugenol concentration from the fibers into the jars. All release experiments were carried out twice.

The accumulative release percentage of eugenol from the PLA fibers was calculated using the following equation (Wang et al., 2016). Where Mt (mg) is the released eugenol at an arbitrary time t, Mt is calculated as described by Dai and Lim (2015), and Mo (mg) is calculated regarding the total extraction of eugenol from the 9*10 cm^2 films to calculate the exact encapsulated amount of eugenol in the fibers. Release results were calculated according to the following equation:

$$\text{Accumulative release } (\%) = \frac{\text{Mt}}{\text{Mo}} \text{x } 100 \quad \text{(Eq. 6.1)}$$

6.2.6. Encapsulation Efficiency of PLA Electrospun Films

The total content of eugenol in PLA fibers was measured according to the solvent extraction method by a slightly modified version as described by Kara et al. (2016). The PLA (9*10 cm) films were dissolved in 10 ml of ethyl acetate using an ultrasonic bath (CP104, CEIA, France) for 1 hr at 100% power. Samples were centrifuged (Universal 320 Hettich Zentrifuger D-78532 Tuffingen, Germany) at 800 rpm for 15min. Hexane (7 ml) was added to the mixture for precipitating the PLA and samples were centrifuged at 800 rpm 15 min again. The supernatant was filtered through a 0.2 μm syringe filter and analyzed by GC at operating conditions in Section 6.2.4. Experiments were repeated three times.

The encapsulation efficiency (EE) of eugenol in fibers was calculated as following equation (Woranuch & Yoksan, 2013b).

$$\text{EE of fibers (\%)} \frac{\text{Mass of eugenol in PLA fiber}}{\text{Mass of eugenol in encapsulated BCNCs emulsions}} \text{x100 (Eq. 6.2)}$$

6.2.7. Fourier Transform Infrared Spectroscopy of Electrospun PLA Films

The infrared spectra of films were measured with a Perkin-Elmer Spectrometer (LX185255 Spectrum BX II, Llantrisant, UK) equipped with an attenuated total reflection (ATR) accessory, a KBr beam splitter and DTGS detector with triple bounce Diamond/ZnSe crystal plate. Film samples were analyzed after taking the background scan of air and spectrum resolution. ATR-FTIR spectra were collected over the range from 4000 to 525 cm^{-1} with 4 cm^{-1} resolution averaging 64 scans. Spectrum software (5.3 version) was used for data analysis.

6.2.8. Antifungal Properties of PLA/Emulsion Fibers-Grafted to PLA Films

The antifungal efficacy of EG-Electrospun PLA/emulsions fibers-grafted to PLA films (containing 6.0 mg/cm^2 eugenol cellulose-emulsion) in headspace was tested against *B.cineria* on agar media. Fungal spores were obtained from 2-week-old potato dextrose agar (PDA) cultures. *B.cineria* surface-inoculated plates (100 µl, approximately 10^4 cells) were placed in an in a clamshell PET box (250 ml) with a piece of antimicrobial film (9*10 cm) which stuck on the lid of the box. Boxes without films were used as controls. The boxes with Potato Dextrose Agar plates were incubated at 25 °C, 80% RH for 3-5 days. The population of *B.cineria* was enumerated by counting the colony forming units (log CFU).

6.2.9. Efficacy of Electrospun PLA/Emulsion Fibers-Grafted to PLA Films on the *B.cinerea* Contaminated Table Grapes

To assess the efficiency of the eugenol vapor on table grapes, the method described by Martínez-Romero et al. (2007), with a modified version, was used. Table grapes (*Vitis vinifera* L.) '' Hatun Parmağı '' cultivar were harvested from a vineyard in Seferihisar region of İzmir. Clusters were selected based on uniform size, color shape, and absence of damage or injuries. Grapes were immersed in 70% ethanol for 1 min and followed, rinsed in sterilized water, and dried under the hood. 2-week-old cultures of *B.cinerea* spores were collected from potato dextrose agar (PDA). The concentration of spores (in 0.5% Tween 20) was determined with a hemocytometer. Grapes were artificially injured using a sterile needle (2mm*4mm), and the berries were inoculated by injecting 10 µl of a diluted *B.cinerea* suspension of 250 x 10^{-1} CFU/mL was injected at inside the each grape. The inoculated plates were placed in a clamshell PET box (250 ml) with an EG-Electrospun PLA/emulsions fibers-grafted to PLA films stuck on the lid of the box. Boxes without films were used as controls. Packed grapes were stored in the climatic test cabinet at 20 ℃ and 90% relative humidity (RH), and samples were analyzed for 5 and 7 days to simulate the commercial marketing conditions. Results were analyzed visually and by stereomicroscope (LEICA EC3). The experiments were repeated two times.

6.2.10. Sensory Analysis

Sensory analyses were carried out by (eugenol) odor trained 20 panelists and panelists evaluated the sensory quality of the treated and untreated grapes as a control. Panelists have evaluated the grapes on a nine-point hedonic scale of 1-9 (1=dislike extremely, 5=neither like nor dislike, 9=like extremely) for appearance, color, odor, and overall acceptability after the five and seven days storage. (n=20).

6.2.11. Statistical Analysis

The statistical analyses were performed using analysis of variance (ANOVA). The mean values were compared by a Tukey's test to examine if differences were considered significant if $p<0.05$. FTIR results statistical analyses were carried out by SIMCA software (14.1, Umetrics, Umea, Sweden).

6.3. Results and Discussions

6.3.1. Composition and Morphology of Electrospun PLA Films

Electrospun PLA fibers-grafted to PLA films that controls films, CE, CF, and CG films (without cellulose, contain eugenol and LA surfactant) (Table 6.1) were produced with the same procedure described in Chapter 5, in Section 5.2.4. The structure of fiber mats was investigated by using SEM analysis. The SEM results showed that the fabricated electrospun PLA fibers-grafted to PLA films have bead free and homogenous fibers (Figure 6.2. b-c-d).

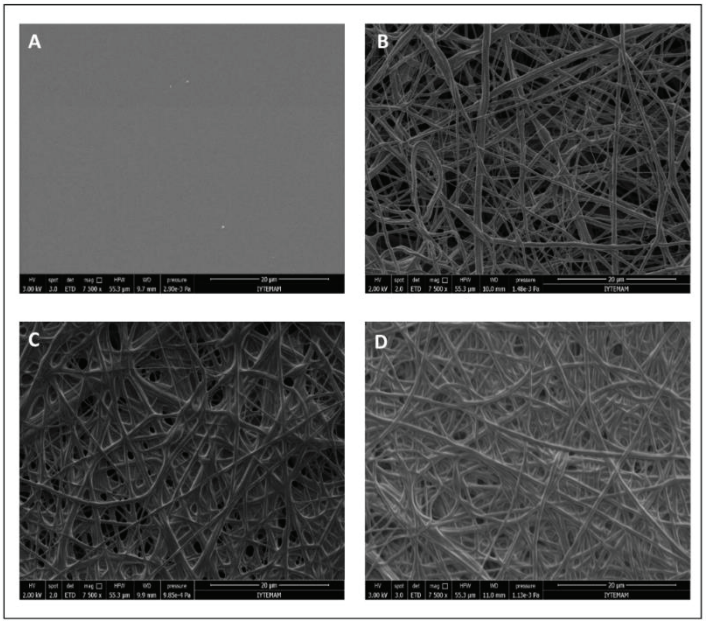

Figure 6.2. Scanning electron microscopy images of a) Solution cast neat PLA Film b) CE, c) CF, d) CG-Electrospun PLA fibers-grafted to PLA films

Table 6.1 Composition of tested films for release test

Films	Composition of tested films for release experiments
EE	Electrospun PLA/emulsion fibers-grafted to PLA film (0.8 mg/cm^2 eugenol containing cellulose-emulsion)
EF	Electrospun PLA/emulsion fibers-grafted to PLA film (1.6 mg/cm^2 eugenol containing cellulose-emulsion)
EG	Electrospun PLA/emulsion fibers-grafted to PLA film (3.2 mg/cm^2 eugenol containing cellulose-emulsion)
CE	Electrospun PLA/fibers-grafted to PLA film (containing 0.8 mg/cm^2 eugenol without cellulose)
CF	Electrospun PLA/fibers-grafted to PLA film (containing 1.6 mg/cm^2 eugenol without cellulose)
CG	Electrospun PLA/fibers-grafted to PLA film (containing 3.2 mg/cm^2 eugenol without cellulose)

E: Emulsion C: Control

6.3.2. Release Kinetics of Eugenol from PLA Films

The release kinetic of eugenol from electrospun PLA fibers-grafted to PLA films (with cellulose emulsions EG film and without cellulose CG) was studied under low (60 %) and high (87 %) relative humidity and, at refrigerated (4±1ºC) and room (22±1ºC) temperature. As shown in Figure 6.3, Figure 6.5, and Figure 6.7 the release of eugenol is triggered at high RH (87 %) in both control and cellulose containing emulsion films at refrigerated and room temperature, as well as the effect of temperature on eugenol release from the fibers investigated under both RH for control and cellulose containing films. As shown in Figure 6.3, the increasing temperature increases the amount of eugenol release under both RH. These results support the hypothesis of this chapter that high relative humidity and high temperature can trigger the release of eugenol from the electrospun PLA fibers-grafted to PLA films. The low amount of eugenol release from the films at low relative humidity and low temperature may be the advantage of fabricated films to store the films without losses of the volatile compound.

The release of volatile compounds might depend on polymer matrix, polymer composition, volatile compound properties, dispersion and diffusion of compound in the polymer matrix, chemical interactions between carrier polymer and volatile compound, the wettability of carrier polymer, and external conditions including temperature and relative humidity, and physicochemical mechanism (Chalier, Area, Guillard, & Gontard,

2009; Dai & Lim, 2015; Dhoot, Auras, Rubino, Dolan, & Soto-valdez, 2009; Kayaci et al., 2013; Kriegel et al., 2010; Lashkari et al., 2017; Vega-Lugo & Lim, 2009).

Relative humidity and temperature were used for triggering the release in many studies. According to the findings of Chalier et al. (2009), increasing relative humidity and temperature increased the carvacrol diffusivity from soy protein coated paper. In their study, Lashkari et al. (2017) also increased the release of ally isothiocyanate from the metallic organic frameworks with high relative humidity and temperature.

The results obtained are compatible with a finding of Mascheroni et al. (2013) the release of β-cyclodextrin encapsulated perillaldehyde from electrospun pullulan membranes was triggered by relative humidity. Also, Mascheroni et al. (2011), triggered the release of carvacrol from wheat gluten/montmorillonite coated papers by high RH in their study. Kayaci et al. (2013) observed that the amount of released eugenol increases with the increasing temperature from the PVA/eugenol/with different cyclodextrins inclusions complexes electrospun fibers. Vega-Lugo and Lim (2009) triggered the release of ally isothiocyanate by relative humidity the from soy protein and poly(lactic acid) electrospun fibers.

For sampling, 0.5 µl of eugenol gas was injected to the GC. We assumed that no release was observed when the time is 0 min. The first sample was taken after 15 min, and the sample preparation took 15 min. During that time, the release of eugenol started in the jar environment. Therefore, the first eugenol released data was obtained after 15 min.

The release study results demonstrated that active eugenol compound could be successfully encapsulated with bacterial nano-cellulose crystals in PLA fibers. Eugenol release can be enhanced by temperature and relative humidity in bacterial cellulose matrix with PLA films and without bacterial cellulose as control PLA films. Both films showed the burst release in first hours, and the release of eugenol from control film is higher than that of cellulose emulsion containing films.

The vapor pressure of an aroma compound and its volatility are affected by the temperature. Hydrophobic-hydrophilic interactions could be responsible for holding eugenol until PLA absorbed sufficient moisture from the headspace to displace eugenol from the PLA and the cellulose matrix. The RH and temperature triggered films, increased the eugenol release in the headspace, at all tested conditions.

The up and down profile of eugenol vapor release was observed which may be due to the non-uniform distribution of the particle sizes of bacterial cellulose emulsions.

Plus, the diameter of the fibers in the whole film were not the same. The similar release profile was reported at volatile hexanal from different cyclodextrins inclusions complexes (Almenar et al., 2007) and was reported the thymol release from zein films (Del Nobile et al., 2008).

Gaseous active agents are volatile and susceptible to heat and unfavorable environmental conditions. To prevent the loss during processing and storage, they are commonly encapsulated. Encapsulated gaseous active agents need to be released from encapsulating material. Electrospinning technique encapsulated active compound and produced the nanofibers with the porous structure and large surface area. The large surface area advantage of electrospun fibers allows the release of the active compounds from fibers. Forces like temperature and moisture should be applied to the trigger systems to start the release at the right time. The diffusion of the volatile active compound is a critical parameter in controlling the release profile. The efficacy of active antimicrobial packaging depends on the release rate of the volatile active compound that accumulates in the headspace and adsorbed on the food surface. Since release mechanisms are a complicated system, they should be triggered and released by controlled diffusivity manner (Yam & Lee, 2012). As discussed in the review of Ayala-Zavala et al. (2008b) high relative humidity created from fresh fruits and vegetables could be an advantage for triggering the release of antimicrobial and antioxidants from the carrier into the headspace of the package.

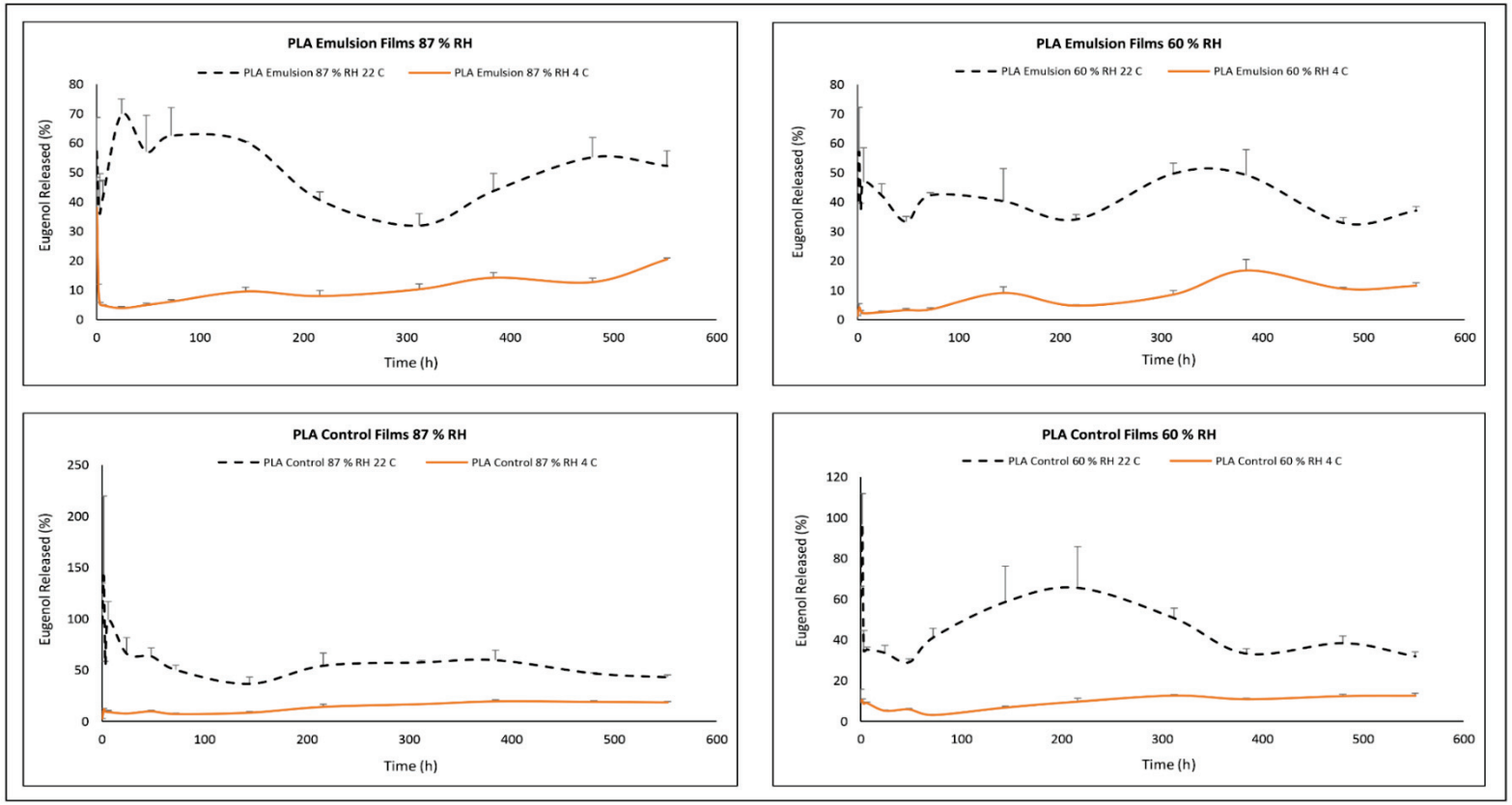

Figure 6.3. Release profile of eugenol from electrospun PLA films (Relative humidity and temperature effect) at 552 h

)

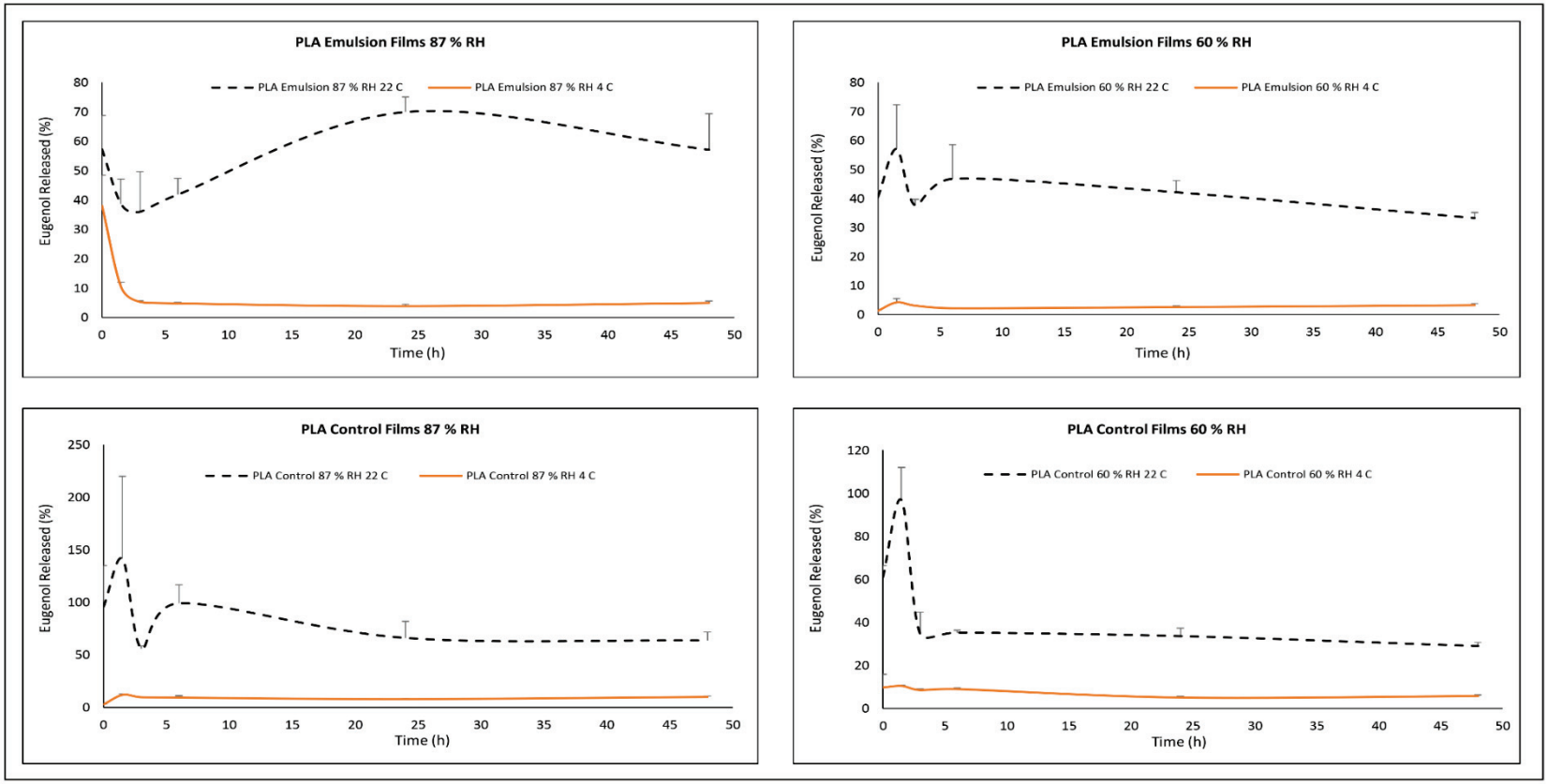

Figure 6.4. Release profile of eugenol from electrospun PLA films (Relative humidity and temperature effect) at 48 h

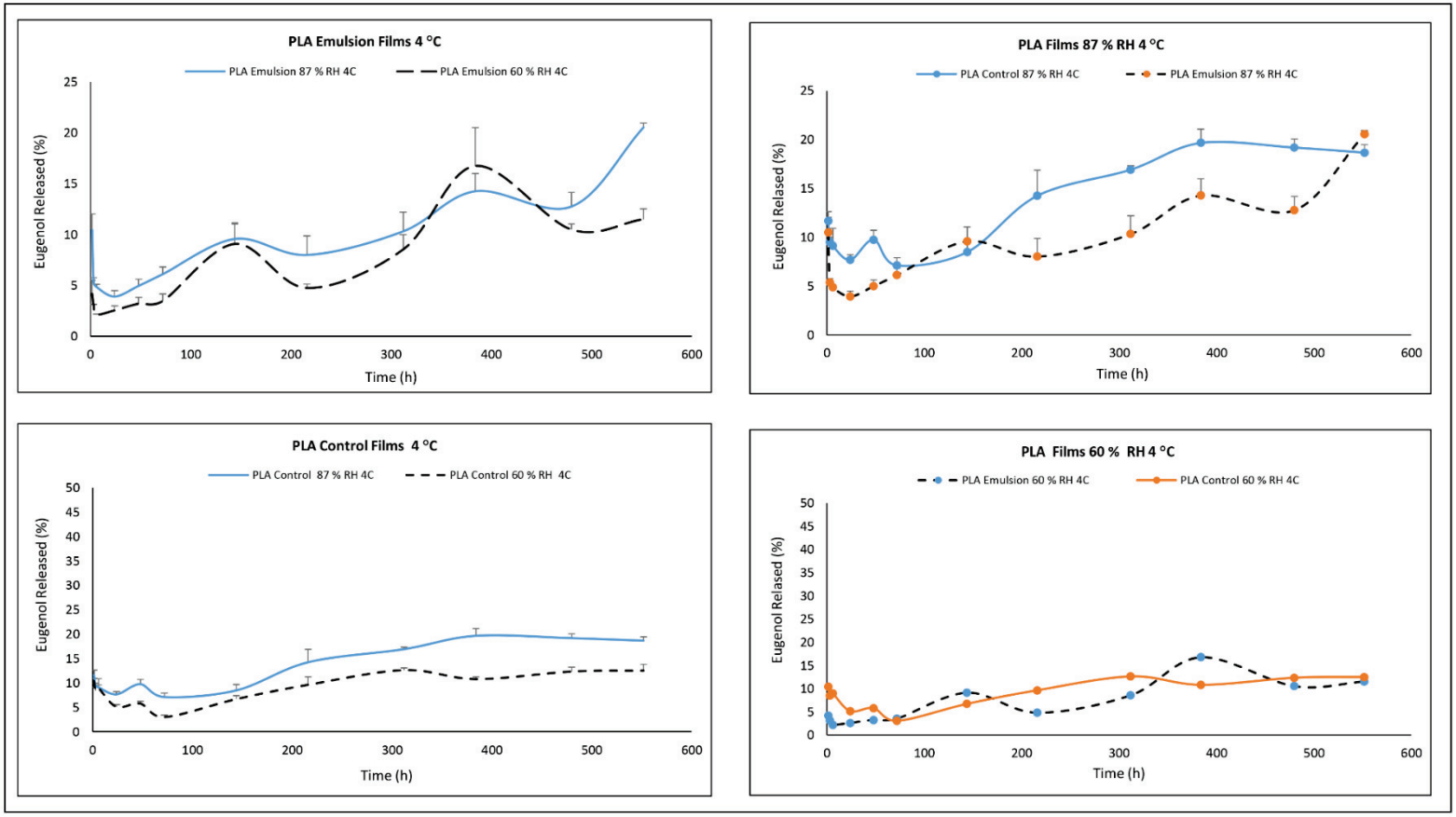

Figure 6.5. Release profile of eugenol from electrospun PLA films at 4±1 ºC for 552 h

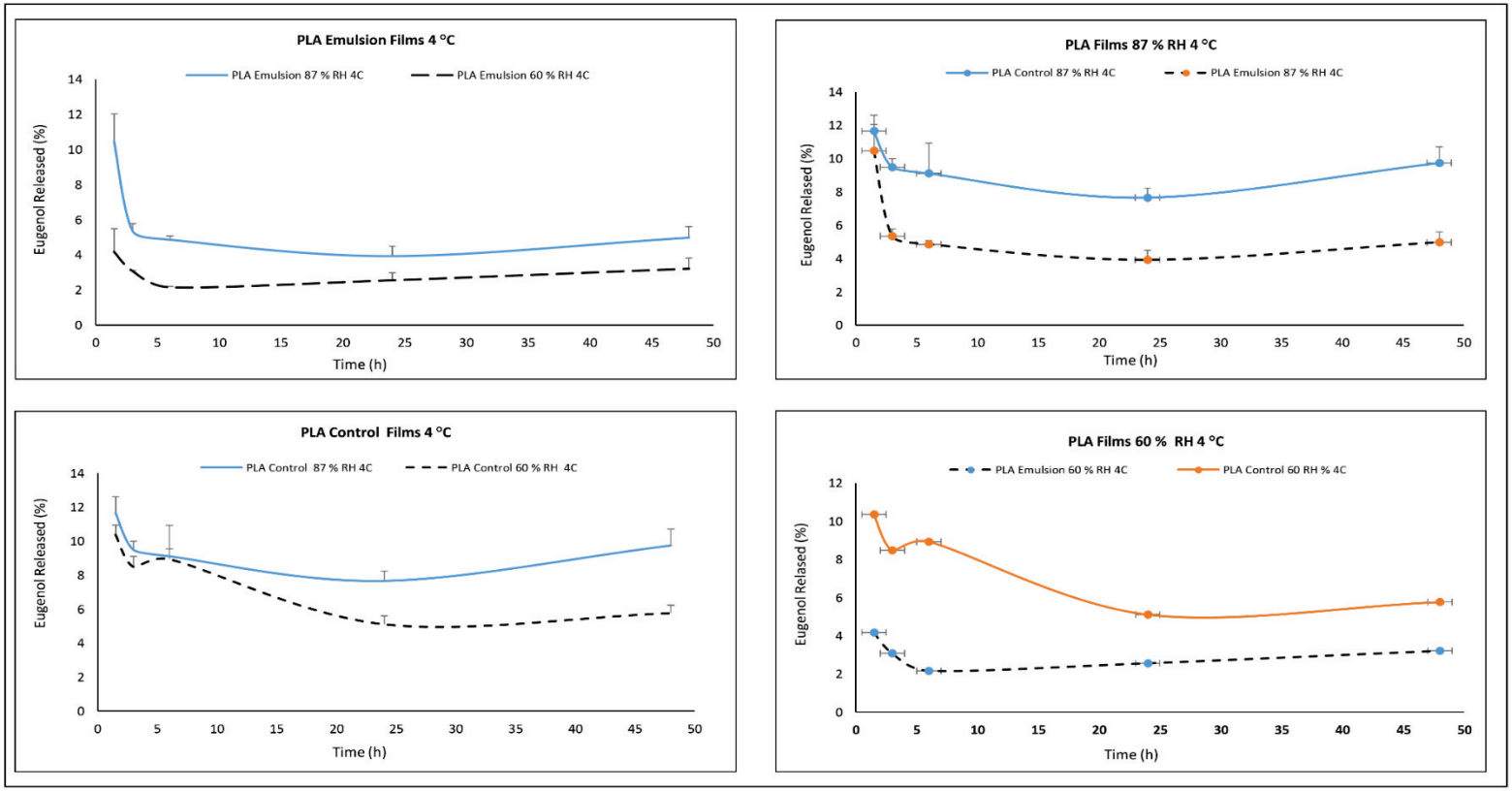

Figure 6.6. Release profile of eugenol from electrospun PLA films at 4±1 °C for 48 h

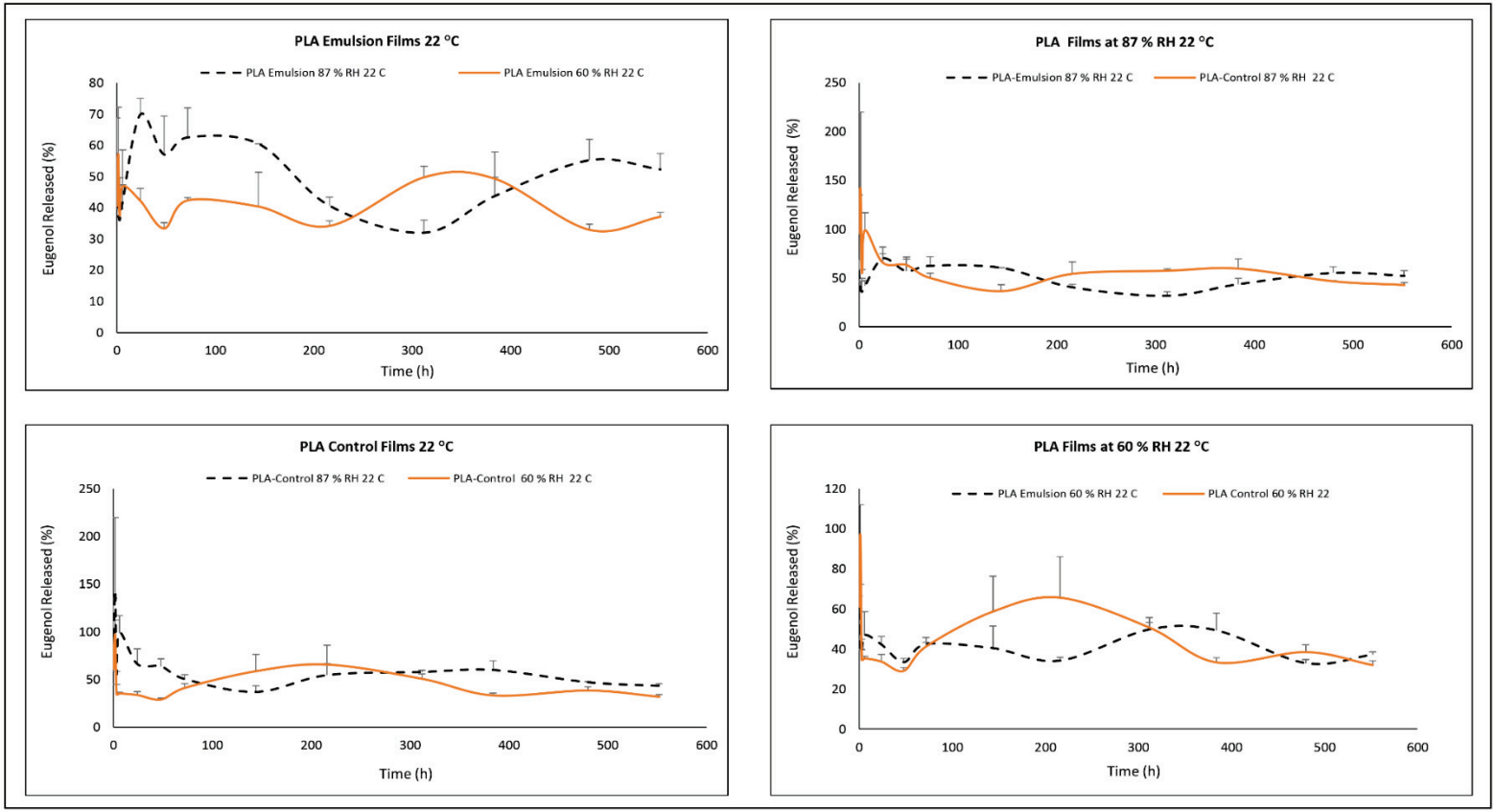

Figure 6.7. Release profile of eugenol from electrospun PLA films at 22±1 ºC for 552 h

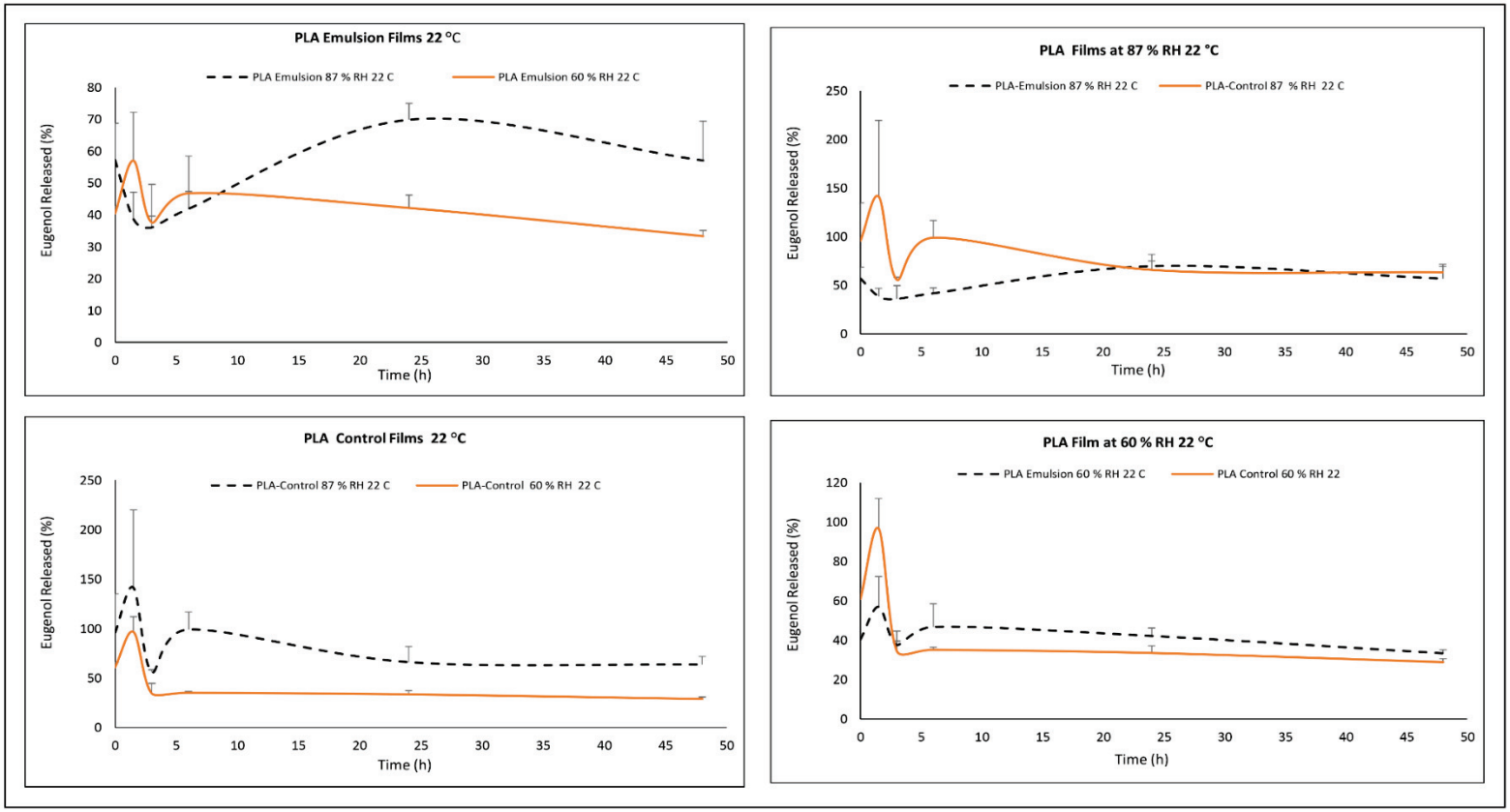

Figure 6.8. Release profile of eugenol from electrospun PLA films at 22±1 ºC for 48 h

6.3.3. Encapsulation Efficiency of Electrospun PLA Films

The encapsulation efficiency was determined by the extraction of eugenol from PLA film. The result showed that eugenol gaseous compound was successfully encapsulated in PLA-emulsion fibers. Cellulose emulsions containing films encapsulation efficiency was higher than that of control PLA films (without cellulose) (Table 6.2). Moreover, the ability of cellulose emulsions containing films to retain eugenol after the release was more than that of control films. In both tested temperatures and RH emulsions containing fibers retained a high amount of eugenol than control films (data were not shown). This result demonstrated the technical feasibility of delivering eugenol vapor via poly(lactic) acid (PLA) emulsion fibers-grafted PLA films with bacterial cellulose into the package headspace. Eugenol is a volatile compound, and it is sensitive to temperature and unfavorable environmental conditions. Therefore, during the spinning process loss of eugenol is also inevitable.

Table 6.2 Encapsulation of Eugenol in PLA Film

Films	Encapsulation Efficiency (%)
EE	88.26
EF	91.83
EG	86.09
CE	84.16
CF	60.05
CG	68.10

E: Films with cellulose C: Films without cellulose

6.3.4. Fourier Transform Infrared Spectroscopy of PLA Films

The chemical structure analysis of the solution cast neat PLA, cellulose, eugenol, electrospun PLA fibers-grafted to PLA films, electrospun PLA-eugenol fibers-grafted to PLA films, EE-EF-EG-electrospun PLA/emulsion fibers-grafted to PLA films (with containing eugenol 0.8, 1.6 and 3.2 mg/cm^2, respectively), electrospun PLA-eugenol fibers-grafted to PLA films CE-CF-CG-electrospun PLA fibers-grafted to PLA films (without containing bacterial cellulose but with containing eugenol as same to EE, EF, EG emulsion films) was carried out through FTIR spectroscopy, as shown in Figure 6.9.

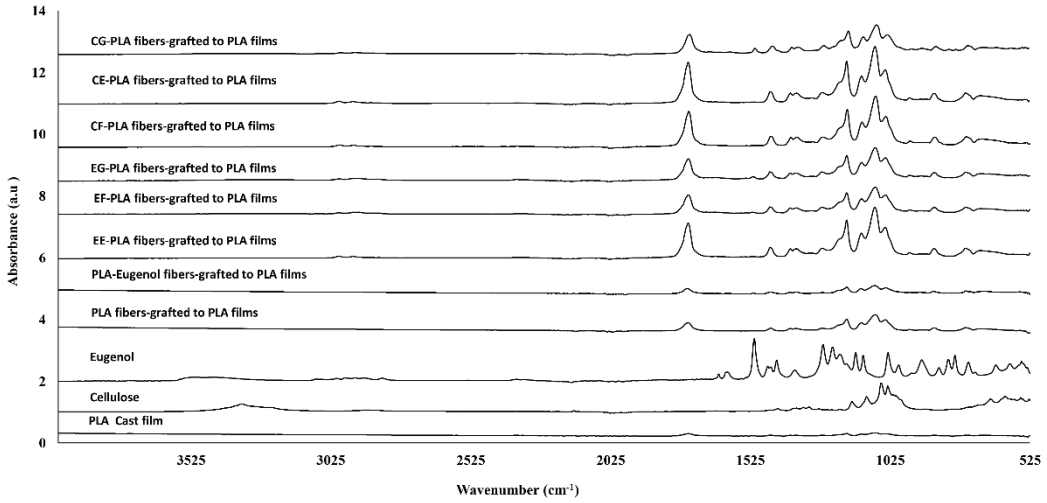

Figure 6.9. FTIR spectra of electrospun PLA films

Eugenol containing EE, EF and EG films showed the characteristic absorption peak of eugenol in all films at 1514, 1608 and 1637 cm^{-1} aromatic C=C stretching, spectra at 3300-3550 cm^{-1} phenol CO-H stretching, peaks at 2870, 2960 cm^{-1} symmetric stretching of methyl (-CH_3) (Dhoot et al., 2009).

In cellulose containing films, cellulose hydrogen bonds characteristic peaks are observed at 3650-3000 cm^{-1} (Castro et al., 2012; Li et al., 2013), cellulosic β-(1-4)-glycosidic linkages at 898 cm^{-1} spectra (Dhar, Tarafder, Kumar, & Katiyar, 2015; Pandey et al., 2014), the bands corresponding to the crystallinity of bacterial cellulose at 1427, 1277, 896 and 667 cm^{-1}.

All PLA films showed the typical spectra of PLA at 1742 cm^{-1} C=C stretching vibration, 1452, 1180, 754, 866-869, 955 cm^{-1} (Braun, Dorgan, & Hollingsworth, 2012; Li et al., 2013; Liu, Yuan, & Bhattacharyya, 2012). Spectral changes in PLA and

electrospun PLA fibers-grafted to PLA film were significantly observed. The presence of cellulose emulsions in the fibers was confirmed with FTIR and the cellulose in the films via fluorescence microscopy.

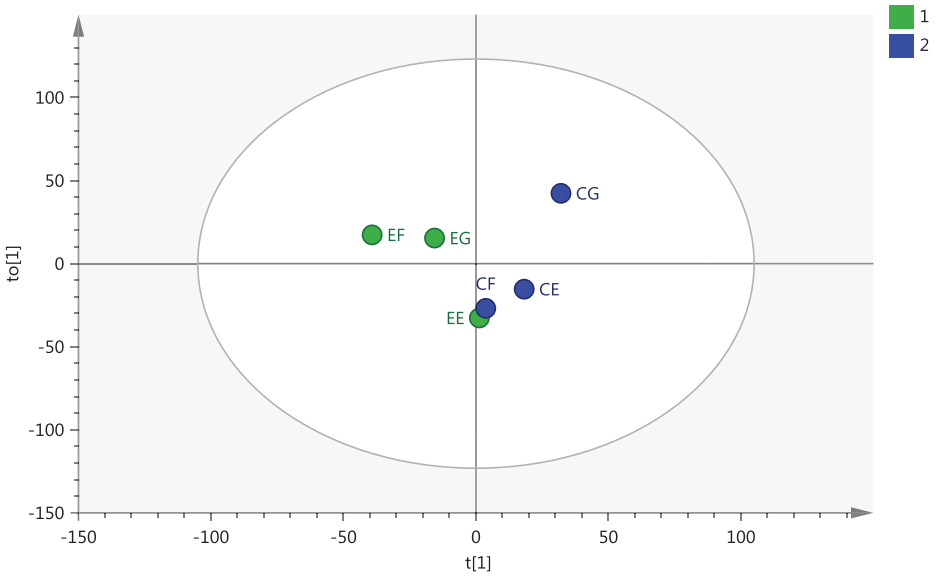

Figure 6.10 OPLS-DA score plots of EE, EF, EG, CE, CF, CG electrospun PLA films

6.3.5. Antifungal Properties of Electrospun PLA/Emulsion Fibers-Grafted to PLA Films

Antifungal activity of fabricated EG electrospun PLA/emulsion fibers-grafted to PLA (6 mg/cm^2 eugenol containing cellulose-emulsion) films against *B.cineria* was tested at headspace on agar media. EG film inhibited the total growth of *B.cineria* on PDA agar media (Figure 6.11). Eugenol antifungal activity against *B.cineria* has been reported by a number of studies in literature (El-Shiekh, El-Din, Shaymaa, & El-Din 2012; Shin et al., 2014; Wang et al., 2010). Wang et al. (2010) examined the mechanism of antifungal activity of eugenol against conidia and mycelial growth, and spore germination of *B.cineria* in detail and they reported that eugenol could be used in the control of *B.cineria*.

The results indicated that eugenol vapor release from PLA fibers active layer significantly inhibited the growth of *B.cineria* on agar media and sustained the release up to 120 h. The obtained nanocomposites have antifungal activity and could be used as an active layer inside the food package. Yam and Lee (2012) demonstrated that EOs vapor release from the fibers to the headspace of the food should be in control manner and

sufficient amount for inactivation/retard the growth of the food spoilage. The release rate/concentration of active compounds in packaged food should match the microbial kinetics of the food.

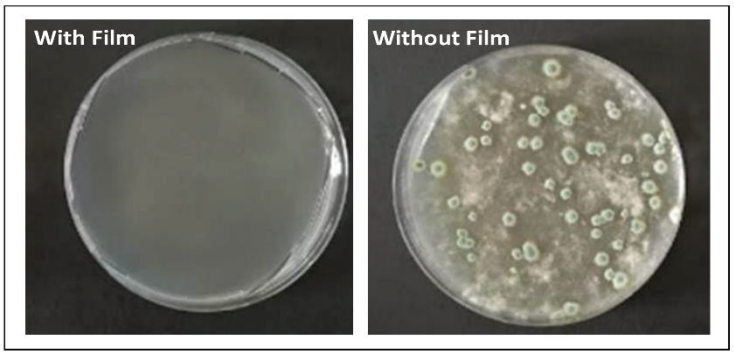

Figure 6.11. Antifungal activity of electrospun EG-PLA films against *B.cineria* with film and without film

6.3.6. Efficacy of Electrospun PLA/Emulsion Fibers-Grafted to PLA Films on the Microbial Safety of Table Grapes

Eugenol vapor released from the fibers and created an antimicrobial atmosphere in the headspace of the package. Eugenol showed a significant antifungal effect and reduced/delayed the decay of table grapes caused by *Botrytis cinerea* compared to control samples (Figure 6.12 and 6.13). According to the obtained results, released eugenol vapor was at the effective concentration for controlling the gray mold decay.

Martinez-Romero et al. (2007) reported the antifungal effect of carvacrol vapor phase on the survival of *B. cinerea* and concluded that carvacrol vapor effect was dose-dependent. The results of their study provided a carvacrol as a natural antifungal compound for preserving the post-harvest grape table losses during storage. Our results are also compatible with the findings of Martinez-Romero et al. (2007). Moreover, the effect of the eugenol and thymol vapor (Volero et al., 2006), eugenol, thymol and carvacrol vapor (Guillén et al., 2007) and thymol, eugenol and menthol vapor (Valverde et al., 2005) with the combination of modified atmosphere packaging, the significant reduction of yeast and mold, and the quality of table grapes during storage have been reported. In addition, Shin et al. (2014) observed that thymol and linalool fumigation significantly reduced *B.cineria* infection on table grapes.

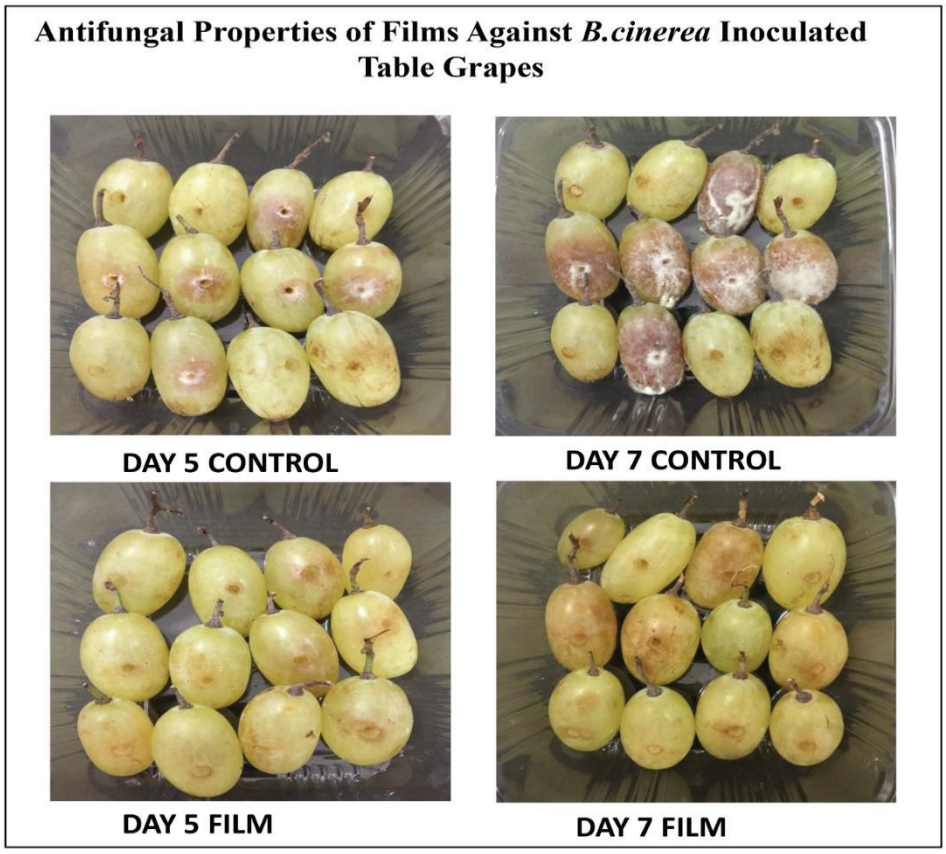

Figure 6.12. Visual images of antifungal activity of electrospun EG-PLA/emulsion fibers-grafted to PLA films against *B.cineria* on grapes after 5 and 7 days storage with film and without film

Table grapes are perishable fruits, and *Botrytis cinerea* infection causes the economically important loss of quality. PLA films with cellulose encapsulated eugenol volatile EOs may provide a new way to enhance the shelf life and microbial safety of the packed table grapes during storage. The antimicrobial vapor of eugenol could be considered as a potential biofumigant for the storage of table grapes, to reduce the post-harvest losses, improve the quality and safety of table grapes and contribute the economic sustainability. High eugenol concentration induced the browning effect on ‘’ Hatun Parmağı ‘’ table grapes cultivar (data were not shown). Further study is needed to optimize the eugenol concentration, which does not affect the color of different table grapes cultivars.

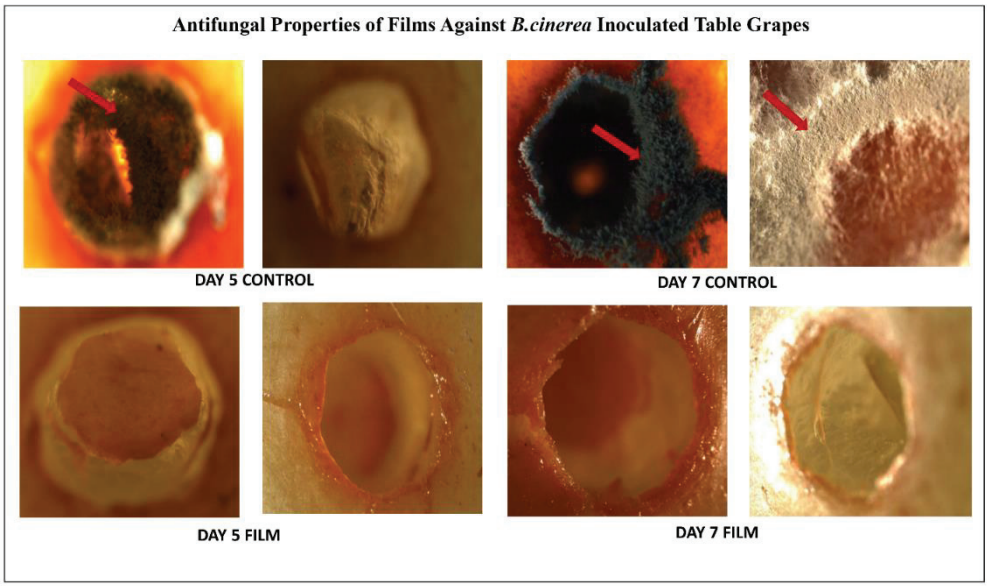

Figure 6.13. Stereo microscope images of the efficacy of eugenol vapor on inhibiting *Botrytis cinerea* population on table grapes after 7 day storage at 20 ℃ and 90% RH.

6.3.7. Sensory Analysis of Table Grapes

Sensory attributes of the table are an important parameter for consumers. The eugenol vapor treated samples had significantly highest scores after 5 and 7 days of storage (Table 6.3) The odor of eugenol in treated samples did not negatively affect the panelists. The eugenol odor rapidly evaporated from the packages when packages were opened for analysis. The panelists liked the eugenol odor in treated samples to some extent. Also, eugenol vapor treated samples had the highest odor score. In the study of the Costa, Lucera, Conte, Contò and Del Nobile (2013) observed that from sensory results, panelists selected the eugenol, ethanol, citrus extract and potassium sorbate as the most suitable compound for ready to eat table grapes.

Table 6.3. Sensory attribute evaluation of eugenol vapor on Film treated and untreated (control) samples after 5 days and 7 days storage at 20 ^{0}C and 90% RH.

Sensory Attribute	Treatments	Days 5	7
Appearance	Control	4.14[a]	4.3[a]
	Film Treated	7.42[a]	7.76[b]
Color	Control	4.85[a]	4.90[a]
	Film Treated	7.47[a]	7.66[b]
Odor	Control	5.52[a]	5.69[a]
	Film Treated	6.71[b]	6.42[a]
Overall Acceptability	Control	4.69[a]	4.73[a]
	Film Treated	7.19[a]	7.47[b]

[a-b]: Means of treatments in the same column with the different lowercase letter are significantly different ($p<0.05$) for each sensory attributes. ($n = 20$).

6.4. Conclusion

Eugenol vapor released from the fibers, created an antimicrobial atmosphere in the headspace of the package, and reduced the decay of table grapes. The result of this study showed the possibility of using the volatile eugenol at headspace as a biofumigant for protecting the quality and safety of packaged grape tables at marketing simulated conditions and this vapor treatment could be promising for organic fruit production. Eugenol vapors could be an alternative to the use of commercial SO_2 for a short term period according to the industrial needs for preserving the quality of table grapes. The release of eugenol vapor from the films in the package headspace should be at an effective concentration for controlling the postharvest decay. The release results gave us the idea about the released amount of antimicrobial into the headspace of the food package. The release of eugenol from the fibers should be matched the microbial kinetics of shelf life requirement. More experimental data are needed to explain this phenomenon and to determine the release rate. Further study is needed to determine release rates in different conditions to match the microbial kinetic. The relative humidity triggering release systems might be used in active packaging of high-moisture foods including meat, fish, and fresh foods products for which the risk of microbial degradation increases at high a_w conditions. To conclude, the weak release rate of eugenol in cellulose emulsions contained films, specifically at low temperature and RH is an advantage to store the antimicrobial packaging films without losses of the antimicrobial agent.

CHAPTER 7

CONCLUSION

Micro and nano scale dimensions of bacterial cellulose nanocrystals (BCNCs) with desired properties such as high thermal stability, high crystallinity, with negatively charged, stable aqueous crystals, and with proper morphology were successfully produced from bacterial cellulose nanofibers (BCNFs). BCNCs were obtained by optimizing the hydrolysis conditions at low acid concentrations, short hydrolysis time and low cellulose acid ratios combining the post-treatment.

Pickering emulsions stabilized by BCNFs and negatively charged BCNCs in the presence of different surfactants. BCNFs Pickering (oil-in-water) emulsions were successfully produced with a negatively charged emulsifier SDS and volatile eugenol essential oil. BCNCs Pickering (oil-in-water) emulsions were produced with eugenol essential oil, in the presence of positively charged emulsifier CTAB and food grade emulsifier LA. Bacterial cellulose-based oil-in water emulsions systems could be a potential carrier for delivering the volatile bioactive compounds in bioactive food packaging applications. Fluorescence microscopy confirmed the adsorption of BCNCs particles at the oil-water interface of the BCNCs stabilized Pickering emulsions.

Active poly(lactic) acid (PLA) fibers composed of eugenol essential oil encapsulated with bacterial cellulose nanocrystals emulsions were prepared by the electrospinning technique and spun onto PLA cast films. The SEM results confirmed that spinning solution formulation parameters are responsible for the formation of uniform, homogenous and beaded free fibers morphology. Bacterial cellulose crystals emulsions contained films (electrospun PLA/emulsion fibers-grafted to PLA films) tensile strength and Young's modulus were increased compared to control films (the electrospun PLA fibers-grafted to PLA films). The presence of cellulose emulsions in the fibers were confirmed with FTIR analysis and via fluorescence microscopy.

Active release of encapsulated eugenol vapors from electrospun PLA/emulsion fibers-grafted to PLA films to the headspace of the package completely inhibited the microbial growth of *L. innocua* and significantly decreased *E. coli* microbial load on agar media. The efficiency of antimicrobial packaging system was validated with

approximately 1.5 log reduction of *E. coli* and *L. innocua* on artificially contaminated tomatoes stem scar with electrospun PLA/emulsion fibers-grafted to PLA films.

The encapsulation of volatile eugenol compound with bacterial nano-cellulose crystals in PLA fibers via the electrospinning method is technically feasible. Temperature and relative humidity triggered the release of eugenol vapor from the fibers in the package headspace at effective levels.

Eugenol showed the controlled release for the long period release profile from the fibers. This may be enough to maintain the minimum inhibitory concentration on the surface of the food regarding the food application results.

The released amount of eugenol vapor from PLA films showed significant antifungal activity against *B. cinerea* on agar media. Eugenol vapor released from the fibers, created an antimicrobial atmosphere in the headspace of the package, and reduced the decay of table grapes. The result of this study showed the possibility of using the volatile eugenol at headspace as a biofumigant for protecting the quality and safety of packaged grape tables at marketing simulated conditions.

Eugenol vapor treatment could be promising for preserving the quality and safety of organic and traditional fresh produce. Eugenol vapors could be an alternative to the use of commercial SO_2 according to the industrial needs to preserve the quality of table grapes.

Novel biodegradable-PLA cellulose composite films may provide a new way for delivering bioactive gaseous compounds for intelligent food packaging applications to improve the food quality, safety, shelf life and may enhance the marketability of fresh produce.

Relative humidity enhanced the release of the volatile eugenol from the fibers, and this system can be used in active packaging of high-moisture foods including meat, fish, and fresh foods products for which the risk of microbial degradation increases at high a_w conditions.

The low amount of eugenol release from the films at low temperature and relative humidity may be the advantage of using fabricated films to store the films without losses of the volatile compound.

The vapor-phase approach appears to be promising way as a controlled release of eugenol and could be applied in active packaging. The obtained films can be directly used as active packaging self-standing film and can be used as labels inside the package.

Further study is needed to assess the safety aspect of eugenol concentration for the storage of grape tomatoes and table grapes.

High eugenol concentration induced the browning effect on ‘’ Hatun Parmağı ‘’ table grapes cultivar. Further study is needed to optimize the eugenol concentration on different table grapes cultivars.

To sum up, the finding of this research support the technical feasibility of delivering eugenol gaseous compound in the packed food via electrospun fibers. Further research will be needed to prove the economic feasibility of eugenol in the food packaging systems in commercial applications.

REFERENCES

Abitbol, T., Marway, H., & Cranston, E. D. (2014). Surface modification of cellulose nanocrystals with cetyltrimethylammonium bromide. *Nordic Pulp & Paper Research Journal*, *29*(1), 46–57.

Acevedo-Fani, A., Salvia-Trujillo, L., Rojas-Graü, M. A., & Martín-Belloso, O. (2015). Edible films from essential-oil-loaded nanoemulsions: Physicochemical characterization and antimicrobial properties. *Food Hydrocolloids*, *47*, 168–177.

Agarwal, S., Wendorff, J. H., & Greiner, A. (2008). Use of electrospinning technique for biomedical applications. *Polymer*, *49*(26), 5603–5621.

Agarwal, S., & Greiner, A. (2011). On the way to clean and safe electrospinning-green electrospinning: Emulsion and suspension electrospinning. *Polymers for Advanced Technologies*, *22*(3), 372–378.

Alila, S., Boufi, S., Belgacem, M. N., & Beneventi, D. (2005). Adsorption of a cationic surfactant onto cellulosic fibers - I. Surface charge effects. *Langmuir*, *21*(18), 8106–8113.

Almenar, E., Auras, R., Rubino, M., & Harte, B. (2007). A new technique to prevent the main post harvest diseases in berries during storage: Inclusion complexes β-cyclodextrin-hexanal. *International Journal of Food Microbiology*, *118*(2), 164-172.

Amano, Y., Ito, F., & Kanda, T. (2005). Novel cellulose producing system by microorganisms such as *Acetobacter sp*. *Journal of Biological Macromolecules*, *5*(1), 3–10.

Ambrosio-Martín, J., Fabra, M. J., Lopez-Rubio, A., & Lagaron, J. M. (2015). Melt polycondensation to improve the dispersion of bacterial cellulose into polylactide via melt compounding: enhanced barrier and mechanical properties. *Cellulose*, 22(2), 1201-1226.

ASTM. (2002). American society for testing and materials. Standard test method for tensile properties of thin plastic sheeting-D882-02.In ASTM (Ed.), *Annual Book of American Standard Testing Methods*. Philadelphia, PA.

Amiri, A., Dugas, R., Pichot, A. L., & Bompeix, G. (2008). In vitro and in vitro activity of eugenol oil (Eugenia caryophylata) against four important postharvest apple pathogens. *International Journal of Food Microbiology*, *126*(1), 13-19.

Andresen, M., & Stenius, P. (2007). Water-in-oil emulsions stabilized by hydrophobized microfibrillated cellulose. *Journal of Dispersion Science and Technology*, *28*(6), 837–844.

Appendini, P., & Hotchkiss, J. H. (2002). Review of antimicrobial food packaging. *Innovative Food Science & Emerging Technologies*, *3*(2), 113-126.

Araki, J., Wada, M., Kuga, S., & Okano, T. (1998). Flow properties of microcrystalline cellulose suspension prepared by acid treatment of native cellulose. *Colloids and Surfaces A: Physicochemical and Engineering Aspects*, *142*(1), 75-82.

Araki, J., Wada, M., Kuga, S., & Okano, T. (1999). Influence of surface charge on viscosity behavior of cellulose microcrystal suspension. *Journal of Wood Science*, 45(3), 258-261.

Araki, J., Wada, M., Kuga, S., & Okano, T. (2000). Birefringent glassy phase of a cellulose microcrystal suspension. *Langmuir*, *16*(6), 2413-2415.

Asker, D., Weiss, J., & McClements, D. J. (2011). Formation and stabilization of antimicrobial delivery systems based on electrostatic complexes of cationic-non-ionic mixed micelles and anionic polysaccharides. *Journal of Agricultural and Food Chemistry*, *59*(3), 1041–1049.

Auras, R., Harte, B., & Selke, S. (2004). An overview of polylactides as packaging materials. *Macromolecular Bioscience*, *4*(9), 835–864.

Aveyard, R., Binks, B. P., & Clint, J. H. (2003). Emulsions stabilised solely by colloidal particles. *Advances in Colloid and Interface Science*, *100–102*, 503–546.

Avinc, O., & Khoddami, A. (2009). Overview of poly lactid acid (PLA) fibre part I : Production , properties, performance , environmental impact , and end-use applications of poly (lactic acid) Fibres. *Fibre Chemistry*, *41*(6), 16–25.

Ayala-Zavala, J. F., Oms-Oliu, G., Odriozola-Serrano, I., González-Aguilar, G. A., Álvarez-Parrilla, E., & Martín-Belloso, O. (2008a). Bio-preservation of fresh-cut tomatoes using natural antimicrobials. *European Food Research and Technology*, *226*(5), 1047–1055.

Ayala-Zavala, J. F., Del-Toro-Sánchez, L., Alvarez-Parrilla, E., & González-Aguilar, G. A. (2008b). High relative humidity in-package of fresh-cut fruits and vegetables: advantage or disadvantage considering microbiological problems and antimicrobial delivering systems?. *Journal of Food Science*, *73*(4).

Aytac, Z., Dogan, S. Y., Tekinay, T., & Uyar, T. (2014). Release and antibacterial activity of allyl isothiocyanate/β-cyclodextrin complex encapsulated in electrospun nanofibers. *Colloids and Surfaces B: Biointerfaces*, *120*, 125-131.

Azizi Samir, M. A. S., Alloin, F., & Dufresne, A. (2005). Review of recent research into cellulosic whiskers, their properties and their application in nanocomposite field. *Biomacromolecules*, *6*(2), 612–626.

Bakry, A. M., Abbas, S., Ali, B., Majeed, H., Abouelwafa, M. Y., Mousa, A., & Liang, L. (2016). Microencapsulation of oils: a comprehensive review of benefits, techniques, and applications. *Comprehensive Reviews in Food Science and Food Safety*, 15(1), 143-182.

Baruah, B., & Kiambuthi, M. (2014). Facile synthesis of silver and bimetallic silver–gold nanoparticles and their applications in surface-enhanced Raman scattering. *RSC Advances*, *4*(110), 64860-64870.

Beck-Candanedo, S., Roman, M., & Gray, D. G. (2005). Effect of reaction conditions on the properties and behavior of wood cellulose nanocrystal suspensions. *Biomacromolecules*, 6(2), 1048–1054.

Bejrapha, P., Choi, M. J., Surassmo, S., Chun, J. Y., & Min, S. G. (2011). Formulation and antimicrobial activity on escherichia coli of nanoemulsion coated with whey protein ısolate. *Korean Journal for Food Science of Animal Resources*, *31*(4), 543–550.

Beuchat, L. R., & Brackett, R. E. (1991). Behavior of Listeria monocytogenes inoculated into raw tomatoes and processed tomato products. *Applied and Environmental Microbiology*, *57*(5), 1367–1371.

Bhushani, J. A., & Anandharamakrishnan, C. (2014). Electrospinning and electrospraying techniques: Potential food based applications. *Trends in Food Science & Technology,* 38(1), 21-33.

Biji, K. B., Ravishankar, C. N., Mohan, C. O., & Gopal, T. S. (2015). Smart packaging systems for food applications: a review. *Journal of Food Science and Technology*, *52*(10), 6125-6135.

Bilia A. R., Guccione C., Isacchi B., Righeschi C., Firenzuoli F., & Bergonzi M. C. (2014). Essential oils loaded in nanosystems: a developing strategy for a successful therapeutic approach. *Evidence-Based Complementary and Alternative Medicine*, 1–14.

Binks, B. P., & Lumsdon, S. O. (2000). Effects of oil type and aqueous phase composition on oil water mixtures containing particles of intermediate hydrophobicity. *Physical Chemistry Chemical Physics*, *2*(13), 2959-2967.

Bondeson, D., & Oksman, K. (2007). Dispersion and characteristics of surfactant modified cellulose whiskers nanocomposites. *Composite Interfaces*, *14*(7–9), 617–630.

Braun, B., Dorgan, J. R., & Hollingsworth, L. O. (2012). Supra-molecular ecobionanocomposites based on polylactide and cellulosic nanowhiskers: synthesis and properties. *Biomacromolecules*, *13*(7), 2013–2019.

Brody, A. L., Bugusu, B., Han, J. H., Sand, C. K., & McHugh, T. H. (2008). Innovative food packaging solutions. *Journal of Food Science*, *73*(8), 107-115.

Burger, C., Hsiao, B. S., & Chu, B. (2006). Nanofibrous materials and their applications. *Annu. Rev. Mater. Res.*, *36*, 333-368.

Burt, S. (2004). Essential oils: their antibacterial properties and potential applications in foods. *International Journal of Food Microbiology*, *94*(3), 223–253.

César, N. R., Pereira-da-Silva, M. A., Botaro, V. R., & de Menezes, A. J. (2015). Cellulose nanocrystals from natural fiber of the macrophyte typha domingensis: extraction and characterization. *Cellulose*, *22*(1), 449–460.

Camarero Espinosa, S., Kuhnt, T., Foster, E. J., & Weder, C. (2013). Isolation of thermally stable cellulose nanocrystals by phosphoric acid hydrolysis. *Biomacromolecules*, *14*(4), 1223–1230.

Camerlo, A., Vebert-Nardin, C., Rossi, R. M., & Popa, A. M. (2013). Fragrance encapsulation in polymeric matrices by emulsion electrospinning. *European Polymer Journal*, *49*(12), 3806–3813.

Capron, I. (2013). Surfactant-free high internal phase emulsions stabilized by cellulose nanocrystals. *Biomacromolecules*, *14*(2), 291–296.

Carrillo, C. A., Nypelö, T. E., & Rojas, O. J. (2015). Cellulose nanofibrils for one-step stabilization of multiple emulsions (W/O/W) based on soybean oil. *Journal of Colloid and Interface Science*, *445*, 166–173.

Casasola, R., Thomas, N. L., Trybala, A., & Georgiadou, S. (2014). Electrospun poly lactic acid (PLA) fibres: Effect of different solvent systems on fibre morphology and diameter. *Polymer*, *55*(18), 4728–4737.

Castro, C., Zuluaga, R., Álvarez, C., Putaux, J. L., Caro, G., Rojas, O. J., Gañán, P. (2012). Bacterial cellulose produced by a new acid-resistant strain of Gluconacetobacter genus. *Carbohydrate Polymers*, *89*(4), 1033–1037.

CDC. (2016). Estimates of foodborne illnes in the United States. Retrieved June 11, 2017, from: https://www.cdc.gov/foodborneburden/pdfs/scallan-estimated-illnesses-foodborne-pathogens.pdf

Chalier, P., Ben Arfa, A., Guillard, V., & Gontard, N. (2008). Moisture and temperature triggered release of a volatile active agent from soy protein coated paper: effect of glass transition phenomena on carvacrol diffusion coefficient. *Journal of Agricultural and Food Chemistry*, *57*(2), 658-665.

Chanjirakul, K., Wang, S. Y., Wang, C. Y., & Siriphanich, J. (2007). Natural volatile treatments increase free-radical-scavenging capacity of strawberries and blackberries. *Journal of the Science of Food and Agriculture*, 87(8), 1463-1472.

Chawla, P. R., Bajaj, I. B., Survase, S. A., & Singhal, R. S. (2009). Microbial cellulose: Fermentative production and applications. *Food Technology and Biotechnology*, *47*(2), 107–124.

Cheng, K.-C., Catchmark, J. M., & Demirci, A. (2009). Enhanced production of bacterial cellulose by using a biofilm reactor and its material property analysis. *Journal of Biological Engineering*, *3(1)*, 12.

Cherhal, F., Cousin, F., & Capron, I. (2016). Structural description of the ınterface of pickering emulsions stabilized by cellulose nanocrystals. *Biomacromolecules*, *17*(2), 496–502.

Chevalier, Y., & Bolzinger, M. A. (2013). Emulsions stabilized with solid nanoparticles: Pickering emulsions. *Colloids and Surfaces A: Physicochemical and Engineering Aspects*, *439*, 23-34.

Choi, M. J., Soottitantawat, A., Nuchuchua, O., Min, S. G., & Ruktanonchai, U. (2009). Physical and light oxidative properties of eugenol encapsulated by molecular inclusion and emulsion–diffusion method. *Food Research International*, *42*(1), 148-156.

Cortés-Rojas, D. F., Souza, C. R., & Oliveira, W. P. (2014). Encapsulation of eugenol rich clove extract in solid lipid carriers. *Journal of Food Engineering*, *127*, 34-42.

Costa, C., Lucera, A., Conte, A., Contò, F., & Del Nobile, M. A. (2013). In vitro and in vivo application of active compounds with anti-yeast activity to improve the shelf life of ready-to-eat table grape. *World Journal of Microbiology and Biotechnology*, *29*(6), 1075-1084.

Cui, H., Yuan, L., Li, W., & Lin, L. (2017). Antioxidant property of SiO_2-eugenol liposome loaded nanofibrous membranes on beef. *Food Packaging and Shelf Life*, *11*, 49–57.

Cunha, A. G., Mougel, J. B., Cathala, B., Berglund, L. A., & Capron, I. (2014). Preparation of double pickering emulsions stabilized by chemically tailored nanocelluloses. *Langmuir*, *30*(31), 9327–9335.

Dai, R., & Lim, L. T. (2015). Release of allyl isothiocyanate from mustard seed meal powder entrapped in electrospun PLA-PEO nonwovens. *Food Research International*, *77*, 467–475.

De Souza Lima, M. M., & Borsali, R. (2004). Rodlike cellulose microcrystals: Structure, properties, and applications. *Macromolecular Rapid Communications*, *25*(7), 771–787.

Del Nobile, M. A., Conte, A., Incoronato, A. L., & Panza, O. (2008). Antimicrobial efficacy and release kinetics of thymol from zein films. *Journal of Food Engineering*, *89*(1), 57-63.

Devi, K. P., Nisha, S. A., Sakthivel, R., & Pandian, S. K. (2010). Eugenol (an essential oil of clove) acts as an antibacterial agent against Salmonella typhi by disrupting the cellular membrane. *Journal of Ethnopharmacology*, 130(1), 107-115.

Deza, M. A., Araujo, M., & Garrido, M. J. (2003). Inactivation of Escherichia coli O157:H7, Salmonella enteritidis and Listeria monocytogenes on the surface of tomatoes by neutral electrolyzed water. *Letters in Applied Microbiology*, *37*(6), 482–487.

Dhar, P., Tarafder, D., Kumar, A., & Katiyar, V. (2015). Effect of cellulose nanocrystal polymorphs on mechanical, barrier and thermal properties of poly (lactic acid) based bionanocomposites. *RSC Advances*, 5(74), 60426-60440.

Dickinson, E. (2009). Hydrocolloids as emulsifiers and emulsion stabilizers. *Food hydrocolloids,* 23(6), 1473-1482.

Dhoot, G., Auras, R., Rubino, M., Dolan, K., & Soto-Valdez, H. (2009). Determination of eugenol diffusion through LLDPE using FTIR-ATR flow cell and HPLC techniques. *Polymer*, *50*(6), 1470–1482.

Ditzel, F. I., Prestes, E., Carvalho, B. M., Demiate, I. M., & Pinheiro, L. A. (2016). Nanocrystalline cellulose extracted from pine wood and corncob. *Carbohydrate Polymers*, *157*, 1577–1585.

Dorman, H. J. D., & Deans, S. G. (2000). Antimicrobial agents from plants: antibacterial activity of plant volatile oils. *Journal of Applied Microbiology*, *88*(2), 308-316.

Dufresne, A. (2013). Nanocellulose: A new ageless bionanomaterial. *Materials Today*, *16*(6), 220–227.

Duran, N., Lemes, A., Duran, M., Freer, J., & Baeza, J. (2011). A minireview of cellulose nanocrystals and ıts potential ıntegration as co-product in bioethanol production. *Journal of the Chilean Chemical Society*, *56*, 672–677.

El-Saied, H., El-Diwany, A. I., Basta, A. H., Atwa, N. A., & El-Ghwas, D. E. (2008). Production and characterization of economical bacterial cellulose. *BioResources*, *3*(4), 1196–1217.

El-Shiekh, Y. W. A., El-Din, N. H., Shaymaa, M. A. A., & El-Din, K. A. Z. (2012). Antifungal activity of some naturally occurring compounds against economically important phytopathogenic fungi. *Nat. Sci*, 10, 114-123.

Elazzouzi-Hafraoui, S., Nishiyama, Y., Putaux, J.L., Heux, L., Dubreuil, F., & Rochas, C. (2007). The shape and size distribution of crystalline nanoparticles prepared by acid hydrolysis of native cellulose. *Biomacromolecules*, *9*(1), 57–65.

Elazzouzi-Hafraoui, S., Putaux, J. L., & Heux, L. (2009). Self-assembling and chiral nematic properties of organophilic cellulose nanocrystals. *Journal of Physical Chemistry B*, *113*(32), 11069–11075.

Eyley, S., & Thielemans, W. (2014). Surface modification of cellulose nanocrystals. *Nanoscale*, *6*(14), 7764–7779.

Fabra, M. J., Lopez-Rubio, A., & Lagaron, J. M. (2013). High barrier polyhydroxyalcanoate food packaging film by means of nanostructured electrospun interlayers of zein. *Food Hydrocolloids*, *32*(1), 106-114.

Fahma, F., Hori, N., Iwamoto, S., Iwata, T., & Takemura, A. (2016). Cellulose nanowhiskers from sugar palm fibers. *Emirates Journal of Food and Agriculture*, *28*(8), 566.

Fan, X., Sokak, K. J. B., Engeman, J., Gurter, J. B., & Liu, Y. (2012). Inactivation of listeria innocua, salmonella typhimurium, and escherichia coli O157:H7 on surface and stem scar areas of tomatoes using ın-package ozonation. *Journal of Food Protection*, *75*(9), 1611–1618.

Fang, J., Wang, X., & Lin, T. (2011). Functional applications of electrospun nanofibers. In Nanofibers-production, properties and functional applications. *InTech*.

FAO. (2011). Food loss and food waste. Retrieved May 21, 2017, from: http://www.fao.org/docrep/014/mb060e/mb060e00.pdf.

FAO. (2017). Save food: Global initiative on food loss and waste reduction. Retrieved July 21, 2017, from: http://www.fao.org/save food/resources/keyfindings/en/

FDA. (1973). Select committee on GRAS substances (SCOGS) opinion: Clove bud extract, clove bud oil, clove bud oleoresin, clove leaf oil, clove stem oil, eugenol. Retrieved July 21, 2017, from: https://www.fda.gov/food/ingredientspackaginglabeling/gras/scogs/ucm261254.htm

FDA. (2002). Inventory effective food contact substance (CFS) notifications. FCN No: 178 (Polylactide Polymers (CAS Reg. No. 9051-89-2). Retrieved July 17, 2017, from:https://www.accessdata.fda.gov/scripts/fdcc/index.cfm?set=FCN&sort=FCN_No&order=DESC&startrow=1&search=9051-89-2

FDA. (2005). Agency response letter RAS Notice No. GRN 000164. (Under 21 CFR 170.30(b)). Retrieved July 17, 2017, from: https://www.fda.gov/food/ingredientspackaginglabeling/gras/noticeinventory/ucm154571.htm

Forslund, A., Ensink, J. H. J., Markussen, B., Battilani, A., Psarras, G., Gola, S., Dalsgaard, A. (2012). Escherichia coli contamination and health aspects of soil and tomatoes (Solanum lycopersicum L.) subsurface drip irrigated with on-site treated domestic wastewater. *Water Research*, *46*(18), 5917–5934.

Farag, R. S., Daw, Z. Y., Hewedi, F. M., & El-Baroty, G. S. A. (1989). Antimicrobial activity of some Egyptian spice essential oils. *Journal of Food Protection*, 52(9), 665-667.

Feng, K., Wen, P., Yang, H., Li, N., Lou, W. Y., Zong, M. H., & Wu, H. (2017). Enhancement of the antimicrobial activity of cinnamon essential oil-loaded electrospun nanofilm by the incorporation of lysozyme. *RSC Advances*, 7(3), 1572-1580.

Friedman, M., Henika, P. R., & Mandrell, R. E. (2002). Bactericidal activities of plant essential oils and some of their isolated constituents against Campylobacter jejuni, Escherichia coli, Listeria monocytogenes, and Salmonella enterica. *Journal of Food Protection*, *65*(10), 1545–1560.

Fu, W., Liu, Y., Yang, C., Wang, W. H., Wang, M., & Jia, Y. Y. (2015). Stabilization of pickering emulsions by bacterial cellulose nanofibrils. *Key Engineering Materials*, *645–646*, 1247–1254.

Gama, M., Gatenholm, P., & Klemm, D. (Eds.). (2012). Bacterial nanocellulose: a sophisticated multifunctional material. *CRC Press.*

Gaysinsky, S., Davidson, P. M., Bruce, B. D., & Weiss, J. (2005). Stability and antimicrobial efficiency of eugenol encapsulated in surfactant micelles as affected by temperature and pH. *Journal of Food Protection*, *68*(7), 1359–1366.

Gea, S., Reynolds, C. T., Roohpour, N., Wirjosentono, B., Soykeabkaew, N., Bilotti, E., & Peijs, T. (2011). Investigation into the structural, morphological, mechanical and thermal behaviour of bacterial cellulose after a two-step purification process. *Bioresource Technology*, *102*(19), 9105–9110.

George, J., Ramana, K. V., Bawa, A. S., & Siddaramaiah. (2011). Bacterial cellulose nanocrystals exhibiting high thermal stability and their polymer nanocomposites. *International Journal of Biological Macromolecules*, *48*(1), 50–57.

George, J. (2012). High performance edible nanocomposite films containing bacterial cellulose nanocrystals. *Carbohydrate Polymers*, *87*(3), 2031-2037.

George, J., & Sabapathi, S. N. (2015). Cellulose nanocrystals: synthesis, functional properties , and applications. *Nanotechnology, Science and Applications*, (8),45–54.

Gestranius, M., Stenius, P., Kontturi, E., Sjöblom, J., & Tammelin, T. (2017a). Phase behaviour and droplet size of oil-in-water Pickering emulsions stabilised with plant-derived nanocellulosic materials. *Colloids and Surfaces A: Physicochemical and Engineering Aspects*, *519*, 60–70.

Ghorani, B., & Tucker, N. (2015). Fundamentals of electrospinning as a novel delivery vehicle for bioactive compounds in food nanotechnology. *Food Hydrocolloids*, *51*, 227–240.

Glasser, W. G., Taib, R., Jain, R. K., & Kander, R. (1999). Fiber-reinforced cellulosic thermoplastic composites. *Journal of Applied Polymer Science*, *73*(7), 1329–1340.

Gong, L., Li, T., Chen, F., Duan, X., Yuan, Y., Zhang, D., & Jiang, Y. (2016). An inclusion complex of eugenol into β-cyclodextrin: Preparation, and physicochemical and antifungal characterization. *Food Chemistry*, *196*, 324–330.

Gong, X., Wang, Y., & Chen, L. (2017). Enhanced emulsifying properties of wood-based cellulose nanocrystals as Pickering emulsion stabilizer. *Carbohydrate Polymers*, *169*, 295–303.

Goñi, P., López, P., Sánchez, C., Gómez-Lus, R., Becerril, R., & Nerín, C. (2009). Antimicrobial activity in the vapour phase of a combination of cinnamon and clove essential oils. *Food Chemistry*, *116*(4), 982–989.

Graupner, N., Herrmann, A. S., & Müssig, J. (2009). Natural and man-made cellulose fibre-reinforced poly (lactic acid)(PLA) composites: An overview about mechanical characteristics and application areas. Composites Part A: *Applied Science and Manufacturing*, 40(6), 810-821.

Gu, J., & Catchmark, J. M. (2012). Impact of hemicelluloses and pectin on sphere-like bacterial cellulose assembly. *Carbohydrate Polymers*, *88*(2), 547–557.

Gu, J., & Catchmark, J. M. (2013). Polylactic acid composites incorporating casein functionalized cellulose nanowhiskers. *Journal of Biological Engineering*, 7(1), 31.

Guillén, F., Zapata, P. J., Martínez-Romero, D., Castillo, S., Serrano, M., & Valero, D. (2007). Improvement of the overall quality of table grapes stored under modified atmosphere packaging in combination with natural antimicrobial compounds. *Journal of Food Science*, *72*(3).

Haaj, S. B., Magnin, A., & Boufi, S. (2014). Starch nanoparticles produced via ultrasonication as a sustainable stabilizer in Pickering emulsion polymerization. *RSC Adv.*, *4*(80), 42638–42646.

Habibi, Y., Lucia, L. A., & Rojas, O. J. (2010). Cellulose Nanocrystals: chemistry, self-assembly, and applications. *Chemical Reviews*, *110(6)*, 3479–3500.

Habibi, Y. (2014). Key advances in the chemical modification of nanocelluloses. *Chemical Society Reviews*, *43*(5), 1519-1542.

Helander, I. M., Alakomi, H.-L., Latva-Kala, K., Mattila-Sandholm, T., Pol, I., Smid, E. J., Von Wright, A. (1998). Characterization of the action of selected essential oil components on gram-negative bacteria. *Journal of Agricultural and Food Chemistry*, *46*(9), 3590–3595.

Henrique, M. Alves, Flauzino Neto, W. Pires, Silvério, H. Alves, Martins, D. Ferreira, Gurgel, L. Vinícius. Alves, Barud, H. da Silva, Morais, L. Carlos de, & Pasquini, D. (2015). Kinetic study of the thermal decomposition of cellulose nanocrystals with different polymorphs, cellulose I and II, extracted from different sources and using different types of acids. *Industrial Crops and Products*, *76*, 128–140.

Heux, L., Chauve, G., & Bonini, C. (2000). Nonflocculating and chiral-nematic self-ordering of cellulose microcrystals suspensions in nonpolar solvents. *Langmuir*, 16(21), 8210-8212.

Hill, L. E., Gomes, C., & Taylor, T. M. (2013). Characterization of beta-cyclodextrin inclusion complexes containing essential oils (trans-cinnamaldehyde, eugenol, cinnamon bark, and clove bud extracts) for antimicrobial delivery applications. *LWT-Food Science and Technology*, *51*(1), 86-93.

Ho, K. W., Ooi, C. W., Mwangi, W. W., Leong, W. F., Tey, B. T., & Chan, E. S. (2016). Comparison of self-aggregated chitosan particles prepared with and without ultrasonication pretreatment as Pickering emulsifier. *Food Hydrocolloids*, *52*, 827–837.

Honary, S., & Zahir, F. (2013). Effect of zeta potential on the properties of nano-drug delivery systems-a review (Part 2). *Tropical Journal of Pharmaceutical Research*, *12*(2), 265-273.

Hu, Z., Ballinger, S., Pelton, R., & Cranston, E. D. (2015). Surfactant-enhanced cellulose nanocrystal Pickering emulsions. *Journal of Colloid and Interface Science*, *439*, 139–148.

Hu, Z., Marway, H. S., Kasem, H., Pelton, R., & Cranston, E. D. (2016). Dried and redispersible cellulose nanocrystal pickering emulsions. *ACS Macro Letters*, *5*(2), 185–189.

Inouye, S., Uchida, K., Maruyama, N., Yamaguchi, H., & Abe, S. (2006). A novel method to estimate the contribution of the vapor activity of essential oils in agar diffusion assay. *Nippon Ishinkin Gakkai Zasshi*, 47(2), 91-98.

Iwatake, A., Nogi, M., & Yano, H. (2008). Cellulose nanofiber-reinforced polylactic acid. *Composites Science and Technology*, 68(9), 2103-2106.

Ji, K., Wang, W., Zeng, B., Chen, S., Zhao, Q., Chen, Y., & Ma, T. (2016). Bacterial cellulose synthesis mechanism of facultative anaerobe Enterobacter sp. FY-07. *Scientific Reports*, *6*, 21863.

Jia, Y., Zhai, X., Fu, W., Liu, Y., Li, F., & Zhong, C. (2016). Surfactant-free emulsions stabilized by tempo-oxidized bacterial cellulose. *Carbohydrate Polymers*, *151*, 907–915.

Jiang, F., & Hsieh, Y. Lo. (2015). Holocellulose nanocrystals: amphiphilicity, oil/water emulsion, and self-assembly. *Biomacromolecules*, *16*(4), 1433–1441.

Jin, T., & Gurtler, J. B. (2012). Inactivation of salmonella on tomato stem scars by edible chitosan and organic acid coatings. *Journal of Food Protection*, *75*(8), 1368–1372.

Jonoobi, M., Harun, J., Mathew, A. P., & Oksman, K. (2010). Mechanical properties of cellulose nanofiber (CNF) reinforced polylactic acid (PLA) prepared by twin screw extrusion. *Composites Science and Technology*, 70(12), 1742-1747

Jorfi, M., & Foster, E. J. (2015). Recent advances in nanocellulose for biomedical applications. *Journal of Applied Polymer Science*, *132*(14), 1–19.

Jirovetz, L., Buchbauer, G., Stoilova, I., Stoyanova, A., Krastanov, A., & Schmidt, E. (2006). Chemical composition and antioxidant properties of clove leaf essential oil. *Journal of Agricultural and Food Chemistry*, 54(17), 6303-6307.

Kalashnikova, I., Bizot, H., Cathala, B., & Capron, I. (2011). New pickering emulsions stabilized by bacterial cellulose nanocrystals. *Langmuir*, *27*(12), 7471–7479.

Kalashnikova, I., Bizot, H., Cathala, B., & Capron, I. (2012). Modulation of cellulose nanocrystals amphiphilic properties to stabilize oil/water interface. *Biomacromolecules*, 13(1), 267-275.

Kalashnikova, I., Bizot, H., Bertoncini, P., Cathala, B., & Capron, I. (2013). Cellulosic nanorods of various aspect ratios for oil in water Pickering emulsions. *Soft Matter*, *9*(3), 952–959.

Kallel, F., Bettaieb, F., Khiari, R., García, A., Bras, J., & Chaabouni, S. E. (2016). Isolation and structural characterization of cellulose nanocrystals extracted from garlic straw residues. *Industrial Crops and Products*, *87*, 287–296.

Kapetanakou, A. E., & Skandamis, P. N. (2016). Applications of active packaging for increasing microbial stability in foods: Natural volatile antimicrobial compounds. *Current Opinion in Food Science*, *12*, 1–12.

Kara, H. H., Xiao, F., Sarker, M., Jin, T. Z., Sousa, A. M. M., Liu, C. K., Peggy, M. T. & Liu, L. (2016). Antibacterial poly(lactic acid) (PLA) films grafted with electrospun PLA/allyl isothiocyanate fibers for food packaging. *Journal of Applied Polymer Science*, *133*(2), 1–8.

Kayaci, F., Ertas, Y., & Uyar, T. (2013). Enhanced thermal stability of eugenol by cyclodextrin inclusion complex encapsulated in electrospun polymeric nanofibers. *Journal of Agricultural and Food Chemistry*, *61*(34), 8156–8165.

Kayaci, F., Umu, O. C. O., Tekinay, T., & Uyar, T. (2013). Antibacterial electrospun poly(lactic acid) (pla) nano fibrous webs ıncorporating triclosan/cyclodextrin ınclusion complexes. *Journal of Agricultural and Food Chemistry*, *61*(16), 3901-3908.

Kasprzyk, H., & Wichłacz, K. (2004). Some aspects of estimation of the crystallinity of gamma radiation wood cellulose by FTIR spectroscopy and X-ray diffraction techniques. *Acta Scientiarum Polonorum Silvarum Colendarum Ratio et Industria Lignaria*, 3(1), 73-84.

Kedzior, S. A., Marway, H. S., & Cranston, E. D. (2017). Tailoring cellulose nanocrystal and surfactant behavior in miniemulsion polymerization. *Macromolecules*, *50*(7), 2645–2655.

Kim, D. Y., Nishiyama, Y., Wada, M., & Kuga, S. (2001). High-yield carbonization of cellulose by sulfuric acid impregnation. *Cellulose*, *8*(1), 29–33.

Kim, J., Montero, G., Habibi, Y., Hinestroza, J. P., Genzer, J., Argyropoulos, D. S., & Rojas, O. J. (2009). Dispersion of cellulose crystallites by nonionic surfactants in a hydrophobic polymer matrix. *Polymer Engineering & Science*, *49*(10), 2054–2061.

Kim, E., Oh, C. S., Koh, S. H., Kim, H. S., Kang, K. S., Park, P. S., & Park, I. K. (2016). Antifungal activities after vaporization of ajowan (Trachyspermum ammi) and allspice (Pimenta dioica) essential oils and blends of their constituents against three Aspergillus species. *Journal of Essential Oil Research*, 28(3), 252-259.

Klemm, D., Kramer, F., Moritz, S., Lindström, T., Ankerfors, M., Gray, D., & Dorris, A. (2011). Nanocelluloses: A new family of nature-based materials. *Angewandte Chemie - International Edition*, *50*(24), 5438–5466.

Kriegel, C., Arrechi, A., Kit, K., McClements, D. J., & Weiss, J. (2008). Fabrication, functionalization, and application of electrospun biopolymer nanofibers. *Critical Reviews in Food Science and Nutrition*, *48*(8), 775-797.

Kriegel, C., Kit, K. M., McClements, D. J., & Weiss, J. (2009). Influence of surfactant type and concentration on electrospinning of chitosan-poly(ethylene oxide) blend nanofibers. *Food Biophysics*, *4*(3), 213–228.

Kriegel, C., Kit, K. M., McClements, D. J., & Weiss, J. (2010). Nanofibers as carrier systems for antimicrobial microemulsions. II. Release characteristics and antimicrobial activity. *Journal of Applied Polymer Science*, *118*(5), 2859-2868.

Kumar, A., Negi, Y. S., Choudhary, V., & Bhardwaj, N. K. (2014). Characterization of cellulose nanocrystals produced by acid-hydrolysis from sugarcane bagasse as agro-waste. *Journal of Materials Physics and Chemistry*, *2*(1), 1–8.

Kumar, A., Bhattacharjee, G., Kulkarni, B. D., & Kumar, R. (2015). Role of surfactants in promoting gas hydrate formation. *Industrial & Engineering Chemistry Research*, *54*(49), 12217-12232.

LaCoste, A., Schaich, K. M., Zumbrunnen, D., & Yam, K. L. (2005). Advancing controlled release packaging through smart blending. *Packaging Technology and Science*, *18*(2), 77-87.

Laird, K., & Phillips, C. (2012). Vapour phase: A potential future use for essential oils as antimicrobials? *Letters in Applied Microbiology*, *54*(3), 169–174.

Lashkari, E., Wang, H., Liu, L., Li, J., & Yam, K. (2017). Innovative application of metal-organic frameworks for encapsulation and controlled release of allyl isothiocyanate. *Food Chemistry*, *221*, 926–935.

Lee, K. Y., Blaker, J. J., Murakami, R., Heng, J. Y. Y., & Bismarck, A. (2014a). Phase behavior of medium and high internal phase water-in-oil emulsions stabilized solely by hydrophobized bacterial cellulose nanofibrils. *Langmuir*, *30*(2), 452–460.

Lee, K. Y., Blaker, J. J., Heng, J. Y. Y., Murakami, R., & Bismarck, A. (2014b). PH-triggered phase inversion and separation of hydrophobised bacterial cellulose stabilised Pickering emulsions. *Reactive and Functional Polymers*, *85*, 208–213.

Li, Y., Ko, F. K., & Hamad, W. Y. (2013). Effects of emulsion droplet size on the structure of electrospun ultrafine biocomposite fibers with cellulose nanocrystals. *Biomacromolecules*, *14*(11), 3801-3807.

Liakos, I. L., Holban, A. M., Carzino, R., Lauciello, S., & Grumezescu, A. M. (2017). Electrospun fiber pads of cellulose acetate and essential oils with antimicrobial activity. *Nanomaterials*, 7(4), 84.

Liu, D., Yuan, X., & Bhattacharyya, D. (2012). The effects of cellulose nanowhiskers on electrospun poly (lactic acid) nanofibres. *Journal of Materials Science*, *47*(7), 3159–3165.

Liu, F., & Tang, C. H. (2013). Soy protein nanoparticle aggregates as pickering stabilizers for oil-in-water emulsions. *Journal of Agricultural and Food Chemistry*, *61*(37), 8888–8898.

Liu, H., Geng, S., Hu, P., Qin, Q., Wei, C., & Lv, J. (2015). Study of Pickering emulsion stabilized by sulfonated cellulose nanowhiskers extracted from sisal fiber. *Colloid and Polymer Science*, *293*(3), 963–974.

Liu, K., Jiang, J., Cui, Z., & Binks, B. P. (2017). PH-Responsive Pickering emulsions stabilized by silica nanoparticles in combination with a conventional zwitterionic surfactant. *Langmuir*, *33*(9), 2296–2305.

Livingstone, R. A., Nagata, Y., Bonn, M., & Backus, E. H. (2015). Two types of water at the water–surfactant interface revealed by time-resolved vibrational spectroscopy. *Journal of the American Chemical Society*, *137*(47), 14912-14919.

López, P., Sánchez, C., Batlle, R., & Nerín, C. (2005). Solid- and vapor-phase antimicrobial activities of six essential oils: Susceptibility of selected foodborne bacterial and fungal strains. *Journal of Agricultural and Food Chemistry*, *53*(17), 6939–6946.

Mari, M., Bautista-Baños, S., & Sivakumar, D. (2016). Decay control in the postharvest system: Role of microbial and plant volatile organic compounds. *Postharvest Biology and Technology*, *122*, 70-81.

Majeed, H., Liu, F., Hategekimana, J., Sharif, H. R., Qi, J., Ali, B., Zhong, F. (2016). Bactericidal action mechanism of negatively charged food grade clove oil nanoemulsions. *Food Chemistry*, *197*, 75–83.

Martínez-Romero, D., Guillén, F., Valverde, J. M., Bailén, G., Zapata, P., Serrano, M., & Valero, D. (2007). Influence of carvacrol on survival of Botrytis cinerea inoculated in table grapes. *International Journal of Food Microbiology*, *115*(2), 144-148.

Martínez-Sanz, M., Lopez-Rubio, A., & Lagaron, J. M. (2011a). Optimization of the nanofabrication by acid hydrolysis of bacterial cellulose nanowhiskers. *Carbohydrate Polymers*, *85*(1), 228–236.

Martínez-Sanz, M., Olsson, R. T., Lopez-Rubio, A., & Lagaron, J. M. (2011b). Development of electrospun EVOH fibres reinforced with bacterial cellulose nanowhiskers. Part I: Characterization and method optimization. *Cellulose*, *18*(2), 335–347.

Mascheroni, E., Guillard, V., Gastaldi, E., Gontard, N., & Chalier, P. (2011). Anti-microbial effectiveness of relative humidity-controlled carvacrol release from wheat gluten/montmorillonite coated papers. *Food Control*, *22*(10), 1582–1591.

Mascheroni, E., Fuenmayor, C. A., Cosio, M. S., Silvestro, G. Di, Piergiovanni, L., Mannino, S., & Schiraldi, A. (2013). Encapsulation of volatiles in nanofibrous polysaccharide membranes for humidity-triggered release. *Carbohydrate Polymers*, *98*(1), 17–25.

McClements, D. J. (2005). Food Emulsions: Principles, Practicles and Techniques. Baco Raton, FL: CRC Press.

Melgarejo-Flores, B. G., Ortega-Ramírez, L. A., Silva-Espinoza, B. A., González-Aguilar, G. A., Miranda, M. R. A., & Ayala-Zavala, J. F. (2013). Antifungal protection and antioxidant enhancement of table grapes treated with emulsions, vapors, and coatings of cinnamon leaf oil. *Postharvest Biology and Technology*, *86*, 321-328.

Mikulcova, V., Bordes, R., Kasparkova, & Vera. (2016). On the preparation and antibacterial activity of emulsions stabilized with nanocellulose particles. *Food Hydrocolloids*, *61*, 780–792.

Mirjalili, M., & Zohoori, S. (2016). Review for application of electrospinning and electrospun nanofibers technology in textile industry. *Journal of Nanostructure in Chemistry*, *6*(3), 207-213.

Munteanu, B. S., Aytac, Z., Pricope, G. M., Uyar, T., & Vasile, C. (2014). Polylactic acid (PLA)/Silver-NP/VitaminE bionanocomposite electrospun nanofibers with antibacterial and antioxidant activity. *Journal of Nanoparticle Research*, *16*(10), 2643.

Nair, D. V. T., Nannapaneni, R., Kiess, A., Mahmoud, B., & Sharma, C. S. (2014). Antimicrobial efficacy of lauric arginate against Campylobacter jejuni and spoilage organisms on chicken breast fillets. *Poultry Science*, *93*(10), 2636–40.

Nedorostova, L., Kloucek, P., Kokoska, L., Stolcova, M., & Pulkrabek, J. (2009). Antimicrobial properties of selected essential oils in vapour phase against foodborne bacteria. *Food Control*, *20*(2), 157–160.

Neo, Y. P., Ray, S., Easteal, A. J., Nikolaidis, M. G., & Quek, S. Y. (2012). Influence of solution and processing parameters towards the fabrication of electrospun zein fibers with sub-micron diameter. *Journal of Food Engineering*, *109*(4), 645-651.

Novo, L. P., Bras, J., García, A., Belgacem, N., & Curvelo, A. A. S. (2015). Subcritical water: a method for green production of cellulose nanocrystals. *ACS Sustainable Chemistry and Engineering*, *3*(11), 2839–2846.

Novo, L. P., Bras, J., Garcia, A., Belgacem, N., & Curvelo, A. A. S. (2016). A study of the production of cellulose nanocrystals through subcritical water hydrolysis. *Industrial Crops and Products*, *93*, 88–95.

Obaidat, M. M., & Frank, J. F. (2009). Inactivation of Salmonella and Escherichia coli O157:H7 on sliced and whole tomatoes by allyl isothiocyanate, carvacrol, and cinnamaldehyde in vapor phase. *Journal of Food Protection*, *72*(2), 315–24.

Oh, S. Y., Yoo, D. Il, Shin, Y., & Seo, G. (2005). FTIR analysis of cellulose treated with sodium hydroxide and carbon dioxide. *Carbohydrate Research*, *340*(3), 417–428.

Ojala, J., Sirviö, J. A., & Limatainen, H. (2016). Nanoparticle emulsifiers based on bifunctionalized cellulose nanocrystals as marine diesel oil-water emulsion stabilizers. *Chemical Engineering Journal*, *288*, 312–320.

Okutan, N., Terzi, P., & Altay, F. (2014). Affecting parameters on electrospinning process and characterization of electrospun gelatin nanofibers. *Food Hydrocolloids*, *39*, 19–26.

Otoni, C. G., Espitia, P. J. P., Avena-Bustillos, R. J., & McHugh, T. H. (2016). Trends in antimicrobial food packaging systems: Emitting sachets and absorbent pads. *Food Research International*, *83*, 60–73.

Otoni, C. G., de Moura, M. R., Aouada, F. A., Camilloto, G. P., Cruz, R. S., Lorevice, M. V., Mattoso, L. H. C. (2017). Antimicrobial and physical-mechanical properties of pectin/papaya puree/cinnamaldehyde nanoemulsion edible composite films. *Food Hydrocolloids* (2014). 41 -*63*.

Ougiya, H., Watanabe, K., Morinaga, Y., & Yoshinaga, F. (1997). Emulsion-stabilizing effect of bacterial cellulose. *Bioscience, Biotechnology, and Biochemistry*, *61*(9), 1541–1545.

Oza, K. P., & Frank, S. G. (1989). Multiple emulsions stabilized by colloidal microgrystalline cellulose. *Journal of Dıspersıon Scıence and Technology*, *10*(2), 163-185.

Painter, J. A., Hoekstra, R. M., Ayers, T., Tauxe, R. V., Braden, C. R., Angulo, F. J. Griffin, P. M. (2013). Attribution of Foodborne Illnesses, Hospitalizations, and Deaths to Food Commodities by using Outbreak Data, United States, 1998–2008. *Emerging Infectious Diseases*, *19*(3), 407-415.

Pandey, M., Mustafa Abeer, M., & Amin, M. C. I. (2014). Dissolution study of bacterial cellulose (nata de coco) from local food industry: Solubility behavior & structural changes. *International Journal of Pharmacy and Pharmaceutical Sciences*, *6*(6), 89–93.

Parafati, L., Vitale, A., Restuccia, C., & Cirvilleri, G. (2015). Biocontrol ability and action mechanism of food-isolated yeast strains against Botrytis cinerea causing post-harvest bunch rot of table grape. *Food Microbiology*, 47, 85-92.

Paria, S., Manohar, C., & Khilar, K. C. (2005). Adsorption of anionic and non-ionic surfactants on a cellulosic surface. *Colloids and Surfaces A: Physicochemical and Engineering Aspects*, *252*(2–3), 221–229.

Park, S., Baker, J. O., Himmel, M. E., Parilla, P. a, & Johnson, D. K. (2010). Cellulose crystallinity index: measurement techniques and their impact on interpreting cellulase performance. *Biotechnology for Biofuels*, *3*(1), 10.

Paximada, P., Tsouko, E., Kopsahelis, N., Koutinas, A. A., & Mandala, I. (2016). Bacterial cellulose as stabilizer of o/w emulsions. *Food Hydrocolloids*, *53*, 225–232.

Peddireddy, K. R., Nicolai, T., Benyahia, L., & Capron, I. (2016). Stabilization of water-in-water emulsions by nanorods. *ACS Macro Letters*, *5*(3), 283–286.

Peng, B. L., Dhar, N., Liu, H. L., & Tam, K. C. (2011). Chemistry and applications of nanocrystalline cellulose and its derivatives: A nanotechnology perspective. *Canadian Journal of Chemical Engineering*, *89*(5), 1191–1206.

Peretto, G., Du, W. X., Avena-Bustillos, R. J., Sarreal, S. B. L., Hua, S. S. T., Sambo, P., & McHugh, T. H. (2014). Increasing strawberry shelf-life with carvacrol and methyl cinnamate antimicrobial vapors released from edible films. *Postharvest Biology and Technology*, *89*, 11-18.

Picheth, G. F., Pirich, C. L., Sierakowski, M. R., Woehl, M. A., Sakakibara, C. N., de Souza, C. F., & de Freitas, R. A. (2017). Bacterial cellulose in biomedical applications: a review. *International Journal of Biological Macromolecules*.

Pickering, S. U. (1907). Cxcvi.-emulsions. *Journal of the Chemical Society, Transactions*, *91*, 2001-2021.

Purwanti, N., Neves, M. A., Uemura, K., Nakajima, M., & Kobayashi, I. (2015). Stability of monodisperse clove oil droplets prepared by microchannel emulsification. *Colloids and Surfaces A: Physicochemical and Engineering Aspects*, *466*, 66–74.

Qiao, C., Chen, G., Zhang, J., & Yao, J. (2016). Structure and rheological properties of cellulose nanocrystals suspension. *Food Hydrocolloids*, *55*, 19–25.

Quintavalla, S., & Vicini, L. (2002). Antimicrobial food packaging in meat industry. *Meat science*, *62*(3), 373-380.

Ramsden, W. (1903). Separation of solids in the surface-layers of solutions and'suspensions'(observations on surface-membranes, bubbles, emulsions, and mechanical coagulation).--preliminary account. *Proceedings of the Royal Society of London*, 72, 156-164.

Rangaswamy, B. E., Vanitha, K. P., & Hungund, B. S. (2015). Microbial cellulose production from bacteria ısolated from rotten fruit. *International Journal of Polymer Science*, *2015*.

Rantuch, P., & Chrebet, T. (2014). Thermal decomposition of cellulose insulation. *Cellulose Chemistry and Technology*, *48*(5-6), 461–467.

Reid, M. S., Villalobos, M., & Cranston, E. D. (2016). Benchmarking cellulose nanocrystals: from the laboratory to industrial production and applications. *Langmuir*, 33(7),1583–1598.

Rieger, K. A., & Schiffman, J. D. (2014). Electrospinning an essential oil: Cinnamaldehyde enhances the antimicrobial efficacy of chitosan/poly (ethylene oxide) nanofibers. *Carbohydrate Polymers*, 113, 561-568.

Robertson, G. L. (2014). Food Packaging. *Encyclopedia of Agriculture and Food Systems*, *3*, 232–249.

Rodriguez-Lafuente, A., Nerin, C., & Batlle, R. (2010). Active paraffin-based paper packaging for extending the shelf life of cherry tomatoes. *Journal of Agricultural and Food Chemistry*, *58*(11), 6780–6786.

Roman, M., & Winter, W. T. (2004). Effect of sulfate groups from sulfuric acid hydrolysis on the thermal degradation behavior of bacterial cellulose. *Biomacromolecules*, 5(5), 1671–1677.

Romanazzi, G., Lichter, A., Gabler, F. M., & Smilanick, J. L. (2012). Recent advances on the use of natural and safe alternatives to conventional methods to control postharvest gray mold of table grapes. *Postharvest Biology and Technology*, *63*(1), 141-147.

Rosa, M. F., Medeiros, E. S., Malmonge, J. A., Gregorski, K. S., Wood, D. F., Mattoso, L. H. C.,Imam, S. H. (2010). Cellulose nanowhiskers from coconut husk fibers: Effect of preparation conditions on their thermal and morphological behavior. *Carbohydrate Polymers*, *81*(1), 83–92.

Rusli, R., Shanmuganathan, K., Rowan, S. J., Weder, C., & Eichhorn, S. J. (2011). Stress transfer in cellulose nanowhisker composites-influence of whisker aspect ratio and surface charge. *Biomacromolecules*, *12*(4), 1363–1369.

Sadeghifar, H., Filpponen, I., Clarke, S. P., Brougham, D. F., & Argyropoulos, D. S. (2011). Production of cellulose nanocrystals using hydrobromic acid and click reactions on their surface. *Journal of Materials Science*, *46*(22), 7344–7355.

Saito, T., Kimura, S., Nishiyama, Y., & Isogai, A. (2007). Cellulose nanofibers prepared by tempo-mediated oxidation of native cellulose. *Biomacromolecules*,8(8), 2485–2491.

Salajková, M., Berglund, L. A., & Zhou, Q. (2012). Hydrophobic cellulose nanocrystals modified with quaternary ammonium salts. *Journal of Materials Chemistry*, *22*(37), 19798-19805

Sanla-Ead, N., Jangchud, A., Chonhenchob, V., & Suppakul, P. (2012). Antimicrobial activity of cinnamaldehyde and eugenol and their activity after ıncorporation into cellulose-based packaging films. *Packaging and Technology and Science*, *25*, 7–17.

Scarlett, A. J., Morgan, W. L., & Hildebrand, J. H. (1927). Emulsification by solid powders. *The Journal of Physical Chemistry*, *31*(10), 1566-1571.

Segal, L., Creely, J. J., Martin, A. E., & Conrad, C. M. (1959). An empirical method for estimating the degree of crystallinity of native cellulose using the x-ray diffractometer. *Textile Research Journal*, *29*(10), 786–794.

Seo, E.-J., Min, S.-G., & Choi, M.-J. (2010). Release characteristics of freeze-dried eugenol encapsulated with *β*-cyclodextrin by molecular inclusion method. *Journal of Microencapsulation*, *27*(6), 496–505.

Shi, Z., Zhang, Y., Phillips, G. O., & Yang, G. (2014). Utilization of bacterial cellulose in food. *Food Hydrocolloids*, *35*, 539–545.

Shin, M. H., Kim, J. H., Choi, H. W., Keum, Y. S., & Chun, S. C. (2014). Effect of thymol and linalool fumigation on postharvest diseases of table grapes. *Mycobiology*, 42(3), 262-268.

Shinde, U., & Nagarsenker, M. (2011). Microencapsulation of eugenol by gelatin-sodium alginate complex coacervation. *Indian Journal of Pharmaceutical Sciences*, *73*(3), 311–5.

Sousa, A. M. M., Souza, H. K. S., Uknalis, J., Liu, S. C., Gonçalves, M. P., & Liu, L. S. (2015). Improving agar electrospinnability with choline-based deep eutectic solvents. *International Journal of Biological Macromolecules*, *80*, 139–148.

Soylu, E. M., Soylu, S., & Kurt, S. (2006). Antimicrobial activities of the essential oils of various plants against tomato late blight disease agent Phytophthora infestans. *Mycopathologia*, *161*(2), 119-128.

Tardy, B. L., Yokota, S., Ago, M., Xiang, W., Kondo, T., Bordes, R., & Rojas, O. J. (2017). Nanocellulose surfactant interactions. *Current Opinion in Colloid and Interface Science*, *29*, 57–67.

Torn, L. H., Koopal, L. K., De Keizer, A., & Lyklema, J. (2005). Adsorption of nonionic surfactants on cellulose surfaces: Adsorbed amounts and kinetics. *Langmuir*, *21*(17), 7768–7775.

Trache, D., Hussin, M. H., Haafiz, M. K. M., & Thakur, V. K. (2017). Recent progress in cellulose nanocrystals: sources and production. *Nanoscale*,9(5), 1763–1786.

Turek, C., & Stintzing, F. C. (2013). Stability of essential oils: a review. *Comprehensive Reviews in Food Science and Food Safety*, *12*(1), 40-53.

Tzortzakis, N. G. (2007). Maintaining postharvest quality of fresh produce with volatile compounds. *Innovative Food Science & Emerging Technologies*, *8*(1), 111–116.

Ugolini, L., Martini, C., Lazzeri, L., D'Avino, L., & Mari, M. (2014). Control of postharvest grey mould (Botrytis cinerea Per.: Fr.) on strawberries by glucosinolate-derived allyl-isothiocyanate treatments. *Postharvest biology and technology*, *90*, 34-39.

Utto, W., Mawson, A. J., & Bronlund, J. E. (2008). Hexanal reduces infection of tomatoes by Botrytis cinerea whilst maintaining quality. *Postharvest Biology and Technology*, *47*(3), 434–437.

Valencia-Sullca, C., Jiménez, M., Jiménez, A., Atarés, L., Vargas, M., & Chiralt, A. (2016). Influence of liposome encapsulated essential oils on properties of chitosan films. *Polymer International*, *65*(8), 979-987.

Valero, D., Valverde, J. M., Martínez-Romero, D., Guillén, F., Castillo, S., & Serrano, M. (2006). The combination of modified atmosphere packaging with eugenol or thymol to maintain quality, safety and functional properties of table grapes. *Postharvest Biology and Technology*, *41*(3), 317-327.

Valverde, J. M., Guillén, F., Martínez-Romero, D., Castillo, S., Serrano, M., & Valero, D. (2005). Improvement of table grapes quality and safety by the combination of modified atmosphere packaging (MAP) and eugenol, menthol, or thymol. *Journal of Agricultural and Food Chemistry*, *53*(19), 7458-7464.

Vanderroost, M., Ragaert, P., Devlieghere, F., & De Meulenaer, B. (2014). Intelligent food packaging: The next generation. *Trends in Food Science & Technology*, *39*(1), 47-62.

Vasconcelos, N. F., Feitosa, J. P. A., da Gama, F. M. P., Morais, J. P. S., Andrade, F. K., de Souza Filho, M. de S. M., & Rosa, M. de F. (2017). Bacterial cellulose nanocrystals produced under different hydrolysis conditions: Properties and morphological features. *Carbohydrate Polymers*, *155*(August), 425–431.

Vega-Lugo, A. C., & Lim, L. T. (2009). Controlled release of allyl isothiocyanate using soy protein and poly(lactic acid) electrospun fibers. *Food Research International*, *42*(8), 933–940.

Vu, K. D., Hollingsworth, R. G., Leroux, E., Salmieri, S., & Lacroix, M. (2011). Development of edible bioactive coating based on modified chitosan for increasing the shelf life of strawberries. *Food Research International*, *44*(1), 198–203.

Walsh, S. E., Maillard, J. Y., Russell, A. D., Catrenich, C. E., Charbonneau, D. L., & Bartolo, R. G. (2003). Activity and mechanisms of action of selected biocidal agents on Gram-positive and-negative bacteria. *Journal of Applied Microbiology*, 94(2), 240-247.

Wang, N., Ding, E., & Cheng, R. (2007). Thermal degradation behaviors of spherical cellulose nanocrystals with sulfate groups. *Polymer*, *48*(12), 3486–3493.

Wang, C., Zhang, J., Chen, H., Fan, Y., & Shi, Z. (2010). Antifungal activity of eugenol against Botrytis cinerea. *Tropical Plant Pathology*, *35*(3), 137-143.

Wang, C., Tong, S. N., Tse, Y. H., & Wang, M. (2011). Conventional electrospinning vs. emulsion electrospinning: a comparative study on the development of nanofibrous drug/biomolecule delivery vehicles. *Advanced Materials Research*, *410*, 118–121.

Wang, H., Hao, L., Niu, B., Jiang, S., Cheng, J., & Jiang, S. (2016). Kinetics and antioxidant capacity of proanthocyanidins encapsulated in zein electrospun fibers by cyclic voltammetry. *Journal of Agricultural and Food Chemistry*, *64*(15), 3083–3090.

Wang, W., Du, G., Li, C., Zhang, H., Long, Y., & Ni, Y. (2016). Preparation of cellulose nanocrystals from asparagus (Asparagus officinalis L .) and their applications to palm oil / water Pickering emulsion. *Carbohydrate Polymers*, *151*, 1–8.

Wen, C., Yuan, Q., Liang, H., & Vriesekoop, F. (2014). Preparation and stabilization of d-limonene Pickering emulsions by cellulose nanocrystals. *Carbohydrate Polymers*, *112*, 695–700.

Wen, P., Zhu, D. H., Wu, H., Zong, M. H., Jing, Y. R., & Han, S. Y. (2016). Encapsulation of cinnamon essential oil in electrospun nanofibrous film for active food packaging. *Food Control*, 59, 366-376.

Woranuch, S., & Yoksan, R. (2013a). Eugenol-loaded chitosan nanoparticles: I. Thermal stability improvement of eugenol through encapsulation. *Carbohydrate Polymers*, *96*(2), 578–585.

Woranuch, S., & Yoksan, R. (2013b). Eugenol-loaded chitosan nanoparticles: II. Application in bio-based plastics for active packaging. *Carbohydrate Polymers*, *96*(2), 586–592.

Xhanari, K., Syverud, K., & Stenius, P. (2011). Emulsions stabilized by microfibrillated cellulose: the effect of hydrophobization, concentration and o/w ratio. *Journal of Dispersion Science and Technology*, *32*(3), 447–452.

Xie, J., & Hsieh, Y. L. (2003). Ultra-high surface fibrous membranes from electrospinning of natural proteins: casein and lipase enzyme. *Journal of Materials Science*, *38*(10), 2125-2133.

Xu, Y., & Hanna, M. A. (2006). Electrospray encapsulation of water-soluble protein with polylactide. Effects of formulations on morphology, encapsulation efficiency and release profile of particles. *International Journal of Pharmaceutics*, *320*(1–2), 30–36.

Yam, K. L., & Lee, D. S. (Eds.). (2012). Emerging food packaging technologies*:* Principles and practice. *Elsevier.*

Yang, Y., Li, X., Qi, M., Zhou, S., & Weng, J. (2008). Release pattern and structural integrity of lysozyme encapsulated in core-sheath structured poly(dl-lactide) ultrafine fibers prepared by emulsion electrospinning. *European Journal of Pharmaceutics and Biopharmaceutics*, *69*(1), 106–116.

Yao, Z. C., Chen, S. C., Ahmad, Z., Huang, J., Chang, M. W., & Li, J. S. (2017). Essential Oil Bioactive Fibrous Membranes Prepared via Coaxial Electrospinning. *Journal of Food Science*, 82(6), 1412-1422.

Zoppe, J. O., Venditti, R. A., & Rojas, O. J. (2012). Pickering emulsions stabilized by cellulose nanocrystals grafted with thermo-responsive polymer brushes. *Journal of Colloid and Interface Science*, *369*(1), 202–209.

APPENDIX A

CALIBRATION CURVE

Six concentration of eugenol (Natural, ≥98 % (W246719) Sigma-Aldrich, St. Louis, MO, USA), namely 0.53 ppm, 1.16 ppm, 2.12 ppm, 5.30 ppm, 21.20 ppm and 53 ppm from the stock solution were used for preparing eugenol headspace calibration curve. All eugenol concentrations were dissolved in dichloromethane (DCM) in 1.8mL vial kits and kits were placed in autosampler (1 ml of injection set) of GC for analysis. Samples were analyzed with an Agilent Technologies 6890N Network Gas Chromatograph (USA) equipped with a flame ionization detector (hydrogen, 40 mL/min; air, 300 mL/min) and a HP-5 5% Phenyl Methyl Siloxane Capillary column (30 m x 0.25 mm, film thickness 0.25 µm Agilent 19091 J-433). The oven temperature was set at 50 to 290 º C at 12 º C/min. Inlet and detector temperatures were adjusted to 50 to 300º C. Helium was used as a carrier gas at a flow rate of 1 mL/min column flow. The standard calibration curve was plotted eugenol concentration against the area under the curve obtained from the GC software for each concentration.

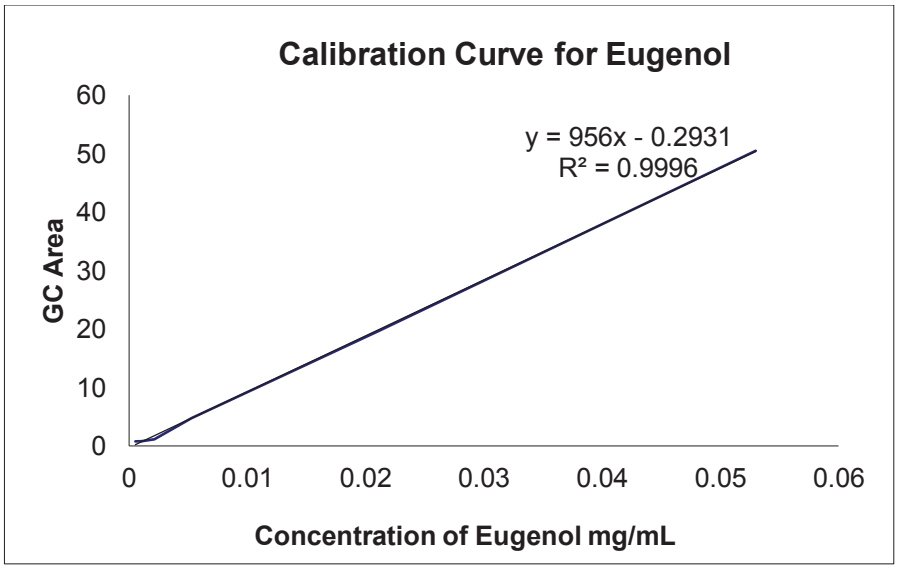

Figure A.1. Standard calibration curve of eugenol

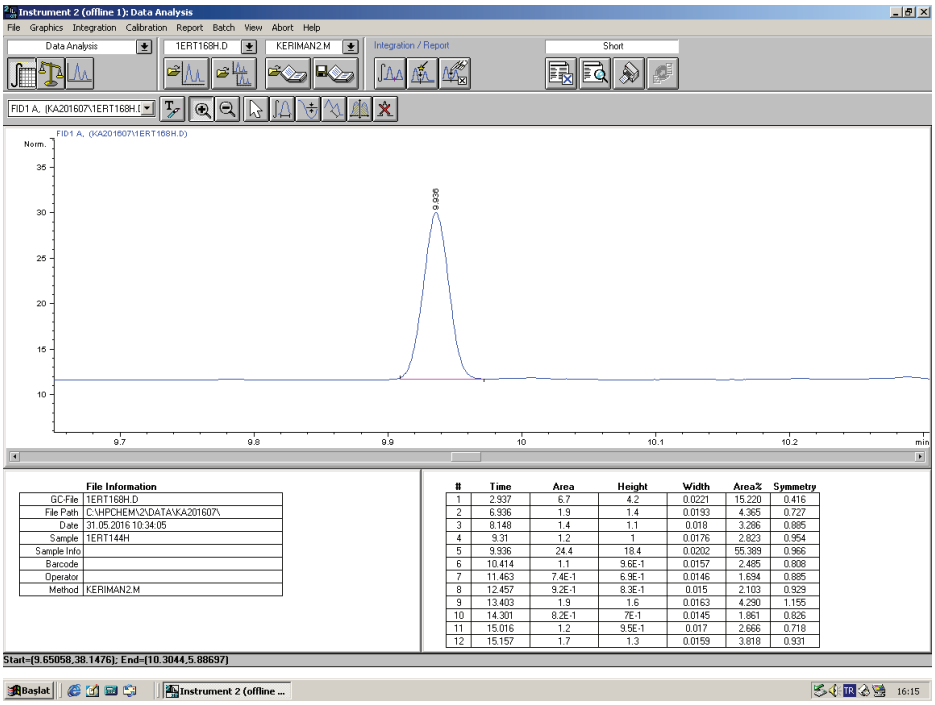

Figure A.2. The eugenol peak position observed in GC experiments

APPENDIX B

RELEASE EXPERIMENTS RH CONTROL

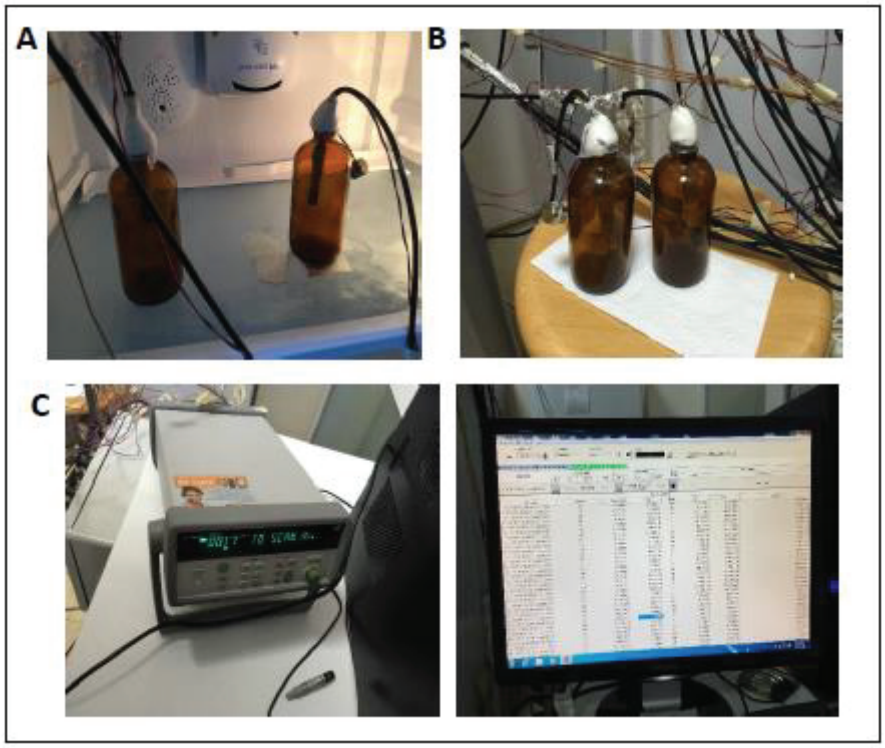

Figure B.1. RH control in a) Refrigerator temperature (4±1°C) b) Room temperature (22±1°C) c) Agilent Data Logger system

VITA

Personal Information

Name: Dılhun Keriman
Surname: ARSERİM UÇAR
Nationality: Turkish
Marital Status: Married
E-mail: kerimanarserim@gmail.com

Education

PhD. in Food Engineering, İzmir Institute of Technology	2011-2017
MSc. in Food Engineering, İzmir Institute of Technology	2006-2009
BSc. in Food Engineering, Mersin University	2000-2004

Academic Work Experience

Project Assistant /İzmir Institute of Technology, İzmir, Turkey	2008-2009
Research Assistant/İzmir Institute of Technology, İzmir, Turkey (35. Madde)	2013-2017
Research Assistant/Bingöl University, Bingöl, Turkey	2013-Present
Research Fellow/Rutgers University, New Jersey, USA	2014-2015

Publications

- Uysal Ünalan, İ., Arserim Uçar, K.D., Arcan, İ., Korel, F., Yemenicioğlu, A. 2011. Antimicrobial potential of polylysine in edible films, Food Science and Technology Research, 17, 375-380

Awards

- 2nd Best Oral Presentation Award. *2nd Congress on Food Structure Design* FSD 2016.
- 2214-A-PhD. Research Fellowship Program award from TUBİTAK (Turkish Scientific Research Council) for Rutgers University 2014-2015
- Scholarship in The Support Program for Scientific and Technological Research Projects from TUBİTAK (Turkish Scientific Research Council-TOVAG 108O591) 2008-2009.